Production and secretion of recombinant proteins using *Bacillus megaterium*

Von der Fakultät für Lebenswissenschaften

der Technischen Universität Carolo-Wilhelmina

zu Braunschweig

zur Erlangung des Grades einer

Doktorin der Naturwissenschaften

(Dr. rer. nat.)

genehmigte

D i s s e r t a t i o n

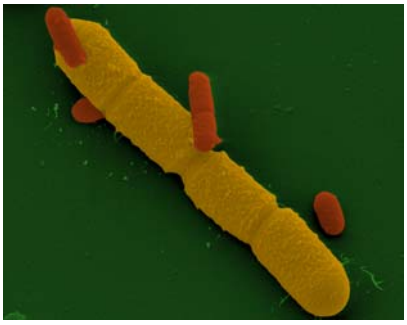

von Yang Yang
aus Tianjin / China

1. Referent: Prof. Dr. Dieter Jahn
2. Referent: apl. Prof. Dr. Siegmund Lang
eingereicht am: 28.02.2007
mündliche Prüfung (Disputation) am: 23.04.2007

Druckjahr 2007

Vorveröffentlichungen der Dissertation

Teilergebnisse aus dieser Arbeit wurden mit Genehmigung der Fakultät für Lebenswissenschaften, vertreten durch den Mentor der Arbeit, in folgenden Beiträgen vorab veröffentlicht:

Publikationen

- Yang, Y., Malten, M., Grote, A., Jahn, D., Deckwer, W.-D. (2007). **Codon optimized *Thermobifida fusca* hydrolase secreted by *Bacillus megaterium***, *Biotech Bioeng*, 96(4):780-794.

- Yang, Y., Biedendieck, R., Wang, W., Gamer, M., Jahn, D., Malten, M., Deckwer, W.-D. (2006). **High yield recombinant penicillin G amidase production and export into the growth medium using *Bacillus megaterium***. *Microb Cell Fact*.5:36.

- Biedendieck, R., Yang, Y., Deckwer, W.-D., Jahn, D., Malten, M. (2007). **Plasmid system for the intracellular production and purification of affinity-tagged proteins in *Bacillus megaterium***, *Biotech Bioeng*, 96(3): 525-537.

- Hollmann, R., Malten, M., Biedendieck, R., Yang, Y., Wang, W., Jahn, D., Deckwer, W.-D., (2006). ***Bacillus megaterium* as a production system for recombinant proteins**, *Chemie-Ingenieur-Technik* **78**, 289-294.

Tagungsbeiträge

- Yang, Y., Malten, M., Wang, W., Jahn, D., Deckwer, W. -D., (2006) **Expression and Secretion of Recombinant proteins in *B. megaterium*,** VAAM-Jahrestagung, Jena, Germany, 19.03.06-22.03.06 (Vortrag).

- Yang, Y., Malten, M., Biedendieck, R., Jahn, D., Deckwer, W. -D. (2006). **Optimization of protein production and secretion in *Bacillus megaterium***, 4th Recombinant Protein Production meeting, Barcelona, Spain, 20.09.06-23.09.06

You have to believe in yourself.
That's the secret of success.

Charles Chaplin

Table of Contents

Abbreviations

AA	amino acid
Amp	ampicillin
6-APA	6-aminopenicillanic acid
ATP	adenosine 5'-triphosphate
bp	base pair
BSA	bovine serum albumin
CAI	codon adaptation index
CcpA	catabolite control protein
CDW	cell dry weight
CHAPS	3-[(3-cholamidopropyl)-dimethyalmino]
Cml	chloramphenicol
Cre	catabolite responsive element
CV	column volume
Da	Dalton
DHAP	dihydroxyacetone phosphate
DNA	deoxyribonucleic acid
dNTP	deoxyribonucleotide triphosphate
DTT	1,4-dithio-D,L-threitol
EDTA	ethylenediaminetetraacetic acid
e.g.	*exempli gratia* (for example)
et al.	*et alteri* (and others)
EMP	Embden-Meyerhof-Parnas Pathway
E4P	erythrose-4-phosphate
FACS	fluorescent activated cell sorting
for	forward
FSC	frontal scatter
g	*centrifugation*: earth gravity *weight*: gram
ß-Gal	ß-galactosidase
GAP	glyceraldehydes-3-phosphate
GFP	green fluorescent protein
G6P	glucose-6-phosphate
h	hour
HCDC	high cell density cultivation
HPLC	high pressure liquid chromatography
H_2O_{deion}	deionised water
IDA	iminodiacetic acid
IMAC	Immobilized Metal Affinity Chromatography
kb	kilo base pair
K_{av}	partition coefficient
kDa	kilo Dalton
λ	wave length
LB	Luria Bertani
M	molar [mol L^{-1}]
μ_{set}	growth rate
MALDI	matrix assisted laser desorption/ionisation
MCS	multiple cloning site
MM	minimal medium
MOPS	3-(N-morpholino)-propan sulfonacid

MOPSO	3-(N-morpholino)-2-hydroxy propan sulfonacid
M_r	relative molecular mass
MS	mass spectrometry
NADH	nicotinamide-adenine dinucleotide
NIPAB	6-Nitro-3-phenylacetamido-benzoic acid
OD_λ	optical density at wavelength λ in nm
ORF	open reading frame
ori	origin of replication
PAA	phenylacetic acid
PAGE	polyacrylamide gel electrophoresis
PBS	phosphate-buffered saline
PCR	polymerase chain reaction
PEG	6000 polyethylen glycol with M_r of 6000
PEP	phosphoenolpyruvate
3-PG	3-phosphoglycerate
PGA	Penicillin G amidase
PI	propidium iodide
PPP	pentose phosphate pathway
PTS	phosphotransferase system
PVDF	polyvinylidene difluoride
RBS	ribosome binding side
rev	reverse
R5P	ribose-5-phosphate
RNA	ribonucleic acid
RNase	ribonuclease
rpm	rotations per minute
RT	room temperature
Ru5P	Ribulose-5-phosphate
SCA	single-chain antibody
SDS	sodium dodecyl sulfate
SDS-PAGE	sodium dodecyl sulfate polyacrylamide gel electrophoresis
SEC	secretion
SF	shake flask
SP	signal peptide
SRP	signal recognition particle
SSC	side scatter
TAT	twin arginine translocation
TCA	trichloroacetic acid
TEMED	tetramethylene diamine
Tet	tetracycline
TFH	*Thermobifida fusca* hydrolase
T_M	hybridisation temperature
TOF	time of flight
TRIS	tris-(hydroxymethyl)-aminomethane
Triton-X100	t-octylphenoxy polyethoxy ethanol
U	unit
UV	ultraviolet
vs.	versus
v/v	volume per volume
w/v	weight per volume

I Summary and outlook

I.1 Summary

The aim of this thesis was to systemically establish the recombinant high level production and secretion of a heterologous hydrolase from *Thermobifida fusca* (TFH) and a homologous penicillin G amidase from *Bacillus megaterium* ATCC 14945 using the Gram positive bacterium *B. megaterium.* First, production and secretion of a TFH in *B. megaterium* MS941 and WH323 was investigated using shake flask and pH controlled bioreactors. Successful TFH production was achieved by adapting the original *tfh* gene to the optimal codon usage of *B. megaterium*. A codon adaptation index close to 1 was reached. The codon optimized *tfh* gene was cloned into an open reading frame with the DNA sequence for the N-terminal signal peptide of *B. megaterium* lipase A and a C- terminal His_6-tag, all under the control of a xylose inducible promoter. The use of WH323 impaired in xylose utilization increased TFH yields via long term promoter induction. Using LB medium 2.9 mg TFH L^{-1} were secreted in shaking flask cultivation. This was further increased to 18.1 mg L^{-1} in a pH controlled batch cultivation. With semi-defined A5 medium in a pH controlled batch cultivation secretion of 13.9 mg L^{-1} was observed. For the first time, significant protein secretion in glucose limited fed batch cultivation was achieved using a semi-defined medium. Finally, continuous cultivation led to 12.3 mg L^{-1} secreted TFH. Productivity was improved 2.3 - fold to 421 U g $_{CDW}^{-1}$ compared to the production in high cell density cultivation. Chromatographically purified TFH carried a specific activity of 439 U mg $_{protein}^{-1}$. Next, the recombinant production and export of penicillin G amidase (PGA) which is used in the reverse synthesis of β-lactam antibiotics were systematically improved. Strain YYBm1 lacking the extracellular protease NprM and deprived in xylose utilization was employed. The PGA leader peptide was replaced by the *B. megaterium* LipA counterpart, which led to an increase in secretion by 1.7-fold. Second, a buffered mineral medium containing calcium ions and defined amino acid supplements was developed and scaled up to a 2 liter bioreactor. With a productivity of up to 40 mg L^{-1} PGA in a batch cultivation, the combination of genetic and medium optimization led to an overall 7-fold improvement. Finally, PGA production was further optimized in high cell density cultivations, which yielded a 30-fold improvement. Nevertheless, continuous cultivation showed the tendency to be a better protein production process than a high cell density cultivation strategy.

I.2 Outlook

In this work *B. megaterium* was shown to produce and secrete high amounts of heterologous and homologous recombinant proteins. However, a further systematic analysis of still limiting steps in protein production and export should follow. For this purpose a system biology analysis currently seems the advised approach.

During the high cell density cultivation a combined transcriptome, proteome and metabalome study might provide insights into the reasons for low protein production and export. A detailed analysis of cell physiology may also help to understand and improve the production and secretion of recombinant proteins in large scale cultivations. The deduced information will help to construct a model for an efficient protein production process after identification of general limitations existing in the *B. megaterium* system.

One strategy would be to minimize proteolytic degradation by knocking out additional proteases as the metalloprotease in *B. megaterium* strain MS941 and YYBm1. Finally, the overall *B. megaterium* system requires strategies for the necessary optimizations on the level of transformation, gene knock out, protein export and extracellular protein folding.

II Introduction

II.1 The genus *Bacillus* and its industrial importance

In 1872, Ferdinand Cohn, a student of Robert Koch, recognized a rod-like bacteria in the soil and named it *Bacillus subtilis*. This organism is part of a large and diverse genus of bacteria, the gene *Bacillus*, and was placed in the family Bacillaceae. Members of the genus *Bacillus* are characterized as Gram-positive, rod-shaped, aerobic or facultative anarobic, endospore-forming bacteria. The nonpathogenity of most species and their ability to secrete proteins make these bacteria interesting for the use in the pharmaceutical, food, and cosmetics industry. *Bacilli* produce many different industrially important enzymes, including amylases, proteases, glucanases, lipases, nucleases, and phosphatases (Priest, 1977). *Bacillus amyloliquefaciens* secretes α-amylase, proteases, and phosphatases. *Bacillus brevis* synthesizes cellulase and tyrocidine (Priest, 1977). *Bacillus stearothermophilus* is of special interest with respect to thermostability as well as chemostability of enzymes (Bergquist *et al*., 1987). *Bacillus licheniformis* is known as an effective producer of degrading enzymes employed in various washing detergents. Moreover, it has been of interest due to its ability to secrete foreign proteins. *Bacillus polymyxa* is of industrial importance because of its broad product range including antibiotics, amylases, cellulases, and proteases (Priest, 1977).

This thesis focuses on one *Bacilli* - *Bacillus megaterium* - which carries all the advantages of the other *Bacilli* such as growth on cheap substrates, ability to secrete high amount of proteins, nonpathogenicity, and the absence of endotoxins common in Gram-negative bacteria like *Escherichia coli*.

II.2 *Bacillus megaterium*

In 1887 it was originally named *Bacillus megatherium*, meaning “big beast” in Greek (Carlsson *et al.*, 2000). By changing the name to *Bacillus megaterium*, it means “big cheese” now. *B. megaterium* is one of the largest *Bacilli* with a cell diameter of 1.2 to 1.5 µm and a length of 2 to 5 µm. It was intensively studied morphologically from the early days of microbiology on. Therefore, it was a model for cell wall and sporulation studies (Frehel & Ryter, 1979; Frehel & Ryter, 1982). It was utilized by industry for the production of several enzymes such as amylases, penicillin amidase, and glucose dehydrogenase and further on for vitamin like B_{12} (Malten, 2005).

II.2.1 General Physiology

Cells grow easily at temperatures from 10 °C to 30 °C but not above 50 °C. Most *B. megaterium* strains grow at 40 and 50 °C. It has a versatile and adaptable arsenal of enzymes, which renders it capable of surviving on numerous carbon sources and in many types of environments. It can utilize all the tricarboxylic acid (TCA) cycle intermediates such as citrate, lactate, malonate, succinate, and also acetate. However, it dose not assimilate nitrite from nitrate but deaminates phenylalanine instead.

II.2.2 Surface Structure

The vegetative cell surface is a laminated structure that consists of the proteins on the outer surface of the plasma membrane, several layers of peptidoglycan sheeting, a proteinaceous surface layer (S-layer) and an outer capsule. The capsule synthesized by *B. megaterium* is composed of both polypeptides and polysaccharides. The polypeptide is located laterally along the axis of the cell. The polysaccharide is located at the poles and at the equator of the cell. The S-layer may play a role in bacteria-metal interactions. The vegetative cell wall is formed by a peptidoglycan containing meso-diaminopimelic acid. In addition to peptidoglycan, the cell wall contains a large amount of teichoic acids which are bound to muramic acid residues.

II.2.3 Spore Physiology

Endospores can be recognized microscopically by their intracellular site of formation and their extreme refractility. They are not formed during cell division and active growth. Rather, they are built in response to environment signals indicating a limiting factor for vegetative growth, such as the exhaustion of an essential nutrient or at high cell density. Typically, one endospore is formed per vegetative cell. The general structure and the chemical composition of the *Bacillus* spore are very different compared to the vegetative cell. For example, the spore wall contains a peptidoglycan which is less cross-linked than that in the vegetative cell. Dipicolinic acid formed in the spores is also not present in the vegetative cells. This compound represents in some cases about 10 to 15 percent of the total spore dry weight and is located within the spore protoplast. Mature spores are highly resistant to environmental stresses such as high irradiation, temperature, strong acids,

disinfectants and so on. They germinate again when the environmental stress is relieved. There is no detectable metabolism. Hence, endospore-formation is a mechanism of survival rather than a mechanism of reproduction. Penicillin-binding proteins (PBPs) have been found to play a major role in the synthesis of the cell wall peptidoglycan during vegetative growth, cell division and sporulation (Foster & Popham, 2001; Popham, 2002).

II.2.4 Stress Responses

Bacteria are highly adapted to a sudden unfavorable environmental change by activation of complex cell defense reactions generally called stress response. One stress can be the depletion of essential nutrients. Under nitrogen, phosphate, or carbon limitation, *B. megaterium* accumulates poly-β-hydroxy butyrate (PHB) as storage compound (Dawes & Ribbons, 1964). It is a nonphosphate containing energy source which accumulates especially during growth in a low-phosphate medium. It is also a major source of energy during sporulation. Because of its industrial applications in thermal plastics and pharmaceuticals a self-disruptive *B. megaterium* strain was constructed which responds to substrate exhaustion (Hori *et al*., 2002). Several groups also investigated the behaviour of *B. megaterium* in response to several osmotic stress conditions. According to the work from Stahl and co workers, *B. megaterium* can not grow in 1.7 M NaCl (Stahl & Olsson, 1977). Nekolny *et al* (2000) investigated a salt concentration-dependent growth delay and a decrease of the maximal growth rate of *B. megaterium* in the range of 0 to 1 M NaCl. Some usually stable cell proteins were degraded very quickly during the adaptation to the salt stress. On the other hand, intracellular non-serine proteases were not significantly affected by the salt stress. However, the production of an extracellular metallo-protease was nearly completely suppressed by 0.5 M NaCl (Nekolny & Chaloupka, 2000). The influence of other stress factors as heat or shear force were not investigated so far.

II.2.5 Products of Industrial Importance

B. megaterium can produce several commercially important enzymes including a neutral protease, amylases, a penicillin amidase, and a glucose dehydrogenase. The neutral protease is used in the leather tanning industry in Indonesia (personal communication, F. Meinhardt, Münster). Millet and co workers (Millet *et al*., 1969)

found that up to 2 % of the total cellular protein consisted of the protease. The enzyme is produced in minimal medium during both logarithmic growth and sporulation. Interestingly, in complex medium it is only produced during sporulation. Amino acids such as leucine, valine, and isoleucine can repress protease production 12 to 32 % (w/v) (Millet *et al*., 1969). Penicillin amidase is used in the production of new β-lactam antibiotics. Amylases are of interest in starch modification and the baking industry. The glucose dehydrogenase catalyzes the metabolism of glucose to gluconic acid under release of NADH. It is widely used for diagnostic purposes. In addition, some species of *B. megaterium* also produce antibiotics, antiviral, antifungal, antitumor substances, and several types of bacteriocins or megacins (Stahl, 1989). The best characterized antiviral agent is oxetanocin, which acted highly efficient against hepatitis B virus.

II.3 Secretion and production of heterologous and homologous proteins in *B. megaterium*

II.3.1 Protein secretion in *B. megaterium*

In contrast to Gram-negative bacteria with an additional outer membrane, secretory proteins of Gram-positive bacteria only need to traverse a single cytoplasmic membrane to enter the extracellular environment. Due to this fact, Gram-positive bacteria are considered especially interesting as host organisms for the secretory production of proteins. Secretion of the produced protein is an advantage over intracellular production often leading to the deposition of the target proteins as aggregates (inclusion bodies). In fact, one of the reasons for the extensive use of certain Gram-positive bacteria with emphasis on *Bacillus* species in industry is their enormous secretion potential of proteins. Several grams proteases, lipases, and amylases are often produced per liter of culture medium by these organism (Aunstrup, 1979; Debabov, 1982; Harwood, 1992).

II.3.1.1 Major protein transport routes

The secretory pathway can be divided into three functional stages: (1) in the first stage, secretory pre-proteins are synthesized, then interacted with chaperones to form a translocation competent conformation and further bound to the secretory translocase; (2) in the second stage, translocation occurs across the cytoplasmic membrane via the translocase; and (3) in the late stage, the signal peptide is

removed, protein is released from the translocase, refolds and passes through the cell wall (Simonen & Palva, 1993). Sec (Secretion) - and Tat (twin arginie translocation) - are the two important different systems in bacteria for the secretion of proteins into the extracellular space (Figure 1). The major protein translocation system (Sec-system) shows a high degree of conservation of central components between Gram-positive and Gram-negative bacteria, proposing similar functions and working mechanisms (van Wely *et al*., 2001).

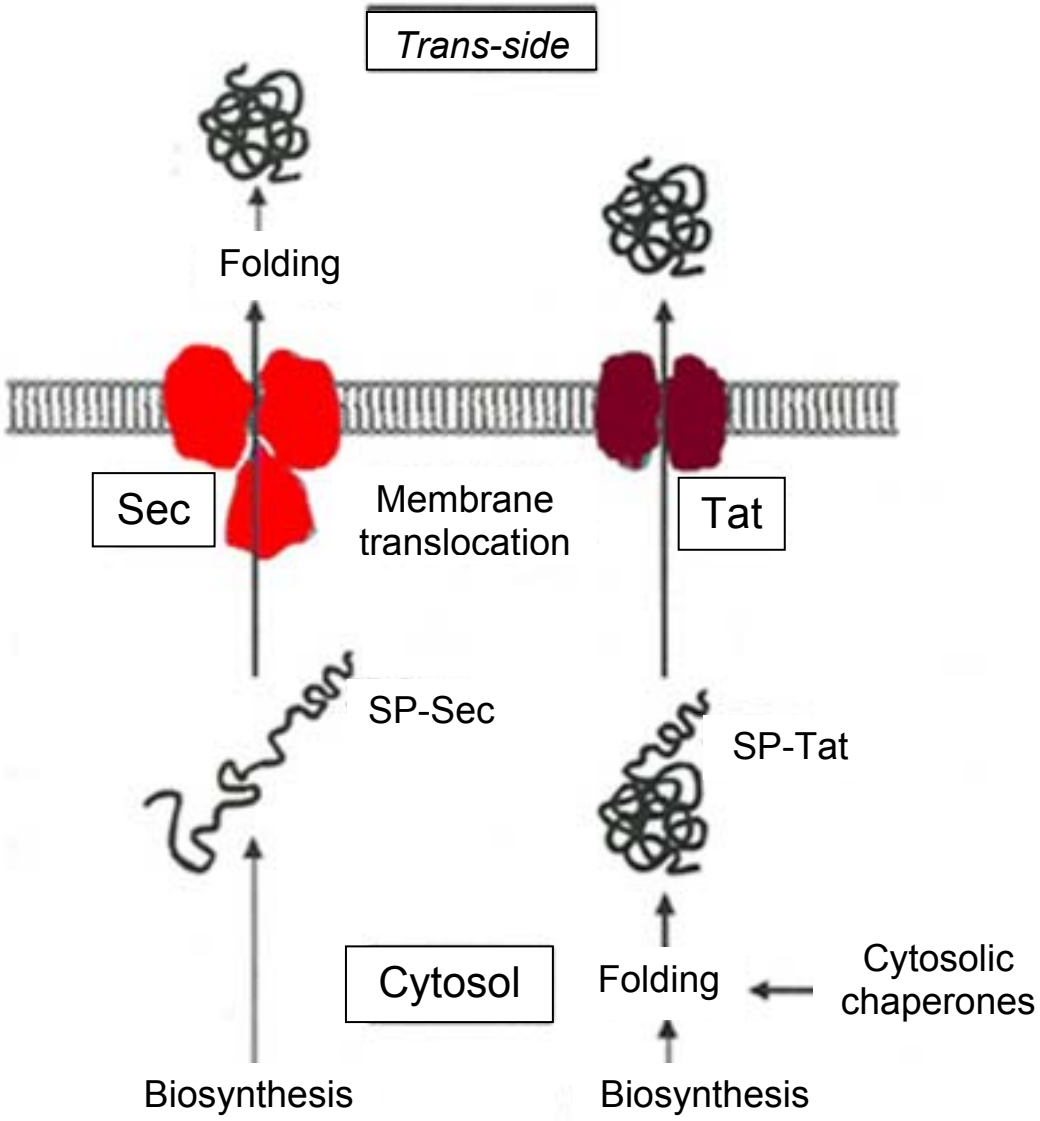

Figure 1. Major protein secretion pathways in Gram-positive bacteria (modified after Gellissen,2002). The general Sec- and Tat-pathways differ greatly with respect to the folding status of their protein substrates. Translocation via the Sec-system requires the exported proteins in an unfolded state. In contrast, completely folded proteins are exported by the Tat systems.

The Tat pathway is named "*t*win-*a*rginine *t*ranslocation pathway" due to the fact that a characteristic amino acid motif includes two consecutive arginine residues which can

be identified in the signal peptide of the respective precursor proteins. The folding status of their respective substrate proteins during the actual translocation step is one of the most remarkable differences between these two systems. Sec-dependent proteins are translocated in an unfolded state. Subsequently, folding takes place on the trans-side of the membrane after membrane translocation. In contrast, the Tat-system tanslocates its protein substrates in a completely folded or even oligomeric form across the membrane. Therefore, many of the Tat substrates are proteins that recruit a cofactor in the cytosol and as a prerequisite need to acquire a folded status prior to export. Cofactor-less proteins are exported via this route, presumably because of their rapid folding kinetics.

II.3.1.2 The general secretion (Sec) pathway

Proteins supposed to exit the cytosol are synthesized as larger precursors containing an N-terminal signal peptide. During or shortly after their synthesis, these precursor proteins are recognized by specific targeting factors – the signal recognition particle (b-SRP) and its receptor FtsY. The bacterial SRP consists of the Ffh protein and the Ffs-RNA. Next, they are delivered to the so-called translocase holoenzyme in the membrane, which consists of the subunits SecA, SecY, SecE, SecG, SecDF and YajC (Figure 1). ATP and an electrochemical membrane potential are required as the energy source for efficient protein translocation. SecA as the key component couples the energy of ATP-hydrolysis to the movement of 20-30 amino acid residues of the translocating polypeptide chain across the membrane during each cycle. SecY and SecE form the protein-conducting channel. SecG and the SecDF/YajC complex increase the efficiency of translocation at the SecY/SecE core translocase by facilitating the SecA cycle. The signal peptide is cleaved from the precursor protein during or shortly after the translocation by specific signal peptidases on the *trans*-side of the membrane (Gellissen, 2002). With the help of specific folding factors, such as the PrsA lipoprotein, the mature protein resumes its final folded structure and is released into the supernatant after transport across the cell wall.

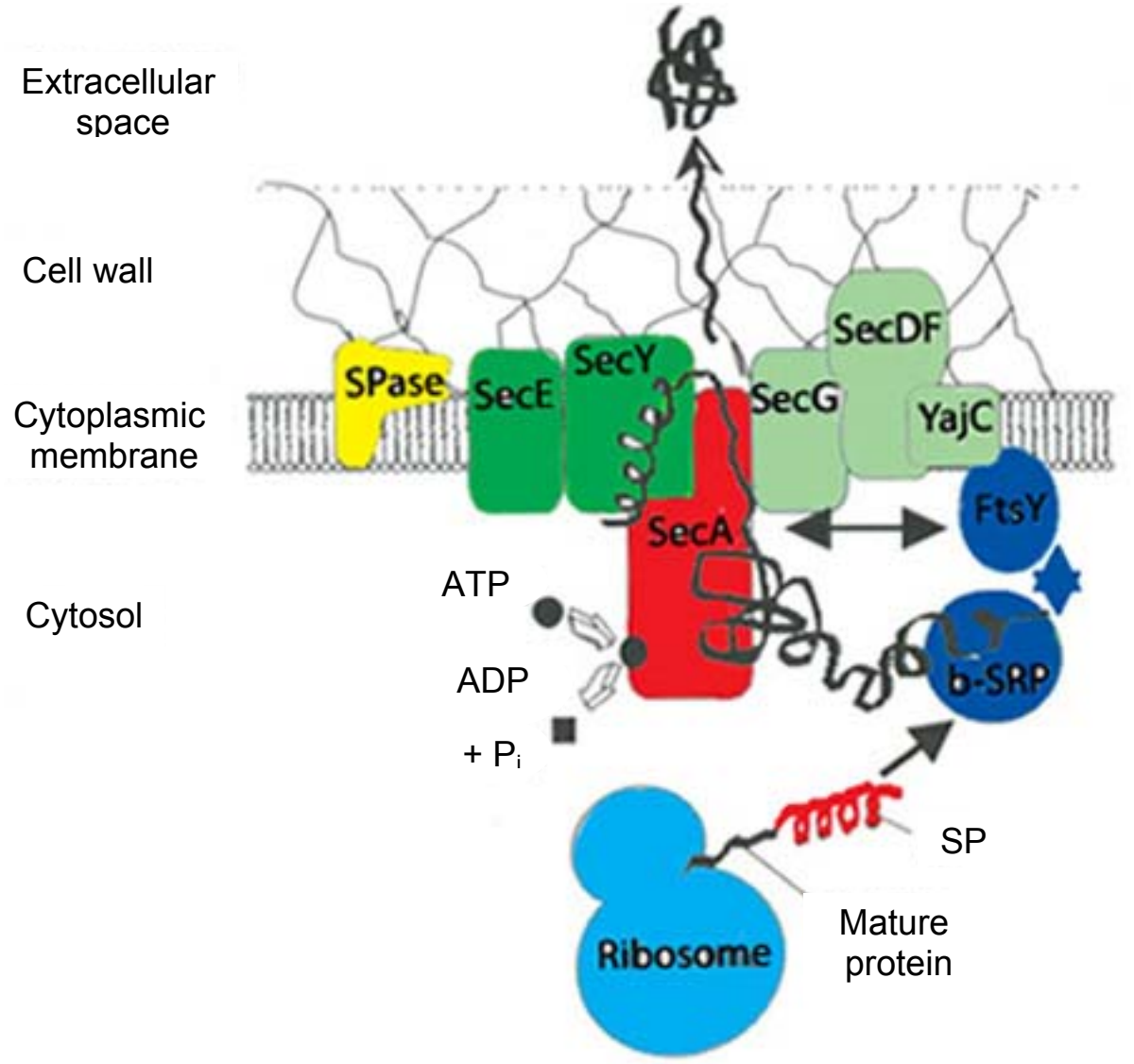

Figure 2. Sec protein export apparatus of Gram-positive bacteria (modified after Gellissen 2002).

II.3.1.3 The secretion signal in Gram-positive organisms

A signal peptide for Gram-positive bacteria is usually 14 to 25 amino acids long and consists of three defined domains, the amino (N-), hydrophobic (H-), and carboxy-terminal (C-) region. The N-region is rich in positively charged amino acids, and is followed by a hydrophobic region that tends to organize into an α-helical conformation when brought into contact with the membrane lipid phase. The C-terminal region is hydrophilic and contains the signal peptidase cleavage site, which in many cases corresponds to an Ala-X-Ala motif. Two classes of signal peptides are known, the general type I and the lipoprotein signal peptides (type II). In contrast to the large number of type I signal peptidases (*sip*S, *sip*T, *sip*V, *sip*U, *sip*W, *sip*P) in *B. subtilis* (Tjalsma *et al*., 1997) and only *sip*M is present in *B. megaterium* (Malten *et*

al., 2005a). Only one type II signal peptidase was identified in *B. subtilis* (Pragai *et al.*, 1997). Its signal peptides largely resemble the type I signal peptides, but within the C-region a so called lipoprotein box with a Leu-Ala-Gly-Cys consensus sequence is formed. The cysteine in this sequence is covalently linked to a lipid in the cytosolic membrane (Tokunaga *et al*., 1982). After lipomodification, the type II signal peptide is recognized by the signal peptidase II, Lsp, and cleaved (Tokunaga *et al*., 1982). Lsp is needed for the processing and sorting of lipoproteins of the outer membrane. The *B. subtilis lsp* null strain accumulates lipomodified proteins with signal peptide but also mature forms of PrsA, a lipoprotein involved in maturation of some secreted proteins (Tjalsma *et al*., 1999).

II.3.1.4 Bottlenecks in protein secretion

Several bottlenecks in the secretory pathway have been identified which dramatically decrease the amount of the desired product in the culture supernatant (Figure 3).

II.3.1.4.1 Inefficient translocation across the cytoplasmic membrane

For Sec-dependent protein export signal peptides and the translocase apparatus are the key players in protein secretion. Secretion of heterologous secretory proteins by Gram-positive bacteria can often be mediated by the authentic signal peptide (Lao & Wilson, 1996; Meens *et al.*, 1993)**.** However, it has also been observed in other cases that the natural signal peptide of a heterologous secretory protein functions only insufficient by the chosen Gram-positive host (Miller *et al.*, 1987). Although attempts have been made, it is still not predictable, whether a certain combination of a signal peptide and a foreign protein will result in membrane tanslocation and processing of the respective hybrid precursor. In *B. subtilis* numerous studies showed that certain signal peptides can support efficient export for a particular protein, but not for another one (Simonen & Palva, 1993)**.** Therefore, when the export of a desired heterologous protein fails, changing the signal peptides might be a promising strategy to pursue.

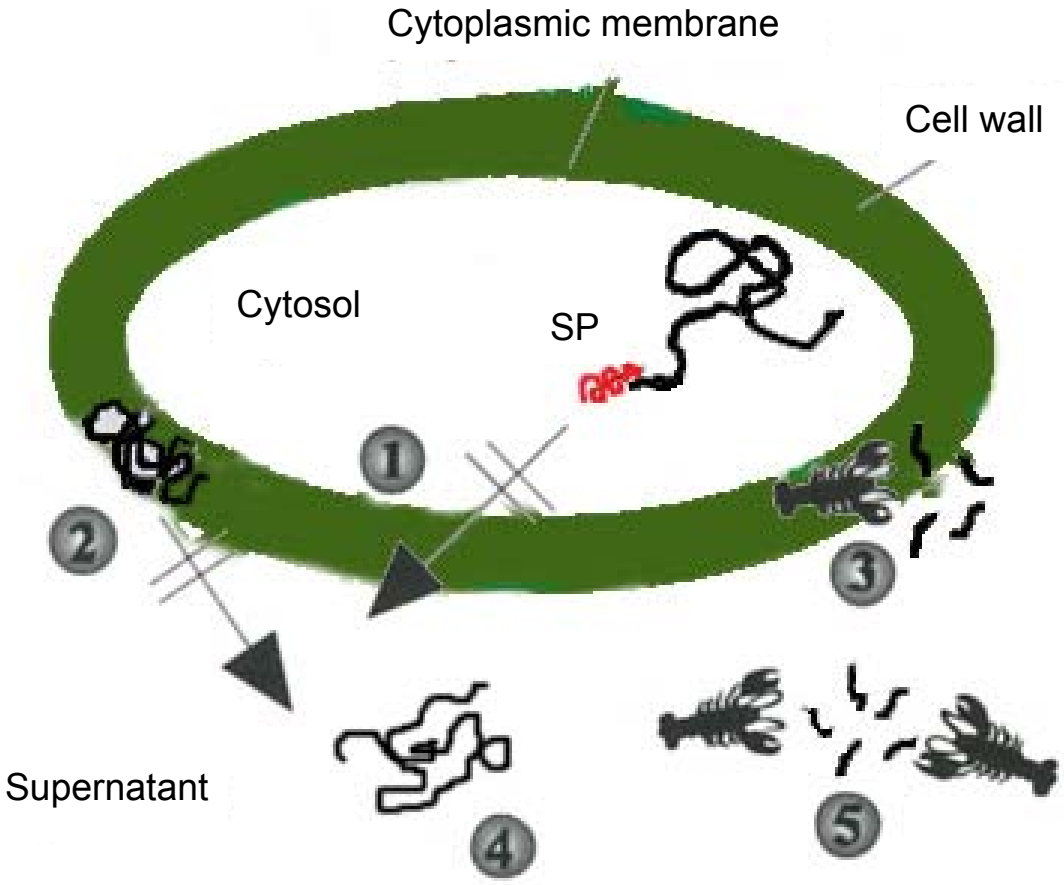

Figure 3. Bottlenecks observed during protein secretion (modified after Gellissen, 2002): (1) translocation across the cytoplasmic membrane; (2) release into the supernatant; (3) degradation by membrane- and/ or cell wall-associated proteases; (4) inefficient or wrong folding; (5) degradation by secreted proteases. SP: signal peptide.

II.3.1.4.2 Inefficient release into the supernatant

The thick cell wall of Gram-positive bacteria may act as a barrier for the secretion of heterologous proteins. It represents the final barrier of protein secretion before proteins are released into the culture medium. It is mainly composed of peptidoglycan and negatively charged polymers such as teichoic or teichuronic acid. Hence, for large proteins and proteins those possess positively charged amino acids residues at their surface, the cell wall acts as a molecular-sieve and ion-exchange absorber, respectively. As an example, human albumin is not released unless the peptidoglycan layer of the cell wall is destroyed, despite the fact that the protein is translocated across the *B. subtilis* plasma membrane (Saunders *et al*., 1987). In such cases, testing different Gram-positive bacteria or mutant strains with altered cell wall compositions (Thwaite *et al*., 2002) might improve the cell wall passage of trapped or

inefficiently released heterologous proteins. For example, cell wall reduced L-forms of Gram-positive bacteria can be used, however, these strains are very fragile to shear force (Gumpert & Hoischen, 1998). Moreover, a major factor important for the post-translocational protein folding is the presence of metal ions in the cell wall or environment. For example, α-amylase and levansucrase secreted by *B. licheniformis* and *B. subtilis* exhibit a weak affinity for calcium ions, and the presence of this divalent cation facilitates their folding (Haddaoui *et al.*, 1997; Leloup *et al*., 1997; Petit-Glatron *et al*., 1993).

II.3.1.4.3 Degradation by cell-associated and secreted protease

In addition to soluble proteases in the supernatant, proteases localized on the outer surface of the plasma membrane and/or in the cell wall of Gram-positive bacteria represent a severe bottleneck (Meens *et al*., 1997). A rapid degradation of newly secreted proteins is observed by cell wall-associated proteases, if the intrinsic folding of the target protein is inefficient (Jacobs *et al*., 1993; Meens *et al*., 1997). For example, an increased yield of secreted α-amylase was observed by a reduced expression of a serine protease WprA which is bound to the cell wall (Stephenson & Harwood, 1998). Therefore, identification and subsequent inactivation of these proteases may improve the performance of Gram-positive bacteria to secrete heterologous proteins.

II.3.1.4.4 Folding drawbacks

B. subtilis has intracellular and extracytoplamic molecular chaperones. The two intracellular major chaperone systems are: GroE and DnaK. PrsA is the only known extracellular folding factor in *B. subtilis* (Figure 4). Chaperones mediate protein folding, minimize aggregation, and can maintain pre-proteins in translocation-competent conformations (Yuan & Wong, 1995). Coproduction of both intracellular and extracytoplasmic molecular chaperones was used in a sequential manner to enhance the single-chain antibody production in *B. subtilis* WB800, which is deficient in eight proteases (Wu et al., 2002).

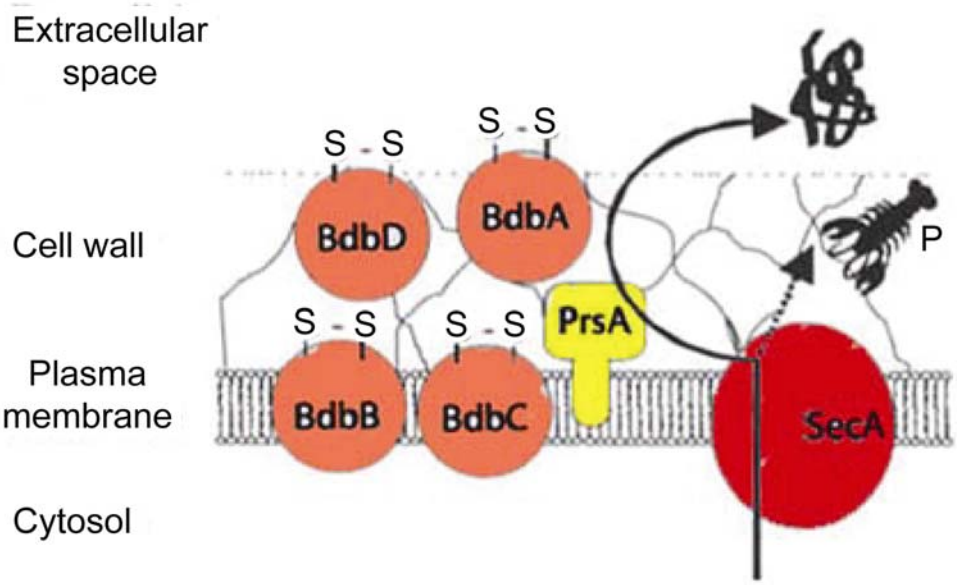

Figure 4. Late stages of Sec-dependent protein secretion in Gram-positive bacteria (modified after Gellissen,2002). The lipoprotein PrsA and the thiol disulfide oxido-reductases BdbABCD are factors assisting protein folding on the trans-side of the cytoplasma membrane.

A significant increase of single chain antibody production in the culture supernatant was only observed when the intracellular molecular chaperones were coproduced. No detectable antibody was observed in the culture supernatant, nor was it detected in the intracellular fraction with coproduction of extracellular PsrA alone. This suggests that these molecular chaperones may act in a sequential order, with intracellular molecular chaperones acting in the first stage. However, limiting the amount or the activity of PrsA results in decreased folding of exported proteins and their subsequent degradation (Jacobs *et al*., 1993). Especially under high-level protein secretion conditions, the amount of available PrsA is a serious bottleneck (Vitikainen *et al*., 2001). Consequently, the overproduction of PrsA as folding factor is a promising tool for improving the yields of correctly folded homologous and heterologous proteins.

The protein disulfide isomerase (thiol disulfide oxido-reductase) has been shown to assist in the folding pathway of disulfide-containing proteins both *in vitro* and *in vivo* (Noiva, 1994)**.** Disulfide bonds are crucial for the activity and stability of many proteins of biotechnological or pharmaceutical interest. Genes encoding four proteins with similarities to thiol disulfide oxido-reductases (BdbA, BdbB, BdbC, BdbD) have been identified in *B. subtilis* (Figure 4). However, proteins containing multiple disulfide bridges such as the human serum albumin or the human pancreatic alpha-

amylase were secreted only very poorly by *B. subtilis,* most likely due to impairments in disulfide bond formation (Bolhuis *et al*., 1999; Saunders *et al*., 1987)**.** Furthermore, not all Gram-positive bacteria seem to be equally capable in catalyzing the formation of disulfide bridges. Therefore, correct choice of the Gram-positive host organism is crucial, if the desired heterologous protein requires disulfide bonds for activity.

II.3.2 Model proteins

Previous investigations using *B. megaterium* focused on the production and the export of a dextransucrase (M_r = 180,000) from *Leuconostoc mesenteroides* (Malten *et al*., 2005b) and a levansucrase (M_r = 110,000) from *Lactobacillus reuteri* (Malten *et al., 2006).* Both enzymes were successfully produced at high levels in *B. megaterium* MS941 and WH320 and secreted into the extracellular medium in batch cultures (shake flasks and pH controlled bioreactors). However, significant export of the proteins into the medium was not detected under conditions of high cell density cultivation. Corresponding cultures were essentially operated at low growth rates to avoid oxygen starvation and production of overflow metabolites (Malten *et al.*, 2005b). This thesis investigates the production and export of *T. fusca* hydrolase TFH and *B. megaterium* penicillin G amidase (PGA) using *B. megaterium*.

II.3.2.1 *Thermobifida fusca* hydrolase TFH

TFH consists of 261 amino acids and has a relative molecular mass of 28,000 (Kleeberg *et al*., 2005). TFH possesses unique hydrolytic properties as it can act as esterase, lipase, cutinase, and is also able to cleave polyesters. In particular, TFH can degrade aromatic copolyesters such as poly (ethylene terephtalate) which are commonly regarded as not susceptible to microbial attack (Müller *et al*., 2005) (Figure 5). Due to these specific properties, TFH is of considerable interest for polyester degradation and textile fibre pre-treatment and modifications (Deckwer *et al*., 2001). Expression and production of TFH in *E. coli* was reported previously (Dresler *et al*., 2006).

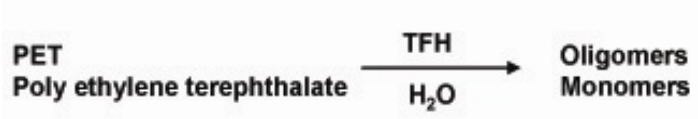

Figure 5. Degradation of PET by using TFH

II.3.2.2 Penicillin G amidase (PGA) of *B. megaterium* ATCC 14945

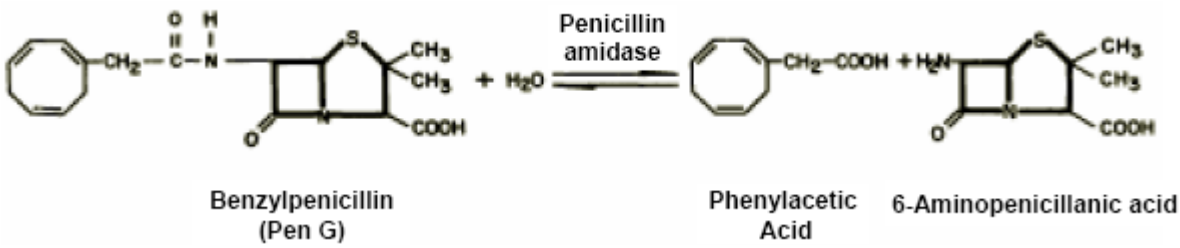

Figure 6. Outline of 6-APA production or Pen G synthesis. Instead of Pen G also other β – lactam derivatives can be produced using PGA in the reverse reaction.

The PGA consists of 802 amino acids and has the relative molecular mass of 90,000. After export, the protein is autocleaved into two subunits, α and β. The crystal structure of a similar *E. coli* enzyme was elucidated. It is a key enzyme in the industrial production of semi-synthetic β – lactam antibiotics. It hydrolyzes penicillin G yielding phenylacetic acid and 6-aminopenicillanic acid (6-APA) (Figure 6). The 6-APA provides the molecular core of all β-lactams to which D-amino acid derivatives can be substituted to create novel antibiotics, *e.g.* amoxicillin. PGA of *B. megaterium* is industrially used for the outlined reverse synthesis reaction due to its higher synthesis rate compared to *E. coli* PGA (Forney & Wong, 1989; Foster & Popham, 2001). In nature, its function is not yet confirmed. It has been suggested that PGA may degrade phenylacetylated compounds generating phenylacetic acid (PAA), which may be used by the organism as carbon source. The intensively studied *E. coli* PGA is predominantly exported into the periplasm (Valle *et al*., 1991). In contrast, using *B. megaterium* to secrete homologous PGA directly into the growth medium should facilitate its purification and consequently decrease the downstream processing and final production costs.

II.3.3 *B. megaterium* strains

In this work different *B. megaterium* strains were utilized for optimizing heterologous protein production. These are MS941, WH320, WH323, and YYBm1, which are all derived from the original strain DSM319. The protease deficient strain MS941 was created by inactivating the chromosomal neutral protease gene (*nprM*) by gene replacement (Wittchen & Meinhardt, 1995). *B. megaterium* WH320 was created by EMS mutagenesis. It has no detectable β-galactosidase activity whereas the wild-type strain shows low but measurable activity (Rygus *et al*., 1991). *B. megaterium* YYBm1 and WH323 are deficient in xylose utilization and were created based on

MS941 and WH320, respectively. This was done by the integration of either a *cml* antibiotic marker or the *lacZ* gene into the chromosomal *xylA* gene by homologous recombination (Rygus & Hillen, 1992).

II.3.4 The xylose inducible promoter system and carbon catabolite repression

The promoter system used in this thesis is the xylose-inducible promoter system of *B. megaterium* which was identified by Rygus and Hillen (Rygus & Hillen, 1991). Induction is mediated by a xylose-triggered release of the repressor XylR from the *xyl* operator (Dahl *et al*., 1994) (Figure 7). The promoter P_{xylA} is located upstream of an operon coding for the xylose isomerase XylA, the xylulokinase XylB, and the xylose permease XylT. XylA and XylB are necessary for the biochemical phosphorylation of xylose to xylose-5-phosphate. XylT can transport the xylose into the cell. The xylose repressor *xylR* gene is located upstream of *xylA* with opposite polarity. The promoter of *xylR* and *xylA* are overlapping. In the absence of xylose, XylR binds to the two tandem operator sequences located in P_{xylA} and prevents transcription of the *xylA* operon (Dahl *et al*., 1994; Gartner *et al*., 1988). In the presence of xylose, the sugar binds to the repressor XylR. Xylose binding results in a conformational change of XylR and its release from the promoter. This enables RNA polymerase to recognize the promoter and to begin transcription of the *xyl* operon. These genes for xylose utilization (*xyl*) are repressed in the absence of xylose and can be 200-fold induced in its presence (Rygus *et al*., 1991). However, the expression of the *xyl* operon is additionally repressed by glucose (Gartner *et al*., 1988; Rygus & Hillen, 1992) (Figure 7). The term carbon catabolite repression (CCR) is currently used to describe the general phenomenon in microorganisms whereby the presence of one carbon source in the medium can repress the expression of certain gene and operons. These gene products are involved in the utilization of alternative carbon source. It helps bacteria to use the best available carbon source efficiently. Glucose alters the activities of specific regulators, such as the catabolic gene activator protein (CAP) in enteric bacteria or the catabolite control protein (CcpA) in low-GC Gram-positive bacteria. The repression in *Bacilli* is mediated by a *cis*-acting DNA element, the catabolite responsive element (*cre*) which is located within the open reading frame of *xylA* (Hueck *et al*., 1994; Jacob *et al*., 1991; Kraus *et al*., 1994), and by the trans-acting protein CcpA (Henkin *et al*., 1991; Hueck *et al*., 1994). Furthermore, also the phosphoenolpyruvate-dependent glucose phosphotransferase system (PTS) is

involved in CCR. In the presence of glucose, a phosphor carrier protein HPr, which is phosphorylated at Ser-46, enhances the CcpA binding to the *cre* sequence (Deutscher *et al*., 1995). Xylose induced gene expression is repressed 13-fold in the presence of glucose. Finally, the XylR repressor contributes to glucose mediated repression since glucose-6-phosphate acts as an anti-inducer (Dahl *et al*., 1995). Hence, even when the *cre* element is deleted a residual repression by glucose is still present.

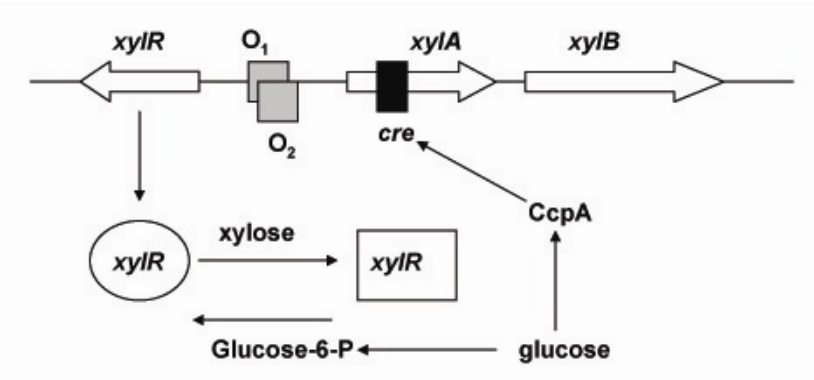

Figure 7. Organisation and regulation of the *B. megaterium xyl* operon (modified after Schmiedel *et al*. 1996). The *xyl* genes are indicated by open arrows. The *xyl* operators O1 and O2 and *cre* are shown as filled boxes. The *xylR* repressor is in the operator-binding form (circle) in the absence of xylose and turns to the non-binding state (square) when xylose acts as inducer. Glucose-6-phosphate acts as an anti-inducer and prevents xylose induction. Furthermore, glucose causes carbon catabolite repression by enhancing the CcpA binding to the *cre* sequence.

Using this xylose-inducible promoter system, the expression plasmid pWH1520 was developed by Rygus and Hillen (1991). Recombinant prokaryotic and eukaryotic proteins were successfully intracellularly produced using this plasmid (Burger *et al.*, 2003; Rygus & Hillen, 1991). Furthermore, in the promoter region of *xylA* the *cre* sequence was eliminated and an enhanced multicloning site (MCS) was inserted (Malten *et al.*, 2005b). The resulting plasmid pMM1520 allows simple cloning of target genes by the use of 15 different DNA restriction enzyme cleavage sites located in the new designed MCS.

II.3.5 Codon usage

In recent years it has become increasingly clear that codon usage plays a crucial role in the expression of recombinant genes (Carbone *et al*., 2003). The heterologous genes are often difficult to express outside their original context because their codons are rarely used in the desired host. The so called codon adaptation index (CAI) which was developed by Sharp and Li (Sharp & Li, 1987), is the prevailing empirical

measure of expressivity. Recently, an easy and rapid method named JCat (Java Codon Adaptation Tool) for the codon usage adaptation to most prokaryotic and some eukaryotic organisms of biotechnological interest was developed by Grote at the Institute of Microbiology (Grote *et al*., 2005). An optimal adapted gene shows a CAI value of 1. This method was also employed in this work for the adaptation of the TFH gene.

II.3.6 Metabolism and protein production

Protein production has to be involved as part of the cellular metabolism. Glycolysis, the pentose phosphate pathway, the reduced nicotinamide-adenine dinucleotide (NADH) and adenosine triphosphate (ATP) turnover, and tricarboxylic acid (TCA) cycle reactions are most likely limiting steps during foreign protein production. These pathways provide key precursors e.g. amino acids for the synthesis of macromolecules and energy for the cell. Hence, an understanding of their regulation and the determination of the amount of the available metabolites are important for the development and optimization of a protein production system.

II.3.6.1 Important metabolic pathways

The carbohydrate glucose is transported into the cell by a phosphoenolpyruvate-dependent sugar-phosphotransferase system (PTS) (Figure 8). The PTS-permeases couples transport and phosphorylation of glucose. The formed glucose-6-phosphate (G6P) can be directly used in glycolysis by the cell. The phosphate donor is phosphoenolpyruvate (PEP).

$$\text{Glucose + PEP} \xrightarrow{PTS} \text{G6P + Pyruvate}$$

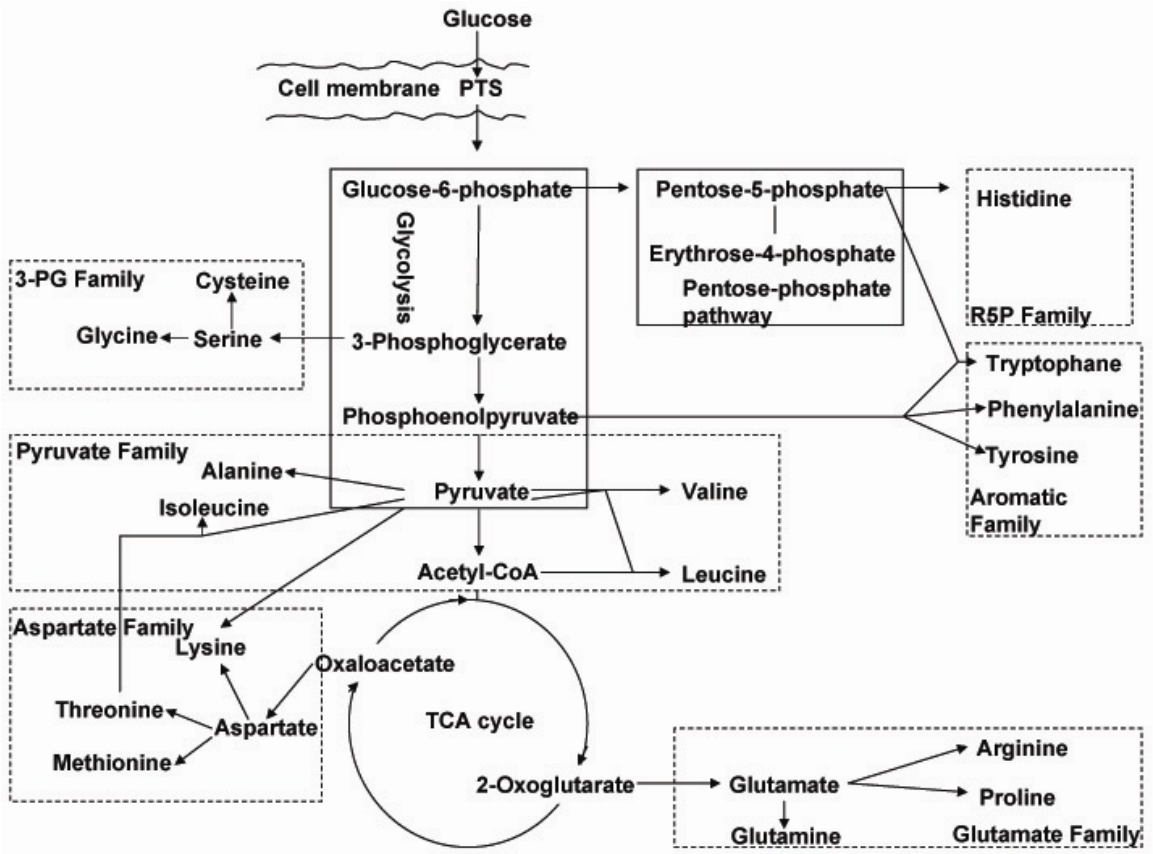

Figure 8. The central pathways of carbon dissimilation (glycolytic pathway, pentose phosphate pathway, and TCA cycle) and branch points at which metabolites are contributed to the amino acids biosynthesis.

II.3.6.1.1 Embden-Meyerhof-Parnas Pathway (Glycolysis)

The Embden-Meyerhof-Parnas (EMP) pathway involves ten enzyme-catalyzed steps which start with glucose and end with pyruvate. During the biosynthesis, dihydroxyacetone phosphate (DHAP), glyceraldehyde-3-phosphate (GAP), 3-phosphoglycerate (3-PG) and phosphoenolpyruvate are produced. Two moles of pyruvate, ATP and NADH are produced per mole of glucose passing through this pathway. Thus, the overall stoichiometry of the EMP pathway is:

$$\text{Glucose} + 2\text{ADP} + 2\text{Pi} + 2\ \text{NAD}^{+} \longrightarrow 2\ \text{Pyruvate} + 2\ \text{ATP} + 2\ \text{NADP} + 2\ \text{H}^{+}$$

II.3.6.1.2 Pentose phosphate pathway

A major function of the pentose phosphate pathway (PPP) is the supply of the cell with NADPH which in turn carries electrons to biosynthetic reactions. Moreover, another advantage is the production of ribose-5-phosphate (R5P) and erythrose-4-phosphate (E4P), as important precursors for purine and pyrimidine biosynthesis.

The PPP has two functions (Figure 9). In the irreversible oxidation part, one mole Ribulose-5-phosphate (Ru5P), one mole CO_2, and two moles NADPH are produced from one mole G6P.

$$G6P + 2NADP^+ + H_2O \longrightarrow Ru5P + 2\ NADPH + CO_2 + 2\ H^+$$

In the following reversible part, different phosphorylized sugars (R5P, E4P, Xu5P, F6P, and GAP) can be produced from Ru5P.

$$3\ Ru5P \longleftrightarrow R5P + 2\ Xu5P$$

$$R5P + 2\ Xu5P \longleftrightarrow 2F6P + GAP$$

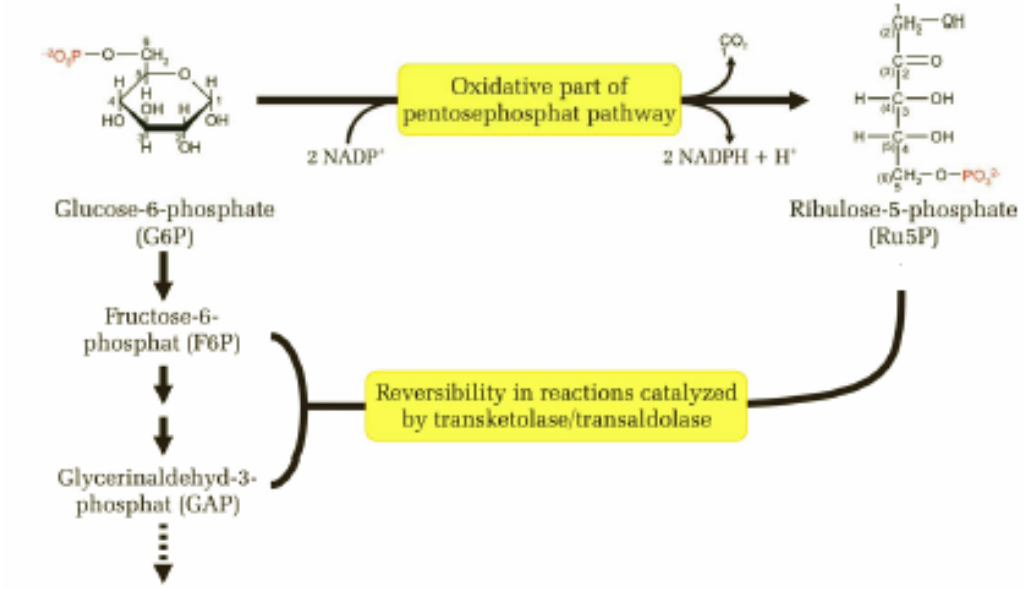

Figure 9. Pentose phosphate pathway

II.3.6.1.3 The tricarboxylic acid cycle

The tricarboxylic acid cycle (TCA) is characterized by the following overall reaction:

$$ACoA + 3\ NAD^+ + FAD + GDP + Pi \longrightarrow CoA + 2\ CO_2 + 3\ NADH + FADH_2 + GTP + 3\ H^+$$

The TCA cycle is not only the process for ATP production after a complete oxidation of the acetyl unit of acetyl-CoA but also provides the key precursors for biosynthesis. Acetyl-CoA, which is produced after glycolysis, provides acetyl units for the citric acid cycle. A complete oxidization to CO_2 of each acetyl group in the TCA cycle can transfer four pairs of electrons (three to NAD^+ and one to FAD). A proton gradient is then generated as electrons flow from the reduced forms of these carriers to O_2. This gradient is used to synthesize ATP by oxidative phosphorylation. Normally, water and carbon dioxide are the metabolic end products of respiration for most aerobic microorganisms. Under abnormal conditions like oxygen limitation, however, the

oxidation of the organic nutrient is not carried to completion, and intermediate products accumulate. Finally, they are released by the cell into the medium. This phenomenon is called “overflow metabolism”.

II.3.6.1.4 The Glyoxylate Cycle

$$2\ ACoA + NAD^+ + 2\ H_2O \longrightarrow succinate + 2\ CoA + NADH + 2\ H^+$$

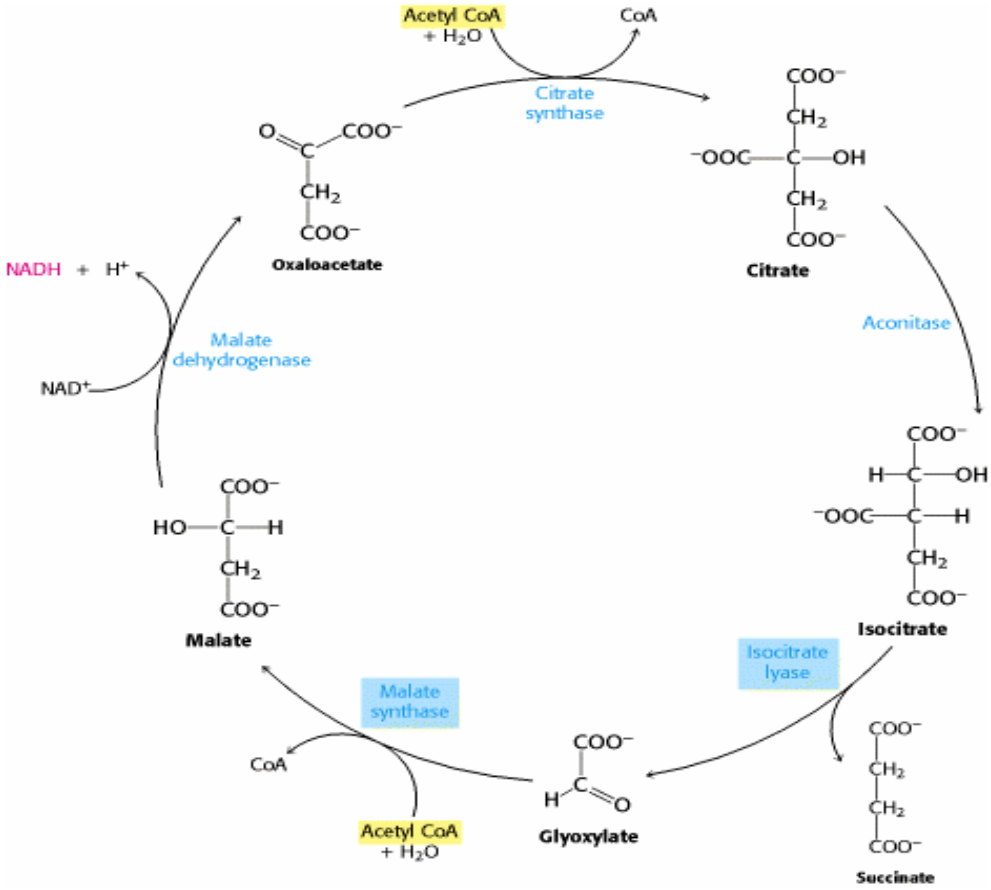

Figure 10. The glyoxylate pathway. The glyoxylate cycle allows plants and some microorganisms to grow on acetate because the cycle bypasses the decarboxylation steps of the citric acid cycle. The enzymes that permit the conversion of acetate into succinate - isocitrate lyase and malate - synthase are in a blue box.

In this study, one significant overflow metabolite was acetate which was produced during the cultivation. Many bacteria and plants are also able to grow on acetate that yield acetyl CoA. They utilize a metabolic pathway that converts two-carbon acetyl units into four-carbon units (succinate) for energy production and biosyntheses. Compared to the TCA the key differences are that this reaction sequence bypasses the two decarboxylation steps and those two molecules of acetyl CoA are needed per cycle (Figure 10).

II.3.6.1.5 Anaplerotic reactions and gluconeogenesis

Several so-called anaplerotic reactions serve to balance the TCA cycle when intermediates are drained off or supplied by connecting anabolic and catabolic pathways. Pyruvate carboxylase and malic enzyme are two examples. Pyruvate carboxylase (Diesterhaft & Freese, 1973) which is strongly activated by acetyl-CoA, helps replenish oxaloacetate by catalyzing the reaction:

$$\text{Pyruvate} + CO_2 + \text{ATP} \longrightarrow \text{Oxaloacetate} + \text{ADP} + \text{Pi}$$

Malic enzyme converts malate into pyruvate by catalyzing the reaction:

$$\text{Malate} + \text{NAD(P)}^+ \longleftrightarrow \text{Pyruvate} + CO_2 + \text{NAD(P)H} + H^+$$

In vivo the major direction of the reaction catalyzed by malic enzyme is the conversion of malate to pyruvate. These two reactions together with the conversion of oxaloacetate to malate by malate dehydrogenase are called futile cycle. Due to its interference with the energy and reduction equivalent metabolism, the activity of the futile cycle increases the overall flexibility of the cell to adapt its metabolism efficiently to environmental changes.

Glucose can be synthesized from noncarbohydrate precursors, such as pyruvate and lactic acid, in the process of gluconeogenesis. PEP carboxykinase is the major enzyme controlling the reverse path from oxaloacetate to PEP, which is apparently involved in the gluconeogenesis when the flow of carbon shifts from down to up. For example, during sporulation, the accumulated substrates like acetate, acetoin or pyruvate are utilized. However, a recent study on central metabolic flux of *B. megaterium* in continuous culture showed that the gluconeogenetic reaction converting oxaloacetate to PEP is not active (Fürch *et al.*, 2006).

II.3.6.1.6 Amino acids biosynthesis

General features of the biosynthesis pathways for the various amino acids are shown in Figure 8. For the purpose of classification, 6 families based on the common precursor are defined (

Table 1). In this study, alanine was placed in a separate 7th family because of its essential role for cell wall construction in Gram positive bacteria. Cysteine was arranged to the aspartate family as proposed by Michal *et al,* 1999 (Michal, 1999).

Table 1. Amino acids classification based on the common precursor

Precursors	**Amino acids**
Pentose-5-phosphate	Histidine
Phosphoenolpyruvate;PPP	tryptophane, phenylalanine, tyrosine
3-phosphoglycerate	serine, cysteine, glycine
pyruvate	alanine, isoleucine, valine, leucine
oxaloacetate	lysine, threonine, methionine, aspartate, asparagines
2-oxoglutarate	glutamate, glutamine, arginine, proline

II.3.6.2 Bacterial cultivation design

II.3.6.2.1 Exponential fed batch cultivation

In biotechnological production processes, the yield coefficient is a crucial parameter for the specific activity of heterologous or homologous proteins. In order to increase the volumetric productivity, large amount of cell mass are needed to be produced, in so called high cell density cultivations. By controlling the feed of a substrate as carbon or nitrogen source, substrate limitation, carbon catabolite repression, and oxygen limitation can be omitted so that the high cell densities are reached. Especially, the formation of overflow metabolites needs to be absent which can be accomplished by reducing the growth rate. The following formula has been used for the exponential feeding strategy (Yamane & Shimizu, 1984):

$$F = \frac{\mu \cdot (X \cdot V)_0 \cdot e^{\mu \cdot t_f}}{Y_{X/S} \cdot S_{f,const}}$$

Here μ [h^{-1}] is the growth rate, $(X \cdot V)_0$ [g] is the biomass at the start of fed batch operation, t_f [h] is the time elapsed since the start of feeding, $Y_{X/S}$ [g g^{-1}] is the biomass yield coefficient on glucose, and $S_{f,const}$ [g L^{-1}] is the glucose concentration of the feed solution. The initial biomass was calculated using the measured OD_{578nm} of a sample taken directly after the end of the batch phase.

II.3.6.2.2 Continuous cultivation

Considering the plasmid replication stability of *B. megaterium*, continuous cultivation has also been applied in this study because of its low cost, constant productivity, great control over concentration dependent factors and the quickly dilution of

overflow metabolites which may otherwise become inhibitory. During cultivation, the fresh medium flows into the fermentor continuously, and part of the medium in the reactor is withdrawn from the fermentor at the same flow rate of the inlet flow. Here, growth rate is equal to the dilution rate: $\mu = D$.

II.4 Objective of this work

The aim of this study was to optimize an established expression system of *B. megaterium* based on a *xylA* promoter system for protein production and secretion. For this purpose a systematical optimization process at the genetic and cultivation level had to be developed. The optimized system had to be tested for the secretion of two recombinant model proteins – the heterologous *T. fusca* hydrolase (chapter IV. 1) and the homologous penicillin G amidase from *B. megaterium* ATCC 14945 (chapter IV.2). Process limitations were expected from the codon usage of the heterologous gene, the xylose - mediated induction of the gene expression, the transport through the cell membrane, the medium composition and the cultivation strategy. Finally, an efficient protein purification strategy was desired after the production and secretion of the model protein into the growth medium. Reached yields of *B. megaterium* produced recombinant model proteins should be compared to analogous *E. coli* based production systems.

III Material and Methods

III.1 Chemicals and Instruments

III.1.1 Chemicals

Bio-Rad protein assay	Bio-Rad
Cell viability kit	BD Bioscience
Chelating sepharose FF	GE Healthcare
PD-10 column	GE Healthcare
Enzymes for molecular biological applications	GE Healthcare Genecraft MBI-Fermentas New England BioLabs Promega
Size standards for agarose gels:	
GeneRuler™ DNA Ladder Mix	MBI Fermentas
MassRuler™ DNA Ladder Mix	MBI Fermentas
Size standards for SDS-PAGE:	
Precision Plus protein standards	Bio-Rad
PageRuler prestained protein ladder	MBI Fermentas
Amino acids	Fluka
Yeast extract	Difco
pH-calibration buffer	Mettler-Toledo

Chemicals and reagents not specifically listed here were purchased from the following manufacturers: Difco, Fluka, GE Healthcare, Gerbu, Merck, Oxoid, Riedel-de-Häen, Roth and Sigma-Aldrich.

III.1.2 Instruments

Agarose gel Documentation	GelDoc	Bio-Rad
Agarose gel Electrophoresis	Agagel	Biometra
Bioreactor	Biostat B2	B. Braun
Blotting	Trans Blot apparatus (semi dry transfer cell)	Bio-Rad
Centrifuges	Labofuge 400R	Heraeus
	Centrifuge 5403	Eppendorf
	Biofuge fresco	Heraeus
	SpeedVac SPD 110B	Savant
	Sorvall RT6000B	Kendro Laboratory
cellulose membrane (10 kDa exclusion size*)*	Ultrafiltration membranes	Amicon
Dialysis cassette (10 kDa)	Slide-A-Lyzer	PIERCE
Exhaust gas analysis	S170 with OxorP and FIN	Maihak

	model	
Electroporation	Gene Pulser® II with Pulse Controller Plus	Bio-Rad
FACS	FACSCalibur	Benton Dickinson
Fluoroskan Ascent reader		Thermo Dreieich
Gel filtration instrument	FPLC system	Pharmacia Biotech
	HiLoad 26/60 Superdex 75 prepgrade	Amersham Biosciences
Gradient Cycler	Tgradient	Biometra
HPLC	Auto sampler 360	Kontron
	Pump 322	Kontron
	RI-detector ERC-7521	Erma
	Column oven K4	Techlab
	UV-VIS-detector 332	Kontron
	Aminex HPX-87H column	Bio-Rad
Microtiter plate incubator	Incubator 1000	Heidolph
	Titramax 1000	Heidolph
Microtiter plate	96-well microtiter plate	Nunc
Oxygen electrode	InPro 6100 with Teflon membrane	Mettler-Toledo
pH determination	pH-meter CG 822	Schott
pH electrode	405-DPAS-Sc-K8S/200	Mettler-Toledo
Purification	ProPur Sample IMAC Pack	Nunc
	Chelating Sepharose Fast Flow Gel	Amersham Bioscience
	Sartobind IDA 75, metal Chelate Membrane Adsorbers	Sartorius AG
SDS-PAGE	Mini Protean II	Bio-Rad
Shaker	Bench Top Shaker, TR	Infors AG HT
Spectrophotometer	Lambda 15	Perkin-Elmer
	Multiskan EX	Thermo Electron Corporation
Titration manager	PHM290, pH-STAT controller	Radiometer, Copenhagen
	Abu 901 AutoBurette	
Thermocycler	Tpersonal	Biometra
Thermomixer	Thermomixer compact	Eppendorf
Vacuum dry box	VT 5042 EK	Heraeus
Water bath shaker	Aquatron	Infors AG HT
Water purification	Milli-Q-System	Millipore

III.2 Plasmids and Strains

All the plasmids and strains used in this study have been listed in Table 2 with regard to the different model proteins.

Table 2. Strains and plasmids used in the study

Name	Description	Reference / source
Strains		
B. megaterium		
WH320	Mutant of DSM319, *lac*$^-$	Rygus and Hillen, 1992
WH323	Mutant of WH320, *lac*$^-$ *xyl*$^-$ φ(Δ*xylA1-spoVG-lacZ)*	Rygus and Hillen, 1992
MS941	Mutant of DSM319, Δ*nprM*	Wittchen and Meinhardt, 1995
YYBm1	Mutant of MS941, Δ*xyl,* Δ*nprM*	This study
E. coli		
DH10B	Strain for construction of plasmid and cloning of gene	Gibco Life Technologies
Plasmids used	**for TFH**	
pMM1520	Shuttle vector for cloning in *E. coli* (*Ap*^{r}) and gene expression under xylose control in *B. megaterium* (*Tc*^{r}); P_{xylA}-MCS	Malten *et al*., 2005a
pMM1522	pMM1520 derivative – vector for intracellular protein production; P_{xylA}- MCS	Malten *et al*., 2006
pMM1525	pMM1522 derivative – vector for protein secretion into the medium; P_{xylA}-SP_{lipA}-MCS	Malten *et al*., 2006
PCYTEXP1-OmpA-EGSE-6his-7	Vector for TFH production in *E. coli* - template for pYYBm1 and pYYBm3	Dresler *et al*., 2006
051392pPCR-Script	Codon optimized *tfh* with His_6-tag cloned into *Kpn*I/*Sac*I of pPCR-Script	This work
pYYBm1	*tfh* (830 bp) cloned into *Bgl*II/*NgoM*IV of pMM1525; P_{xyA}-SP_{lipA}-*tfh*	This work
pYYBm3	*tfh* (830 bp) cloned into *Bgl*II/*NgoM*IV of pMM1520; P_{xylA}-*tfh*	This work
pYYBm9	Codon optimized *tfh* with His_6-tag cloned into *Bgl*II/*Eag*I of pMM1525	This work
Plasmids used	**in PGA**	
pMM1520	Shuttle vector for cloning in *E. coli* (*Ap*^{r}) and gene expression under xylose control in *B. megaterium* (*Tc*^{r}); P_{xylA}-MCS	Malten *et al*., 2005a
pMM1525	pMM1522 derivative – vector for protein secretion into the medium; P_{xylA}-SP_{lipA}–MCS	Malten *et al*., 2006
pRBBm23	sp_{pga}- *pga* (2476 bp) (*B. megaterium* strain ATCC 14945) cloned into *Bsr*GI/*Sac*I of pMM1522; P_{xylA}-SP_{pga}-*pga*	This work

pRBBm48	*pga* (2407 bp) (*B. megaterium* strain ATCC 14945) without coding sequence for sp_{pga} cloned into *Bgl*II/*Eag*I of pMM1525; P_{xylA}-SP_{lipA}-*pga* with *Sfo*I-spacer	This work
pRBBm49	pRBBm48 without *Sfo*I-spacer; P_{xylA}-SP_{lipA}-*pga*	This work
pHBIntE	*B. megaterium* with temperature sensitive *ori*	Barg 2003
pHV33	Ap^r in *E. coli*, Cm^r in *B. subtilis*, Cm^r in *E. coli*, Tc^r in *E. coli*	Primrose *et al*, 1981
pYYBm4	pHBIntE derivative with *xylA* from *B. megaterium* genome sequence	This study
pYYBm8	pYYBm4 derivative –*xylA*'-*cmL*-'*xylA*	This study

III.3 Growth medium

III.3.1 Complex medium for *E. coli* and *B. megaterium* in shaking flask and batch cultivation

A high salt Luria Bertani (LB) medium containing 5 g L^{-1} NaCl, 5 g L^{-1} yeast extract, and 10 g L^{-1} tryptone from Bacto (Heidelberg, Germany) or Oxoid (Wesel, Germany) was used.

III.3.2 Semi-defined medium for *B. megaterium* in shaking flask, batch and continuous cultivation

Semi-defined A5 medium contained glucose 30 g L^{-1}, $(NH_4)_2SO_4$ 5 g L^{-1}, KH_2PO_4 2.2 g L^{-1}, $MgSO_4 \cdot 7H_2O$ 300 mg L^{-1}, yeast extract 1 g L^{-1} and trace element solution 2 mL L^{-1}. The trace element solution contained 40 g $MnCl_2 \cdot 4H_2O$, 53 g $CaCl_2 \cdot 2H_2O$, 2.5 g $FeSO_4 \cdot 7H_2O$, 2 g $(NH_4)_6Mo_7O_{24} \cdot 4H_2O$, and 2 g $CoCl_2 \cdot 6H_2O$ per liter. For continuous cultivation, feed 1 solution contained the same components as in the batch phase except that the glucose concentration was increased from 30 to 50 g L^{-1}. Furthermore, glucose concentration was increased to 100 g L^{-1} in the feed 2 solution. After induction, the feed solutions were changed to the ones also containing 5 g L^{-1} xylose.

III.3.3 Defined medium for *B. megaterium* in shaking flask and 96 well microtiter plate cultivation

The minimal medium containing 50 mM MOPSO (pH 7.0), 5 mM tricine (pH 7.0), 520 µM $MgCl_2 \cdot 6H_2O$, 276 µM K_2SO_4, 50 µM $FeSO_4 \cdot 7H_2O$, 2.5 mM $CaCl_2$, 100 µM $MnCl_2 \cdot 4H_2O$, 50 mM NaCl, 10 mM KCl, 37.4 mM NH_4Cl, 1.32 mM K_2HPO_4, 0.4 % (w/v) glucose, 1 mL L^{-1} trace element solution, and 1 mL L^{-1} vitamine solution with 0.5 % xylose as inducer. The trace element solution contained 3.7 mg $(NH4)_6Mo_7O_{24} \cdot 4H_2O$, 24.7 mg H_3BO_3, 7.1 mg $CoCl_2$, 2.5 mg $CuSO_4$, 15.8 mg $MnCl_2$, and 2.9 mg $ZnSO_4$ per liter. The vitamine solution consisted of 6 mg biotin, 20 mg niacin amid, 20 mg p-amino benzoate, 10 mg Ca-panthotenate, 100 mg pyridoxal/HCl, 20 mg folic acid, 50 mg riboflavin, 50 mg DL-6,8-thioctic acid and 10 mg thiamine dichloride per liter. For medium optimization, minimal medium was supplemented with different concentrations of amino acid solution. Unconcentrated amino acid solution (1 x) was defined as: 1 mg alanine, 1 mg argine, 100 µg aspartic acid, 100 µg cysteine, 4 mg glycine, 400 µg isoleucine, 200 µg leucine, 1 mg lysine, 500 µg methionine, 500 µg proline, 250 µg phenylalanine, 500 µg serine, 500 µg threonine, 160 µg glutamic acid, 100 µg tryptophane, 5.5 µg tyrosine, 800 µg valine, 400 µg histidine, 300 µg asparagine, and 300 µg glutamine per liter.

III.3.4 Solid medium

For solid media, 15 g agar per liter was added. For selection of *B. megaterium* deficient in xylose utilization M9 medium was used consisting of 500 mg NaCl, 1 g NH_4Cl, 3 g KH_2PO_4, 7.5 g $Na_2HPO_4 \cdot 2H_2O$, 4 g glucose, 120 mg $MgSO_4$, and 10 mg $CaCl_2$ per liter (Marsic *et al*., 1993).

Tetracycline was added to all media at a final concentration of 10 µg mL^{-1}.

III.4 Molecular biology techniques

III.4.1 Preparation of chromosomal DNA from *B. megaterium*

Up to 35 µg *B. megaterium* genomic DNA were used for amplifying genomic fragments by PCR. Therefore, 4 x 10^9 cells of an overnight culture were harvested by centrifugation (14,000 x g; 15 min; 4 °C) and suspended in 50 µL of lysozyme solution (10 µg mL^{-1} of lysozyme in 100 mM of sodium phosphate buffer, pH 7.0). Incubation occurred at 37 °C and 1,000 rpm (Thermomixer; Eppendorf; Germany) for

1 h. In an interval of 10 min, the cell suspension was intensively mixed to enhance cell lysis. After an additional incubation for 15 min at 99 °C, the cell debris was separated from the DNA by centrifugation (12,000 x g; 10 min; 4 °C). Before use, the DNA-supernatant was diluted 1: 10.

III.4.2 Preparation of plasmid DNA from *E. coli*

High quality plasmid DNA for protoplast transformation of *B. megaterium* was prepared from *E. coli* DH10B carrying the corresponding plasmid. Five mL of an overnight culture were harvested (14,000 x g; 2 min). The cells were suspended in 300 µL of buffer P1. After addition of 300 µL of buffer P2, the tube was inverted 6 times and incubated for 2 min. Then 300 µL of buffer P3 were added and mixed carefully by 6 times inverting the tube. Afterwards, the samples were centrifuged for 30 min at 14,000 x g. The supernatant was gently mixed with 600 µL isopropanol to precipitate the plasmid DNA followed by centrifugation. Recovered DNA was washed with 400 µL of 70 % (v/v) ethanol. Finally, the DNA precipitate was dried and dissolved in 50 µL of H_2O_{deion}.

All steps were performed at RT.

Solution for Plasmid DNA Preparation:

Buffer P1	Tris-HCl (pH 8.0)	50.0	mM
	EDTA	10.0	mM
	RNase A	100.0	mg L^{-1}
	dissolved in H_2O_{deion}		
Buffer P2	NaOH	200.0	mM
	SDS	1.0	% (w/v)
	dissolved in H_2O_{deion}		
Buffer P3 (pH 5.5)	CH_3COOH	3.0	M
	dissolved in H_2O_{deion}		

III.4.3 Determination of DNA concentration

For determination of the prepared plasmid DNA concentration, the plasmid was enzymatically linearized and visualized on an agarose gel (see III.4.4). Using the Quantity One software for gel documentation (Bio-Rad; Munich; Germany), the concentration of the respective band in the agarose gel was determined in comparison to two bands of known concentration.

III.4.4 Agarose gel electrophoresis

For separation of DNA fragments, 0.7 to 2.5 % (w/v) agarose gel electrophoresis was performed. The DNA samples were mixed with 6 x DNA loading dye to facilitate loading and to indicate the progress of the samples in the gel. GeneRuler™ DNA Ladder Mix or MassRuler™ DNA Ladder Mix (MBI Fermentas; St. Leon-Rot; Germany) were used as size standards according to the manufacturer's instructions. Depending on the size of the gel, a voltage of 80 – 100 V was applied. The DNA fragments migrate towards the anode with a velocity that is proportional to the negative logarithm of their length. After electrophoresis, gels were incubated in an ethidium bromide solution for 30 min and briefly rinsed with H_2O_{deion}. The DNA was detected via its fluorescence under UV light (λ =312 nm)

Solutions and Marker for Agarose Gel Electrophoresis:

TAE buffer (pH 8.0)	Tris-acetate	40.0	mM
	EDTA	1.0	mM
	dissolved in H_2O_{deion}		
6 x DNA loading dye	Bromophenol blue	350.0	µM
	Xylene cyanol FF	450.0	µM
	Glycerol	50.0	% (w/v)
	dissolved in H_2O_{deion}		
Ethidium bromide solution	Ethidium bromide	0.1	% (w/v)
	dissolved in H_2O_{deion}		

GeneRuler DNA Ladder Mix (MBI Fermentas; St. Leon-Rot; Germany) contains the following fragments (given in base pairs): 10,000; 8,000; 6,000; 5,000; 4,000; 3,500; 3,000; 2,500; 2,000; 1,500; 1,200; 1,031; 900; 800; 700; 600; 500; 400; 300; 200; 100.

MassRuler DNA Ladder Mix (MBI Fermentas; St. Leon-Rot; Germany) contains the following fragments (given in base pairs): 10,000; 8,000; 6,000; 5,000; 4,000; 3,000; 2,500; 2,000; 1,500; 1,031; 900; 800; 700; 600; 500; 400; 300; 200; 100; 80.

III.4.5 Amplification of DNA by Polymerase Chain Reaction (PCR)

For amplification of DNA by PCR, oligonucleotide primers for each DNA fragment of interest were designed. Recognition sequences for restriction endonucleases were inserted via these primers at both ends of the corresponding fragment. Primers were

purchased from MWG Biotech AG (Ebersberg; Germany) or Biomers.net GmbH (Ulm; Germany). For amplification of the DNA of interest, PCR reactions of a total volume of 20 µL were prepared. For amplification of smaller DNA fragments, the BioTherm® *Taq* polymerase (Genecraft; Lüdinghausen; Germany) was used, which may create one mismatch in 1,000 base pairs.

Concentrations used in the PCR reaction:

template DNA	10 pg (plasmid) / 200 ng (genomic DNA)
forward primer	20 pmol
reverse primer	20 pmol
dNTPs (10 mM)	200 µM
Taq polymerase	1 U
10 x reaction buffer	2 µL
H_2O_{deion}	ad 20 µL

The lid of the PCR-machine was pre-heated to 10 °C over the denaturation temperature. Before insertion of the reaction tubes, the PCR-machine was pre-heated to the denaturation temperature. After an initial DNA denaturation step, a cycle consisting of the three steps denaturation, primer annealing and primer elongation was repeated 30 times. The reaction was terminated every cycle with a final elongation step. Time and temperature for denaturation, time of annealing and elongation temperature remained unchanged for each reaction. Annealing temperature (T_m) depended on oligonucleotide length and G+C content. It was calculated as follows:

$$\mathbf{T_m\ [°C] = 69.3 + 0.41\ (\%\ G+C) - 650/\mathit{n}}$$

% G+C represents the G+C content in the primer; n represents the number of nucleotides.

III.4.6 Digestion of DNA with restriction endonucleases

Digestion of DNA was carried out using restriction endonucleases purchased from New England BioLabs (Ipswich; USA) or MBI Fermentas (St. Leon-Rot; Germany). Reaction buffers, concentrations of enzymes and DNA as well as incubation temperatures were chosen according to the manufacturer's instructions. The digestion was allowed to proceed for up to 16 h and was, if possible, followed by heat inactivation of the restriction endonucleases (20 min; 65 °C or 80 °C).

III.4.7 Purification of PCR products and plasmid fragments

After PCR or plasmid digestion, an aliquot of the reaction mixture was analyzed by agarose gel electrophoresis (section III.4.4). If only one DNA fragment was detected in the gel, the entire sample was subjected to purification with the QIAquick PCR purification kit (QIAgen; Hilden; Germany). If more than one DNA fragment was visible in the gel, the entire reaction mixture was separated electrophoretically. The DNA was visualised using the GelStar® Nucleic Acid Gel Stain (Biozym; Hessisch Oldendorf; Germany) on a blue light detector (Flu-O-blu) and a yellow filter. This avoids damaging the DNA by UV-light as used in DNA detection employing ethidium bromide. The DNA fragment of interest was excised from the gel and purified using the QIAquick Gel Extraction Kit (QIAgen; Hilden; Germany).

All kits were used according to the manufacturer's instructions using H_2O_{deion} for elution of the DNA from the columns.

III.4.8 Ligation of DNA

To avoid re-circularisation of a previously digested DNA vector, the 5' phosphate groups of the linearised vector were removed prior to the ligation reaction. The dephosphorylation was achieved by adding 1 unit of calf intestinal alkaline phosphatase (New England BioLabs; Ipswich; USA) per µg of DNA to the sample immediately after restriction. An incubation at 37 °C for 3 h followed. The DNA was purified using the PCR purification kit (QIAgen; Hilden; Germany) following the manufacturer's instructions.

In one ligation reaction, 25 – 200 ng of plasmid DNA were used. Insert DNA was added in excess to a final volume of 8.5 µL. Insert to vector ratio with regard to molar concentrations was 2 : 1 to 10 : 1. After incubation of the DNA for 5 min at 45 °C, the reaction buffer supplied by the manufacturer and 200 U of T4 DNA ligase (New England BioLabs; Ipswich; USA) were added. The reaction was performed at 25 °C for 20 min followed by 16 °C for 16 h. After that, the ligation reaction was dialysed against H_2O_{deion} for 1 h at RT and was used for electroporation (section III.4.9.1) of competent *E. coli* cells.

III.4.9 Transformation of Bacteria

III.4.9.1 Electroporation of *Escherichia coli* cells

Starting out from an individual *E. coli* DH10B colony, a 5 mL overnight culture was inoculated. This culture was used to inoculate 500 mL of LB medium. The bacteria were incubated at 37 °C and 200 rpm in baffled flasks until the culture reached an OD_{578nm} of 0.6. After cooling the cultures in ice water for 15 min, the cells were harvested by centrifugation (4,500 x g; 15 min; 4 °C). The cells were washed twice with 20 mL of ice-cold water (2,600 x g; 8 min; 4 °C) and suspended in 20 mL of 10 % (v/v) glycerol. After a further centrifugation step (2,600 x g; 8 min; 4 °C), the obtained cells were dissolved in 1 mL of 10 % (w/v) glycerol. Competent cells were either used directly for transformation experiments or were shock frozen and stored at - 80 °C.

The competent *E. coli* cells were transformed with dialysed ligation reactions (section II.5.10) by electroporation using a Gene Pulser™ apparatus (Bio-Rad; Munich; Germany). For this purpose, 20 – 200 ng of plasmid DNA were mixed with 40 µL of prepared competent *E. coli* cells in a 2 mm electroporation cuvette. The electroporation was carried out in the Gene Pulser™ at settings of 2.5 kV at 25 µF and 200 Ω. The transformed cells were regenerated for 1 h by incubation in 500 µL of LB medium at 37 °C and smooth shaking. The transformation volume was streaked out onto a LB medium agar plate with appropriate antibiotics. The plate was incubated overnight at 37 °C.

III.4.9.2 Protoplast transformation of *Bacillus megaterium* cells

Starting out from an individual *B. megaterium* colony, an overnight culture was inoculated. One mL aliquot of this culture was used to inoculate 50 mL of LB medium. The culture was incubated at 37 °C and 250 rpm in a baffled flask until it reached an OD_{578nm} of 1.0. Cells were separated from the growth medium by centrifugation (2,600 x g; 15 min; 4 °C) and suspended in 5 mL of freshly prepared SMMP. After adding 100 µL of freshly prepared sterile lysozyme solution (100 µg of lysozyme mL^{-1} in SMMP), the protoplast suspension was incubated at 37 °C for 30 min and smooth shaking. Forming of protoplasts was controlled microscopically. After up to 80 % of the rod shaped bacterium cells formed coccoid protoplasts, the protoplasts were harvested (1,300 x g; 10 min; RT). The supernatant was decanted carefully and the protoplasts were suspended in 5 mL of SMMP. After a second washing step, the

protoplasts were suspended in 5 mL of SMMP and 750 µL of 87 % (w/v) glycerol were added. They were either used directly for transformation or were frozen and stored in portions of 500 µL at - 80 °C for a period of not longer than two months.

Before starting the transformation, protoplasts were tested for viability. Therefore, a 500 µL aliquot of protoplast solution was mixed with 2.5 mL of CR5-top agar as described below and was streaked out on a LB medium agar plate without antibiotics. After incubation overnight, a thick film of *B. megaterium* cells should be seen.

For transformation of the protoplasts, 5 µg of plasmid DNA were dissolved in 10 µL of SMMP for 20 min at 37 °C. A 500 µL aliquot of protoplasts suspension was mixed with the DNA and was added into 1.5 mL of PEG-P solution. After incubation for 2 min at RT, 5 mL of SMMP were added and the reaction was mixed gently. The protoplasts were harvested by centrifugation (1,300 x g; 10 min; RT), carefully suspended in 500 µL of SMMP and incubated at 30 °C for 45 min without shaking followed by 45 min of smooth shaking at 300 rpm (Thermomixer compact; Eppendorf; Germany). The regenerated protoplasts were mixed with 2.5 mL of 42 °C CR5-top agar and poured onto a pre-heated LB medium agar plate containing the required antibiotics. For outgrowth, the plates were incubated at 30 °C for up to 24 h. Colonies seen after this period of incubation were streaked out on new LB medium agar plates containing the required antibiotics.

Solutions for Protoplast Transformation:

SMMP	2 x AB3 and 2 x SMM; mixed 1 : 1		
2 x AB3	Antibiotic medium No. 3 (Difco)	35.0	g L^{-1}
2 x SMM (pH 6.5)	Malic acid	40.0	mM
	$MgCl_2 \cdot H_2O$	40.0	mM
	NaOH	80.0	mM
	Sucrose	1.0	M
	dissolved in H_2O_{deion}, sterilized by filtration		
PEG-P solution	PEG 6000	40.0	% (w/v)
	dissolved in 1 x SMM (pH 6.5)		
cR5 top-agar (2.5 mL)	Solution A	1.25	mL
	Solution B	713.0	µL
	8 x cR5-salts	288.0	µL
	L-proline (12 % (w/v))	125.0	µL
	D-glucose (20 % (w/v))	125.0	µL
Solution A (pH 7.3)	Sucrose	602.0	mM
	MOPS	58.0	mM
	NaOH	30.0	mM
	dissolved in H_2O_{deion}, sterilised by filtration		

Solution B	Agar agar	4.0 % (w/v)
	Casamino acids	0.2 % (v/w)
	Yeast extract	10.0 % (v/w)
	dissolved in H_2O_{deion}	
8 x cR5-salts	K_2SO_4	11.0 mM
	$MgCl_2$ x 6 H_2O	394.0 mM
	KH_2PO_4	3.0 mM
	$CaCl_2$	159.0 mM
	dissolved in H_2O_{deion}	

III.4.10 Plasmids construction

III.4.10.1 Plasmids for heterologous TFH protein production

All strains and plasmids used in the study of TFH are listed in (Table 2). Employed molecular biology methods were described. The wild type *tfh* gene was amplified by PCR from plasmid pCYTEXP1-OmpA-EGSE-6his-7 (Dresler *et al.*, 2006) using the primers bta1-1_for and bta1-1_rev. The resulting PCR product and the target plasmids pMM1522 and pMM1525 (Malten *et al*., 2006) were cut with the restriction enzymes *Bgl*II/*NgoM*IV. The PCR product and the plasmid were ligated and transformed into *E. coli* DH10B cells. Single colonies were grown in Luria-Bertani (LB) medium with 100 µg mL^{-1} ampicillin. Positive clones identified via restriction digestion of plasmid preparations were verified by DNA sequencing (MWG Biotech, Ebersberg, Germany). Using this strategy, the plasmids pYYBm3 and pYYBm1 were constructed from the parental plasmids pMM1522 and pMM1525, respectively.

Primers

bta1-1_for 5’-ggg*aagatc*ttggccaacccctacgagc-3’
bta1-1_rev 5’-gact*gccggcc*tagaacgggcaggtggagc-3’

Next, the *tfh* codon usage was optimized using the program JCat (Grote *et al*., 2005), a coding region for a C-terminal His_6-tag added, and the corresponding gene sequences were synthesized by Geneart GmbH (Regensburg; Germany). This optimized *tfh* gene was subcloned into pMM1525 via introduced *Bgl*II/*Eag*I restriction sites from the plasmid 051392pPCR-Script (Geneart GmbH; Regensburg; Germany). After cutting out a part of the linker region with *Sfo*I pYYBm9 was generated (Figure 11). Constructed plasmids were transformed into *B. megaterium* strains MS941 and WH323 by protoplast transformation (III.4.9.2). The used strains are derivatives of the wild type DSM319. MS941 has a defined deletion of the gene for the major

extracellular protease NprM (Wittchen and Meinhardt, 1995). WH323 is derived from WH320 (a chemically obtained β-galactosidase deficient mutant of DSM319) by inserting the *E. coli lacZ* gene in the *xylA* gene (Rygus and Hillen, 1992). Hence, WH323 (Δ*xylA*) does not consume xylose after induction (Table 2).

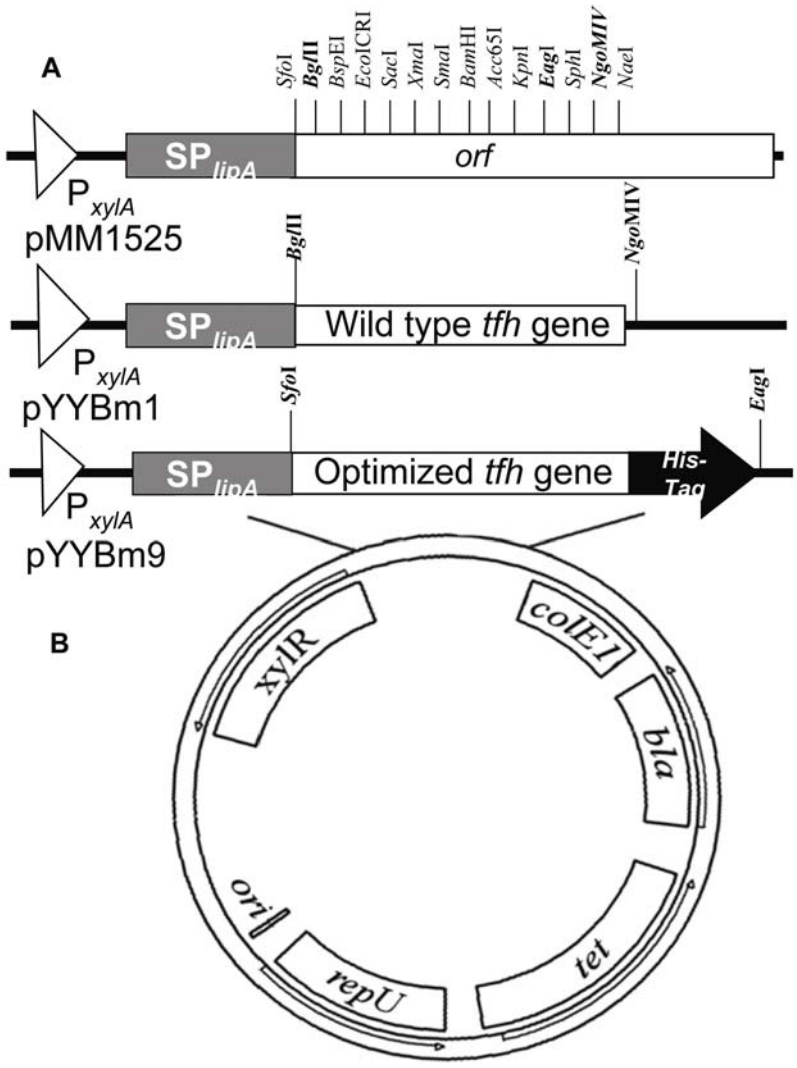

Figure 11. (A) Structure of the employed plasmids: the promoter P_{xylA} is the xylose inducible *B. megaterium xylA* promoter, the signal peptide (SP) is from the *B. megaterium* extracellular lipase LipA. The open reading frame carries the multiple cloning site for the in frame insertion of target genes (*orf*), synthetic or wild type *tfh* gene and His-tag. Both genes were cloned into the vector pMM1525 via introduced *Bgl*II/*Eag*I restriction sites in pYYBm9 and *Bgl*II/*NgoM*IV sites in pYYBm1. In order to place the *tfh* gene directly downstream of the signal peptide SP_{lipA} encoding sequence in pMM1525 a *Sfo*I restriction site was inserted upstream of the *tfh* gene, allowing the removal of a linker between sp_{lipA} and the *tfh* gene. (B) Details of expression vector pMM1525: *xylR* is the gene for the xylose repressor. Elements for plasmid replication in *Bacillus sp*. are the origin of plasmid replication (*ori*), a gene essential for plasmid replication (*repU*) and the *tet* resistance gene. Elements for plasmid replication in *E. coli* are the origin of replication *colE1* and the ampicillin resistance gene *bla*.

III.4.10.2 Plasmids for homologous recombinant PGA protein production

All strains and plasmids used in the study of PGA are listed in Table 1. The complete wild type *pga* gene encoding also its native signal peptide was amplified by PCR from *B. megaterium* ATCC 14945 using the primers pga_23_for and pga_23_rev and was then cloned into the *BsrG*I/*Sac*I site of pMM1522 (Malten *et al*., 2006). The wild type *pga* gene was combined with the signal peptide of LipA encoded on pMM1525 by cloning the amplified fragment from *B. megaterium* ATCC 14945 using the primers

pga_49_for and pga_49_rev into *Bgl*II/*Eag*I of pMM1525 (Malten *et al*., 2006). Positive clones selected with 100 µg mL^{-1} ampicillin were identified by restriction digestion of plasmid preparations and verified by sequencing (MWG Biotech; Ebersberg; Germany). From the parental plasmids pMM1522 and pMM1525 the plasmids pRBBm23 and pRBBm49 were constructed, respectively.

Primers (introduced restriction endonuclease size are given in italics)

pga_23_for	tacata*gtaca*atgaagacgaagtggctaatatca
pga _23_rev	Tatca*gagctc*atcaatagtataggctctttatgc
pga_49_for	ttatt*agatctt*ggcgcc*c*ggggaggataagaatgaagg
pac_49_rev	tatca*cggcca*gcataaagagcctatactattgat

III.4.11 Xylose utilization deficient *Bacillus megaterium* strain development

The xylose deficient strain was developed from *B. megaterium* MS941 by integration of the *cat* antibiotic gene into the chromosomal *xylA* gene via a double crossover (Rygus & Hillen, 1992). The *xylA* gene was amplified by PCR from *B. megaterium* MS941 using the primers xylA_as and xylA_s and then cloned into the *Sac*I/*Sac*I site of pHBIntE (Barg, 2003). The resulting plasmid was called pYYBm4 (Table 2). The plasmid contained a temperature sensitive origin of replication. The *cat* marker gene was amplified by PCR from pHV33 (Primrose & Ehrlich, 1981) using the primers cml_as and cml_s and cloned into *Nde*I/*Xba*I of pYYBm4. The resulting plasmid was called pYYBm8 (Table 2). Constructed plasmids were transformed in *B. megaterium* strain MS941 by protoplast transformation at 30 °C (Barg *et al*., 2005). The double crossover was achieved by dividing the process into two easily screenable steps: (i) single-crossover recombination by cultivation at 42 °C and addition of 3 mg L^{-1} chloramphenicol; (ii) excision of the carrier replicon by screening for a colony deficient in xylose utilization. The colony after the second crossover was selected on chloramphenicol containing M9 agar plates with glucose or xylose as carbon source. *B. megaterium* strain YYBm1 grew on the chloramphenicol agar plate and only used glucose as carbon source.

Primers

xylA_as	ttcatgagctcttaagtgttgttcttgtgtcattcc
xylA_s	gcaacgagctcagcagtgtatttacttgagagg
cmL_as	tgattcatatggtcgacaaaaagaaggatatggatctggagc
cmL_s	acacctctagagtcgacacaaacgaaaattggataaagtggg
cmL_for	ggttatactaaaagtcgtttgttgg
cmL_rev	cgggtgataaactcaaatacagc

xylB_rev	cctattgattcctgctaattgg
xylR_for	cggtgcaaatctttgatattcc
xylR_for'	cgttaagatagtcgactcc
xylB_rev'	ccacaataacttaggaaga
putative4_for	ccattatatattctggggcg
ery_s	cgtcaattcctgcatgttttaagg
ery_antis	ccaaatcggctcaggaaaag

III.5 Cultivation

III.5.1 The 96-well microtiter plate and shaking flask cultivation

For the inoculum *B. megaterium* was cultivated in 50 mL of the adequate medium at 37 °C and 120 rpm for 16 h. For microtiter plate cultivation 200 µL culture medium with an adjusted initial optical density of 0.1 to 0.2 was transferred to a 96-well microtiter plate except the outer wells which were filled with water due to the evaporation problem. The plate was cultivated in the Fluoroskan Ascent fluorescence reader (Thermo electron corporation; Dreieich; Germany) at 37 °C and 1020 rpm with an orbital shaking diameter of 1 mm as described previously (John *et al*., 2003).

For shaking flask cultivation *B. megaterium* strains were grown in 100 mL LB or semi-defined A5 medium at 37 °C and 250 rpm. Gene expression was induced by addition of 5 g L^{-1} xylose to the growth medium, when the culture reached an optical density of 0.4 measured at 578 nm.

III.5.2 Bioreactor cultivation

III.5.2.1 Bioreactor

Table 3. The parameters of two bioreactors

Geometrical Parameter	**B1**	**B2**	
Total volume	1.5	3	L
Working volume	1	2	L
Inside diameter D	108	130	mm
Total height H	205	285	mm
Fill height h	86-173	104-208	mm
Agitator diameter d	45	53	mm
Agitator height h_R	7	10	mm
h/D	0.8-1.6	0.8-1.6	
d/D	0.41	0.41	

In this study bioreactors from the Biostat B Reihe (Satorius BBI Systems; Melsungen; Germany) were utilized. Batch and Fed batch cultivation were carried out in Biostat

B2 and continuous cultivation in Biostat B1. The parameters of these two bioreactors are summarized in the Table 3.

III.5.2.2 Instrument configuration

A schematic bioreactor setup is shown in Figure 12. The bioreactor was controlled with its Biostat Digital Control Unit (DCU). A constant temperature for the cultivation was kept by a water filled double jacket connected to an external heating unit. Base and acid were fed into the bioreactor by the integrated DCU pumps after calibration. The consumption of base was measured by a balance in order to calculate the volume at the end of the cultivation. This was not required for the acid consumption because of the production of acids as metabolites during the cultivation. After the cooling process, in a 2 °C extern thermostat, the exhaust gas was divided into two parts. One part as waste was directly bleeded off in a flask with a constant water surface. Another part was analyzed in an exhaust gas analyzer. The connecting tubes in the pilot-plant were made of silicon, except the ones between the bioreactor and exhaust gas analyzer were gas-proof.

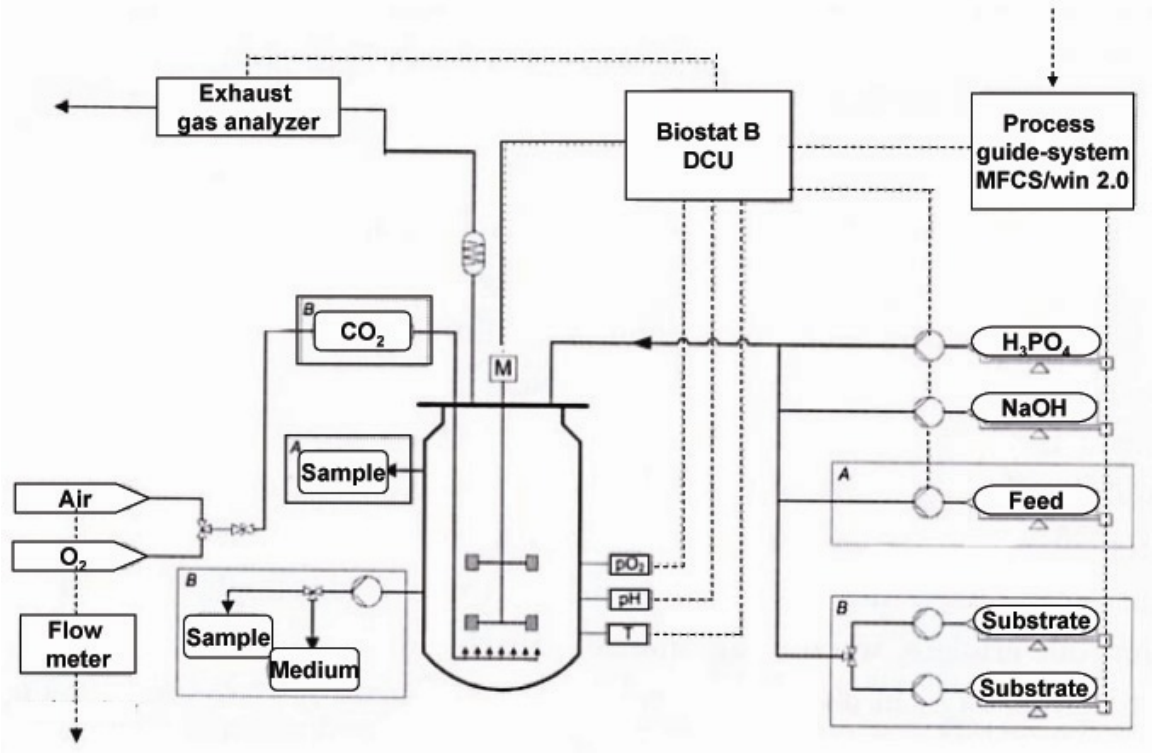

Figure 12. Schematic diagram of the bioreactor setup, A: Fed-batch, B: continuous cultivation (Modified after Hollmann 2006)

During the cultivation, data were collected and the parameters were further regulated by the process guide-system MFCS/win 2.0 (BBI Systems; Melsungen; Germany). Dissolved oxygen concentration (pO2), calibrated with air and nitrogen, was kept

above 20 % initially via a concomitant increase in stirrer speed and aeration which was measured by a flow meter (Maihak; Hamburg; Germany). In a later stage of fed batch cultivation oxygen enriched inlet air was used. Foam was controlled by the manual addition of antifoam agent (Sigma Antifoam 204; Sigma-Aldrich; USA) when necessary.

III.5.2.3 Batch cultivation with pH control

For bioreactor cultivation, a Biostat B2 (B. Braun; Melsungen; Germany) with 2 L working volume connected to an exhaust gas analysis unit (S710; Sick Maihak; Germany) was used. The bioreactor was inoculated with 1 %(v/v) cells and cultivated at 37 °C with controlled pH at 7 as previously described (Malten *et al.*, 2005b). In batch cultivation, LB or A5 medium containing 30 g L^{-1} glucose were used and xylose was added as inducer of gene expression right from the beginning.

III.5.2.4 High cell density cultivation (HCDC)

With a 2 L working volume Biostat B2 bioreactor fed-batch cultivations were started with an initial batch cultivation also using A5 medium containing 30 g L^{-1} glucose. After the glucose consumption, an exponential feeding profile with a growth rate of 0.14 h^{-1} was set. The first feed solution was prepared as described previously (Hollmann & Deckwer, 2004). Expression of *tfh* was induced by addition of 5 g L^{-1} xylose at a cell dry weight (CDW) of approximately 15 g L^{-1}. Simultaneously, the feed solution was changed to the second feed solution (Hollmann & Deckwer, 2004) additionally containing 5 g L^{-1} xylose and 5 g L^{-1} yeast extract. During fed-batch cultivation trace elements were added discontinuously summing up to 24 mL of trace element solution and 1.8 g $MgSO_4$.

III.5.2.5 Continuous cultivation

In a 1 L working volume Biostat B2 bioreactor the cultivation was started with a semi-defined A5 medium in the batch phase containing 30 g L^{-1} glucose. After the batch phase the glucose concentration was increased to 50 g L^{-1} in the medium. The temperature was kept constant at 37 °C and the pH was controlled at 7 by the addition of 5 M NaOH and 1 M H_3PO_4. In order to keep a constant volume the agitation rate was set at 500 rpm and a constant airflow of 1 L min^{-1}. The starting volume in the batch phase was 450 mL. Thereafter, the volume was kept constant using an overflow device at 350 mL. Three dilution rates were investigated in this

study with D = 0.1 h^{-1} at the beginning, D = 0.25 h^{-1} in the second phase and D = 0.4 h^{-1} in the last phase. Induction was carried out by keeping a constant concentration of 5 g L^{-1} xylose in the fermentor when dilution rate was 0.1 and 0.4 h^{-1}. Steady state was defined after four residence times when stable carbon dioxide production and oxygen consumption rates as well as constant cell dry weight were observed.

III.6 Analytical procedures

III.6.1 Optical density and cell dry weight measurement

Culture samples for biomass, metabolites, and enzyme activity were taken at regular intervals. In microtiterplate cultivation OD_{580nm} was measured in the Multiskan Ascent photometer (Thermo Electron Corporation; Dreieich; Germany). The relationship between OD_{580nm} measured from microtiterplate and OD_{578nm} measured from 1 cm cuvette was determined as $OD_{578nm,\ 1\ cm\ cuvette} = 3.719 * OD_{580nm,\ microtiter\ plate}$. The OD_{578nm} was measured in triplicates with an Ultrospec 3100 Pro spectrophotometer (Amersham Pharmacia; UK). The relationship between CDW and OD_{578nm} was determined as CDW [g L^{-1}] = 0.346 * OD_{578nm} for WH323, as CDW [g L^{-1}] = 0.334 * OD_{578nm} for MS941 and as CDW [g L^{-1}] = 0.395 * OD_{578nm} for YYBm1.

III.6.2 High performance liquid chromatography

The concentration of glucose and produced metabolites was determined by high performance liquid chromatograph (HPLC) (Shimadzu; Japan) using an Aminex HPX-87H column (Biorad; USA) and 10 mM H_2SO_4 as the mobile phase. In order to separate xylose from pyruvate a flow rate of 0.6 mL min^{-1} at 60 °C was used.

III.6.3 SDS-PAGE

For SDS–PAGE analysis 6 x 10^9 cells were harvested, lysed and intracellular proteins were separated by centrifugation into soluble and insoluble protein fractions (Malten *et al.*, 2005b). SDS-PAGE was performed using a Mini Protean 3 apparatus (Bio-Rad; USA) and proteins were stained by Commassie Blue G250. For the immunochemical detection, the separated proteins were transferred onto a polyvinylidene difluoride (PVDF) membrane using a Trans-Blot Semi-Dry Transfer Cell (Bio-Rad; Munich; Germany) as described by the manufacturer. Mouse anti-His_6-tag antibodies (Amersham-Pharmacia Biotech; Freiburg; Germany) were used

1:2,000 diluted in PBS buffer with 5 %(w/v) skim milk powder for detection of the His_6-tagged TFH. The N-terminal amino acid sequences of blotted proteins were determined by Edmann degradation (HZI; Braunschweig; Germany).

III.6.4 Fluorescent Staining and Flow Cytometry

Cells from fed-batch samples were diluted with ice cold PBS buffer (pH = 7) to a final concentration of (0.5 – 5) x 10^8 per mL (Biedendieck *et al.*, 2007). Dead cells as a negative control were prepared by adding 70 % ethanol to the sample for 10 min. Aliquots of 500 µL were stained with 2.5 µL propidium iodide (PI) (Cell Viability Kit; BD Bioscience; San Jose, CA; USA). Flow cytometric analysis was performed using a FACSCalibur (BD Bioscience; San Jose, CA; USA) and analyzed using CellQuestPro and Summit software (DakoCytomation; Fort Collins, CO; USA). Side (SSC) and frontal scatter (FSC) triggers were adjusted to show the whole cell population. Red fluorescence for PI detection was collected in the FL3 and green autofluorescence in the FL1 channel. All triggers during the measurements were kept constant. On the FCS and SSC dot blot a gate containing all events from stained dead cells was set up according to the negative control. All gated events were separated via their position in the FL1 – FL3 dot blot into either live or dead subpopulation.

III.6.5 Enzyme tests

III.6.5.1 TFH activity assay

III.6.5.1.1 pNPP test

TFH activity was measured spectrophotometrically (Ultrospec 3100 pro; Amersham Biosciences; Sweden) via released p-nitrophenol from p-nitrophenylpalmitate as described previously (Schmidt-Dannert *et al.*, 1994). Fresh pNPP solution was prepared by mixing 1 mL of 3 g L^{-1} pNPP dissolved in 2-propanol and 9 mL 20 mM phosphate buffer (pH 7.1, sodium taurocholate 2.3 g L^{-1}, arabic gum 1.1 g L^{-1}). After addition of the enzyme sample, the absorption was immediately measured for 2 min at 400 nm and 25 °C and plotted against a control reaction without addition of enzyme. TFH activity was measured in the initial linear phase of velocity. Protein concentration was employed accordingly. After the cell disruption with lysozyme intracellular TFH activity was measured against a control reaction by adding a lysis buffer instead of the enzyme. One unit of TFH activity was defined as the amount of

enzyme that caused the release of 1 µmol p-nitrophenol per minute under the test conditions. The extinction coefficient of p-nitrophenol is 9.62 cm^2 $µmol^{-1}$.

III.6.5.1.2 Titration test

The activity was monitored via the release of free acids during ester cleavage with an auto-titration system (PHM290 pH-STAT controller and Abu 901 AutoBurette; Radiometer; Copenhagen) at pH 7 in a sterile 9 g L^{-1} NaCl solution. A total of 6 mL of NaCl solution and the enzyme sample were filled into a 10 mL thermostated glass reactor. The reaction was started by the addition of a nanoparticle suspension containing 700 µg polymers. The monomer includes a diol – 1, 4-butandiol and a dicarboxylic acid – adipic acid. During the cleavage an acid is formed. Hence, the ester cleavage rate was calculated from the consumption of 100 mM NaOH used to keep the solution neutral.

III.6.5.2 ß-galactosidase activity assay

The ß-galactosidase activity was determined spectrophotometrically via released o-nitrophenol from o-nitrophenyl-β-D-galactopyranosid (ONPG) as described previously (Mason *et al*., 1988). First, 6 x 10^9 cells were harvested, washed 2 times with 25 mM ice cold Tris / HCl, buffer (pH 7.4). After removing the supernatant, cells were resuspended in 640 µL Z–buffer (60 mM Na_2HPO_4, 40 mM NaH_2PO_4, 10 mM KCl, 1 mM $MgSO_4$, and 50 mM ß-mercaptoethanol (pH 7.0). After adding 160 µL of 2.5 mg mL^{-1} lysozyme, the solution was incubated at 37 °C for 30 min. Disrupted cells were extracted by adding 8 µL 10 % Triton-X100 for 3 min at 31 °C. Subsequently, 200 µL of a freshly prepared 4 mg of ONPG per mL Z–buffer solution were added into the reaction vessels for the colour reaction and incubated at 31 °C until the colour changed. The reaction was stopped by adding 400 µL of 1 M Na_2CO_3. The supernatant was collected after centrifugation and measured at 420 nm against a standard without addition of enzyme. Miller units were determined using the following formula:

[OD_{420nm}/ (OD_{578nm} of cells x volume of culture x length of incubation)] x 1000

III.6.5.3 Protease activity measurement by azocasein assay

Azocasein solution was freshly prepared by dissolving of 20 g L^{-1} azocasein (Sarath *et al*., 1989) in 100 mM of phosphate buffer (pH 6.5), with 360 µM calcium chloride and 5 mM sodium azide. The growth medium was diluted 1:10 in 100 mM phosphate buffer. 150 µL of this sample were added to 250 µL of the azocasein solution and

incubated at 37 °C for 1 h. The reaction was stopped by adding 1 M NaOH. After precipitation of the proteins using trichloroacetic acid the absorption of the released azodye was measured at 440 nm against culture medium. One unit was defined as the amount of enzyme causing an absorbance change of 1.0 in a 1 cm cuvette.

III.6.5.4 PGA activity measurement by NIPAB assay

Directly after sampling, PGA activity was measured spectrophotometrically (Ultrospec 3100 pro, Amersham Biosciences, Sweden) via release of the 6-nitro-3-phenylacetamido-benzoic acid (NIPAB) as described previously [29]. Freshly prepared NIPAB solution was prepared by dissolving 60 mg 6-nitro-3-phenylacetamido-benzoic acid in 100 mL 50 mM Na-Phosphate buffer. After addition of the enzyme sample, the absorption was immediately measured at 405 nm and 37 °C for 60 s after a 20 s delay against a standard without addition of enzyme. One unit was defined as the amount of enzyme that caused the release of 1 µmol 6-nitrophenol per minute under the test conditions. The extinction coefficient of 6-nitrophenol is 8.98 cm^2 μmol^{-1}.

III.7 Protein Purification

III.7.1 Protein purification with Chelating Sepharose™ Fast Flow Gel

Prior chromatography filtrated culture medium (0.25 µm) was divided into 3 samples of 10 mL. The first sample was kept as control, the second was heated at 50 °C for 10 min. One mM Pefabloc protease inhibitor (FluKa; Deisenhofen; Germany) was added to the third sample before it was dialysed at 4 °C in a Slide-A-Lyzer dialysis cassette with a 10 kDa cut-off (10 k MWCO, PIERCE; Bonn; Germany) for 18 h. Then 1 mg Ni-charged Chelating Sepharose Fast Flow Gel (Amersham Bioscience; Freiburg; Germany) per 0.85 U TFH was added to the TFH containing growth medium. The suspension was carefully stirred at room temperature until unbound TFH activity in the supernatant decreased to a constant low level. After centrifugation (9,000 x g; 35 min; 4 °C) the suspension was filled into in a Poly-Prep chromatography column (Bio-Rad; Munich; Germany). The column was washed with 3 column volumes (CV) binding buffer containing 20 mM Tris (pH 7.5), 500 mM NaCl and 10 mM imidazole and then eluted with 6 CV elution buffer containing 20 mM Tris (pH 7.5), 500 mM NaCl and 500 mM imidazole. Fractions were collected and analyzed by the TFH activity test (III.6.5.1.1) and SDS-PAGE (III.6.3). Protein was

quantified by Roti-Nanoquant (Roth; Germany) as described by the manufacturer. In order to minimize the influence of imidazole (Hefti *et al*., 2001) elution samples were diluted and the calibration curve was measured with bovine serum albumin dissolved in buffer with the same imidazole concentration as in the samples.

III.7.2 Purification with ProPur Sample IMAC Pack

In order to remove any cellular debris 1 mL sample was filtered through a 0.2 µm pore size syringe filter. 650 µL filtered cleared lysate was pipetted into the pre-equilibrated IMAC Mini column (Nunc; Wiesbaden; Germany). The spin column was equilibrated two times by centrifugation at 1,800 g for 1 min with 650 µL binding buffer (50 mM sodium phosphate buffer, 300 mM NaCl, 10 mM imidazole (pH 7.4)). For purification the column was first centrifuged at 640 x g for 6 min then it was washed up to 5 times with the same amount washing buffer (50 mM sodium phosphate buffer, 300 mM NaCl, 30 mM imidazole (pH 7.4)). Finally, bound His-tagged protein was eluted two times by centrifugation at 1,800 g for 1 min with 650 µL elution buffer (50 mM sodium phosphate buffer, 300 mM NaCl, 300 mM imidazole (pH 7.4)).

III.7.3 Purification with Sartobind IDA 75 metal chelate membrane adsorbers

Sartobind IDA 75 metal chelate membrane adsorbers (Sartorius AG; Goettingen; Germany) was first pre-loaded by filling in 10 mL 500 mM imidazole then washed two times with distilled water in order to remove unbound metal ions. Before the sample was loaded it was first filtered through a 0.4 µm and a 0.2 µm pore size syringe filter. Next, the sample was loaded by gravity flow until the fluid level reached the bottom of the syringe again. After that 10 mL binding buffer (20 mM Tris, pH 7.5, 500 mM NaCl and 10 mM imidazole) was used to wash the unit. Finally, His-tagged protein was eluted with 5 mL elution buffer (20 mM Tris, pH 7.5, 500 mM NaCl and 500 mM imidazole).

III.7.4 Desalting and concentration

Fractions with activity were pooled and concentrated by ultrafiltration (Amicon Stirred Cell 1050 or 1010; Amicon; USA) using a regenerated cellulose membrane (YM Ultrafiltration Membranes, cut off: 10 kDa; Amicon; USA).

III.7.5 Size exclusion chromatography

6 ± 0.5 mL of the concentrated enzyme was applied manually to the column (HiLoad 26/60 Superdex 75 prep grade; Amersham Bioscience; Germany) equilibrated with 0.9 % NaCl. The flow rate was set to 2 mL min^{-1} to elute proteins. Fractions with activity were pooled and stored at -20 °C until further use. Whenever necessary, TFH solution was concentrated by ultrafiltration. The calibration equation of partition coefficient K_{av} (Y) to the logarithmic value of protein's molecular weight (x) was determined to be : Y = -0.3453 x + 2.098 (Xia, 2005).

IV Results and Discussion

IV.1 Production and secretion of a heterologous *Thermobifida fusca* hydrolase (TFH) after codon optimization

IV.1.1 Influence of codon usage on *tfh* gene expression in *B. megaterium*

IV.1.1.1 Wild type *tfh* gene expression in *B. megaterium*

For the heterologous production and secretion of TFH in *B. megaterium* MS941 in a first step, the *tfh* gene with and without encoded signal peptide was cloned into *B. megaterium* plasmids under the control of a xylose inducible promoter system (Rygus & Hillen, 1991). The plasmid pMM1525 encoding the signal peptide of *B. megaterium* extracellular lipase LipA was used for the secretion of proteins into the growth medium. Plasmid pMM1520 was employed for the intracellular protein production. The resulting *tfh* carrying plasmids were named pYYBm1 and pYYBm3, respectively. Complete DNA sequence determination confirmed the integrity of the used plasmids. However, no obvious TFH activity was detected in the used complex or semi-defined A5 medium although various xylose addition schemes for the induction of *tfh* expression were tested (Table 5). For a better quantitative determination of enzyme activity, a more sensitive assay via the release of free acids during ester cleavage with an auto-titration system at pH 7 using a sterile 9 g L^{-1} NaCl solution was employed. However, no TFH was detected in the culture supernatant. Inspection of the intracellular soluble and insoluble protein fractions by SDS-PAGE analysis yielded identical results.

IV.1.1.2 Adaptation of the *tfh* gene to the codon bias of *B. megaterium*

The codon bias of heterologous genes is often a limiting factor for the expression in certain host system. Gene expression limiting regulatory elements may exist within the coding sequence resulting in a decreased expression level. Therefore, a codon usage table was deduced from the predicted 4814 open reading frames of an ongoing *B. megaterium* sequencing project (Table 4 - genome %). Using the recently developed program JCat, the relative adaptiveness of each codon was computed (Table 4 – genome w_i) (Grote *et al*., 2005). This calculation is based on an iterative algorithm searching in the genome for genes with the highest codon bias, so called highly-expressed genes. The multiplication of the relative adaptivenesses for each codon in the *tfh* gene divided by the number of codons gives the codon adaptation

index (CAI). A CAI of 1 represents optimal codon usage. The average CAI for all 4814 open reading frames of *B. megaterium* is 0.35. The codons used in the *T. fusca tfh* gene (Table 4 – wt *tfh*) differ largely from the codon bias of *B. megaterium* evident by a CAI of 0.16.

Table 4**.** Codon usage of *Bacillus megaterium* and of the *tfh* gene before and after optimization. The codon usage of the genome was determined from 4814 predicted open reading frames of an ongoing genome sequencing project. The given percentage is the abundance of a codon used for one amino acid. The relative adaptiveness of each codon was computed by an algorithm, which was further used for the optimization of the *tfh* gene (Grote et al., 2005). For the wild type *tfh* gene from *T. fusca* and the optimized *tfh* gene the usage of each codon in the DNA sequence was counted. [aa = coded amino acid; wi = relative adaptiveness of a codon]

aa	codon	genome %	w_i	w. t. *tfh*	opt. *tfh*
Ala	GCA	34.6	0.89	2	0
Ala	GCC	11.8	0.03	15	0
Ala	GCG	16.9	0.14	7	0
Ala	GCU	36.7	1.00	1	25
Arg	AGA	22.4	0.07	0	0
Arg	AGG	6.7	0.01	0	0
Arg	CGA	18.1	0.01	1	0
Arg	CGC	19.4	0.33	6	0
Arg	CGG	5.9	0.02	6	0
Arg	CGU	27.5	1.00	2	15
Asn	AAC	37.0	1.00	14	14
Asn	AAU	63.0	0.46	0	0
Asp	GAC	27.8	0.56	12	0
Asp	GAU	72.2	1.00	0	12
Cys	UGC	38.9	0.49	2	0
Cys	UGU	61.1	1.00	0	2
Gln	CAA	64.8	1.00	0	4
Gln	CAG	35.2	0.05	4	0
Glu	GAA	40.0	1.00	2	12
Glu	GAG	11.9	0.15	10	0
Gly	GGA	20.0	0.52	2	1
Gly	GGC	9.7	0.49	18	0
Gly	GGG	6.3	0.03	1	0
Gly	GGU	12.1	1.00	1	21
His	CAC	31.6	1.00	6	6
His	CAU	68.4	0.72	0	0
Ile	AUA	14.5	0.00	0	0
Ile	AUC	19.3	0.58	17	1
Ile	AUU	66.3	1.00	0	16
Leu	CUA	6.4	0.17	0	0
Leu	CUC	3.0	0.01	9	0
Leu	CUG	6.1	0.01	11	0
Leu	CUU	13.7	0.41	0	0
Leu	UUA	21.6	1.00	0	21
Leu	UUG	7.3	0.05	1	0
Lys	AAA	76.0	1.00	1	7
Lys	AAG	24.0	0.11	6	0
Met	AUG	100.0	1.00	3	3
Phe	UUC	20.8	1.00	9	9
Phe	UUU	79.2	0.84	0	0
Pro	CCA	30.2	1.00	0	18
Pro	CCC	7.8	0.01	7	0
Pro	CCG	22.0	0.15	12	0
Pro	CCU	40.0	0.76	0	1
Ser	AGC	17.5	0.59	15	0
Ser	AGU	16.1	0.22	0	0
Ser	UCA	23.6	1.00	0	26
Ser	UCC	8.0	0.04	11	0
Ser	UCG	9.0	0.04	0	0
Ser	UCU	25.8	0.99	0	0
Thr	ACA	34.1	1.00	1	18
Thr	ACC	9.9	0.00	15	0
Thr	ACG	25.0	0.14	3	0
Thr	ACU	15.5	0.42	1	2
Trp	UGG	15.6	1.00	4	4
Tyr	UAC	30.9	0.95	10	9
Tyr	UAU	69.1	1.00	0	1
Val	GUA	35.7	1.00	0	13
Val	GUC	11.3	0.03	10	0
Val	GUG	20.6	0.16	3	0
Val	GUU	32.5	0.81	0	0

Hence, the codon usage was adapted using the relative adaptiveness (w_i) of the codon usage chart. For the six histidines in the tag also the less used CAT codon was used twice. The sequence was optimized avoiding internal promoters, ribosomal binding sites and RNA secondary structures and synthesized by Geneart (Regensburg, Germany). After optimization, the codon usage (Table 4 – opt. *tfh*) is very well adapted to the preferences in *B. megaterium* as demonstrated by a CAI of 0.98. Moreover, during the whole *tfh* gene optimization process *cis*-acting sequence motifs such as internal –10 regions, *chi*-sites, ribosomal entry sites, repetitive sequences, and RNA secondary structures were avoided. In addition, regions of very high (> 80%) or very low (< 30%) GC content was excluded.

IV.1.1.3 Expression of the codon optimized *tfh* gene in *B. megaterium*

The codon optimized *tfh* gene was cloned into pMM1525. The successfully constructed plasmid was named pYYBm9. The expression was first tested using a 100 mL LB shaking flask cultivation at 37 °C (Table 5). The *B. megaterium* MS941 carrying pYYBm9 encoding the optimized *tfh* gene secreted 563 U g_{CDW}^{-1} TFH. Under the identical cultivation conditions MS941 carrying pYYBm1 encoding the wild type *tfh* gene failed to produce or secrete any TFH. With regard to the successful gene expression of a dextransucrase from *Leuconostoc mesenteroides* (Malten *et al.*, 2005b) and a levansucrase from *Lactobacillus reuteri* (Malten *et al*., 2006) which

Table 5. Comparison of the production of secreted TFH in U g_{CDW}^{-1}. *B. megaterium* strains carrying different plasmids were first grown aerobically in 100 mL LB or A5 shaking flask cultures at 37 °C. Gene expression was induced by the addition of 0.5 % (w/v) xylose at an OD_{578nm} of 0.4. Strain WH323-pYYBm9 was selected for further bioreactor cultivation. Gene expression of recombinant *B. megaterium* grown using pH controlled batch fermentation in LB and A5 medium was induced with 5 g L^{-1} xylose right at the beginning of the cultivation. In glucose limited HCDC *tfh* expression was induced at a biomass of 15 g L^{-1} (16.8 h) by adding constantly xylose to a concentration of around 5 g L^{-1}.

Strain	Vector	Shaking flask		Bioreactor with pH control		HCDC
		LB	A5	LB	A5	A5
MS941	pYYBm1	0	0			
MS941	pYYBm3	0	0			
MS941	pYYBm9	563	0			
WH323	pYYBm9	694	0	2651	116	187

have a high CAI value over 0.7 the codons of the *tfh* gene required an initial

adaptation to the *B. megaterium* codon usage due to their low CAI value of 0.16. Talarico *et al*. also observed that the expression of a pyruvate decarboxylase from the Gram positive bacterium *Sarcina ventriculi* in *B. megaterium* was successful with a CAI value of 0.60. But genes isolated from other organisms like *Acetobacter pasteurianus*, *Zymononas mobilis* and *Saccharomyces cerevisiae* were not expressed (Talarico *et al*., 2005). The CAI values were merely 0.19, 0.32 and 0.34, respectively. These observations underscore that in the same production host the formation of enzymes originating from different organisms often varies significantly in dependence of their CAI. Clearly, the CAI value seems to be a valuable tool for estimating the expression level of heterologous genes.

IV.1.2 TFH production and secretion in *B. megaterium*

IV.1.2.1 Shaking flask cultivation with *B. megaterium* strain deficient in xylose utilization

For enhanced secretion of TFH a long lasting gene induction phase by xylose was desired. However, when glucose became limiting xylose was rapidly consumed by *B. megaterium*. Therefore, induction conditions were hardly predictable especially in fed-batch cultivations. Hence, the *B. megaterium* strain WH323 (Rygus & Hillen, 1992) deficient in xylose utilization (Δ*xylA*) was used. After cultivation of WH323 (Δ*xylA*) carrying pYYBm9 in shake flasks with 100 mL LB medium and *tfh* induction, secretion of 694 U g_{CDW}^{-1} TFH was observed. This was 1.2 fold more TFH than produced by extracellular protease NprM deficient strain MS941 (Δ*nprM*) under the same conditions (Table 5 and Figure 13). SDS-PAGE analysis of precipitated extracellular proteins showed only one dominant protein with a relative molecular mass of 28,300. This is in good agreement with its gene deduced molecular weight of 28,172 Da. This protein was first detectable 4 hours after induction and not observed in a cultivation of *B. megaterium* carrying a geneless plasmid. In accordance with the activity assay the protein band was stronger in samples from WH323 (Δ*xylA*). Hence, further studies were performed using *B. megaterium* strain WH323 (Δ*xylA*).

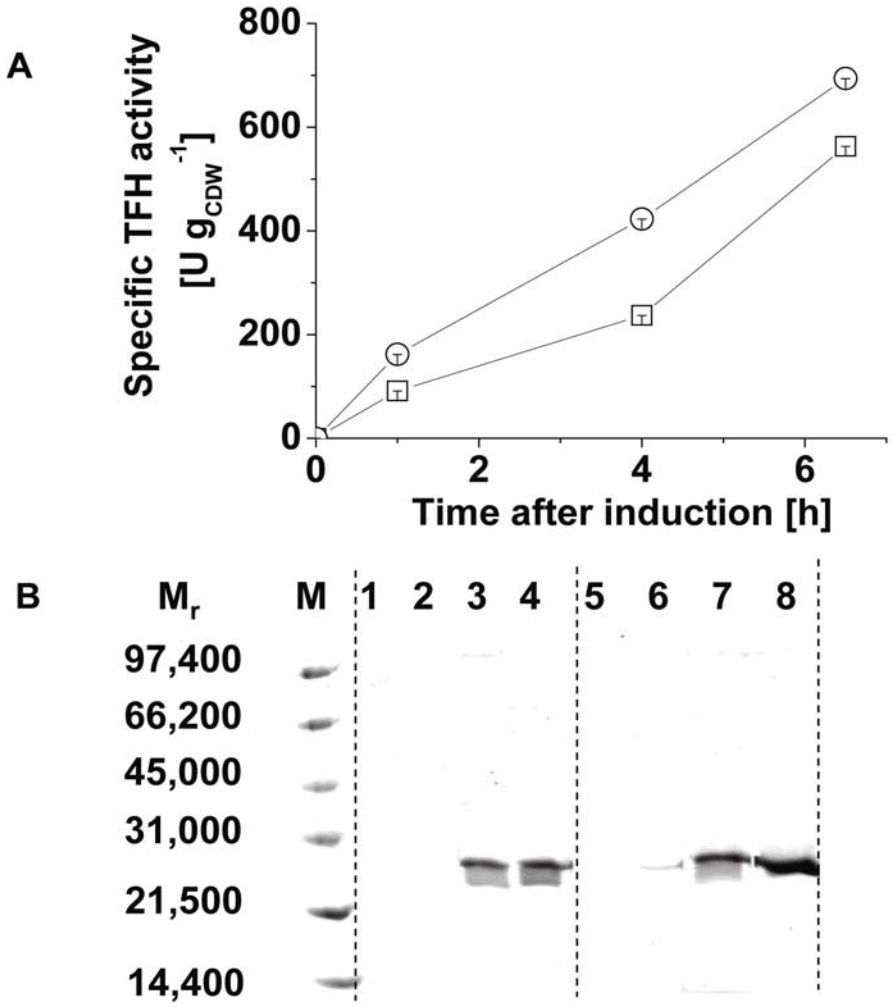

Figure 13. Recombinant production and export of TFH into growth medium by *B. megaterium* MS941 (Δ*nprM*) (□) and WH323 (Δ*xylA*) (○) transformed with pYYBm9 in LB complex medium. At an OD_{578nm} of 0.4, production of TFH was induced by the addition of 0.5 % (w/v) xylose to the growth medium. Samples were taken at various time points after induction. (A) Specific activity curve of TFH produced and secreted by MS941 (Δ*nprM*) (□) and WH323 (Δ*xylA*) (○). (B) Proteins of 1.5 mL growth medium were concentrated by ammonium sulphate precipitation, separated by SDS-PAGE and visualized using Coomassie Brilliant Blue G250. Proteins exported by MS941 carrying pYYBm9 before, 1 h, 4 h and 6.5 h after induction are shown in lane 1, 2, 3 and 4, respectively. Proteins exported by WH323 carrying pYYBm9 before, 1 h, 4 h and 6.5 h after induction are shown in lane 5, 6, 7 and 8, respectively.

IV.1.2.2 Secretion of TFH in batch cultivation

A shake flask cultivation of *B. megaterium* in A5 semi-defined medium grew to 2.2 fold higher cell densities (4 g_{CDW} L^{-1}) compared to a culture with LB complex medium. Hence, a higher TFH yield was expected using A5 medium. However, we failed to detect TFH activity in the growth medium of MS941 carrying pYYBm9 and of WH323 carrying pYYBm9 (Table 5). One reason might be that after induction of gene

expression the pH of the cultivation in A5 medium decreased in 2.5 h from 7 to 5.5 and further to 4. Previously, it was observed that below a pH of 6.5 TFH activity decreased to 60 % at pH 5.5 and 10 % at pH 4 (Kleeberg *et al*., 2005). In these acidic conditions TFH is probably partly unfolded and more prone to proteolytic attack.

In order to control the pH, cultivation of *B. megaterium* WH323-pYYBm9 in complex LB and semi-defined A5 medium was continued in batch cultivations using a 2 L bioreactor (Figure 14). Five g L^{-1} xylose was added as inducer of gene expression at the beginning of the fermentation because a previous study with intracellular green fluorescent protein (Biedendieck *et al.*, 2007) and a secretion of penicillin G amidase in this study (Figure 24) suggested that early induction was preferable to late induction. Using A5 medium, 886 U L^{-1} corresponding to 116 U g_{CDW}^{-1} of TFH were produced after 21 h of cultivation (Figure 14, Table 11). In contrast, after 26 h of cultivation in LB medium 7953 U L^{-1} corresponding to 2651 U g_{CDW}^{-1} TFH were produced and secreted (Table 11). Therefore, the specific TFH activity was found 23 fold higher than the specific TFH activity after cultivation in A5 medium and 4 fold higher than after cultivation with LB medium in shake flask. On the contrary, *B. megaterium* cell densities reached with 12 g_{CDW} L^{-1} a 4 fold higher cell concentration after cultivation in A5 medium than in LB medium. *B. megaterium* grown in complex LB medium exhibited a longer lag phase (10 h) than cells grown in A5 medium (5 h). HPLC analysis (Figure 14) revealed that different metabolites were produced by *B. megaterium* during cultivation in these two media. In A5 medium, acetate and succinate were found as the major metabolites, whereas only negligible amounts of acetate were detected in LB medium. Acids produced in the exponential phase with A5 medium were consumed again in the stationary phase.

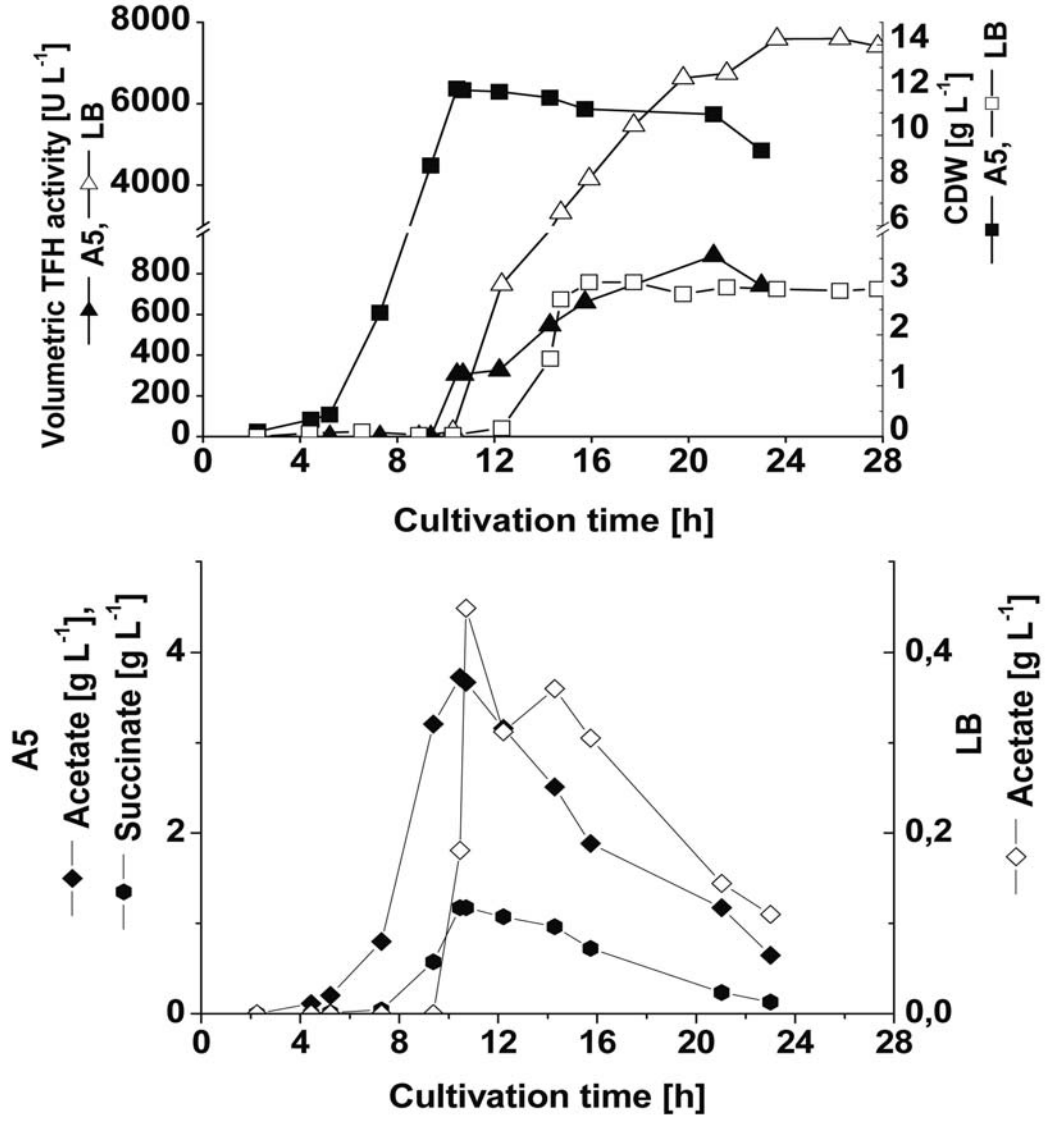

Figure 14. TFH production and metabolites concentrations during batch cultivation under pH control *of B. megaterium* WH323 (Δ*xylA*) carrying pYYBm9 in LB (empty) and A5 (solid) medium. As inducer of gene expression 0.5 % (w/v) xylose was added at the beginning of the cultivation.

SDS-PAGE analysis of all extracellular proteins demonstrated that TFH was again the dominant protein of the secretome, but other proteins were present as well (Figure 15). The density of the TFH bands correlated well with the enzyme activity determined for the corresponding cultivation medium. Interestingly, in a culture with LB medium TFH was secreted from the beginning of the exponential growth phase and during the stationary phase. For cultures with A5 medium TFH production was exclusively observed only during the stationary phase.

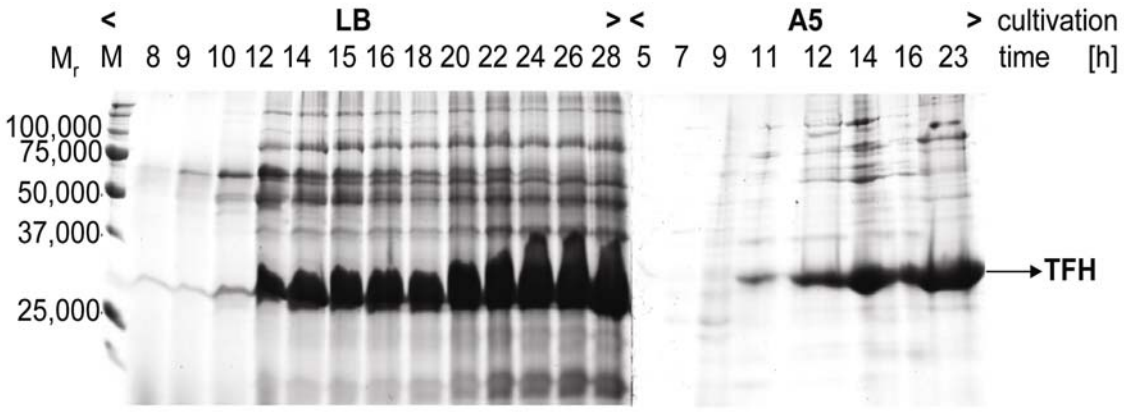

Figure 15. SDS–PAGE analysis of proteins from 1.5 mL growth medium samples were taken at indicated time points, precipitated by ammonium sulphate, and stained by Coomassie Brilliant Blue G250.

A Western blot analysis (summarized in Table 6) revealed the cell-associated localization of the remaining TFH. From the previous work of Malten *et al*. (2005) and many other reports on protein secretion it was concluded that pre-proteins which still carry their signal peptides are located in the cytoplasm. Mature cell-associated protein is usually located outside the cytoplasmic between cell-wall and cytoplasma membrane. The size difference between the pre-protein with its signal peptide and the mature protein without signal peptide can be observed by Western blotting**.** During cultivation in LB medium mature TFH was found outside the cytoplasm mostly as soluble protein. Its accumulation correlated well with the volumetric TFH activity curve. Cytoplasmic TFH carrying its signal peptide was barely detectable. Hence, TFH transport through the cytoplasmic membrane was not the limiting step, however, some limitation in the transport through the cell wall might occur. In contrast, *B. megaterium* cells cultivated in A5 medium accumulated considerable amounts of insoluble TFH with its signal peptide in the cytoplasm. This was observed already at the start of TFH secretion. Under these conditions the transport through the cell membrane was found limiting leading to cytoplasmic retention and aggregation of TFH. The increased intracellular accumulation of TFH in *B. megaterium* grown in A5 medium compared to cells grown in LB medium is in consistence with the decreased secretion of TFH per cell (Figure 14).

Table 6. Cell-associated TFH forms detected by Western blot analysis in the soluble and insoluble protein fraction. Cells from a batch cultivation of *B. megaterium* WH323 (Δ*xylA*) carrying pYYBm9 in LB and A5 medium were disrupted. Cell-free extracts were separated into soluble (S) and insoluble (I) protein fraction by centrifugation. The information given here is from the analysis of approximately 30 samples from different cultivations in separate Western blots.

Medium	Cell associated fraction	Mature TFH	TFH with SP_{lipA}.
LB	soluble	++	-
	insoluble	+	(+)
A5	soluble	+	-
	insoluble	-	+++

In *B. megaterium* WH323 (Δ*xylA*), a β-galactosidase gene (*lacZ*) was integrated into the chromosomal *xylA* locus placing the β-galactosidase under control of the xylose-inducible promoter P_{xylA}. Hence, *lacZ* is under the same transcriptional and translational control as the *tfh* gene on the multicopy plasmid. However, a glucose repression mediated by the catabolite responsive element (*cre*) is still present for the chromosomal *lacZ* gene. Consequently, in the batch cultivation of *B. megaterium* WH323 (Δ*xylA*) carrying pYYBm9 in glucose-free LB medium the measurement of the ß-galactosidase activity enables to measure the promoter activity independent of influences from secretion or multicopy plasmid caused protein overproduction. Furthermore, extracellular proteases were assayed using azocasein allowing insights into the secretion of homologous proteins (Figure 16). In the cultivation in LB medium the secretion pattern of general proteases and TFH were found quite similar. Only low protease levels of 0.04 U mL^{-1} were detected at 14.7 h after cultivation start. After nearly 7 hours the protease activity decreased parallel to the TFH activity. The β-galactosidase activity increased rapidly in the exponential growth phase from 97.3 Miller units (10.7 h) to 1515 Miller units (14.7 h) and reached slowly to a maximal value of 1683 Miller units at 17.7 h. In this period the TFH secretion rate was nearly constant. Thereafter, the β-galactosidase activity decreased followed by a decrease of the TFH secretion rate (Figure 16A). Hence, β-galactosidase production and TFH secretion seemed to follow the similar patterns. In the stationary phase not only expression from the P_{xylA} promoter was decreased but also the production of homologous extracellular proteins decreased as observed for the proteases. These effects are probably caused by a slow down of general protein biosynthesis in the cell or an increased intracellular proteolytic activity.

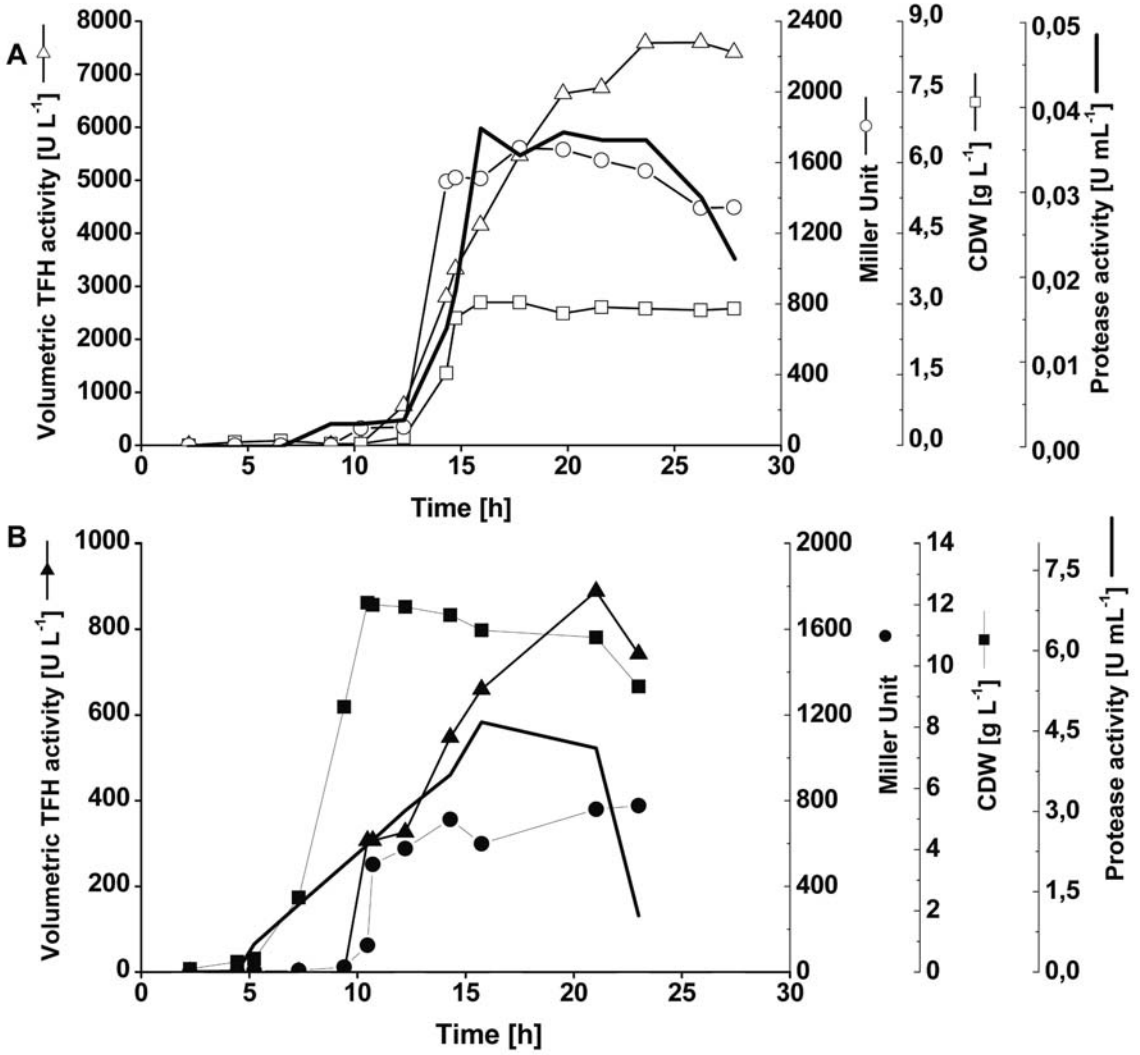

Figure 16. Homologous general proteases, heterologous TFH and β-galactosidase (Miller units) production by *B. megaterium* WH323 (Δ*xylA*) carrying pYYBm9 were compared for batch cultivations with two different growth media: (A) LB, (B) A5.

A completely different behaviour was observed for the secretion of TFH, proteases including NprM, and for the intracellular production of the β-galactosidase during growth in A5 medium (Figure 16B). Similar to LB medium secretion of proteases started during the exponential growth phase, but increased slower. It reached 10-fold higher levels due to the increased demand for amino acids and peptides in the defined medium. The heterologous proteins under control of the xylose inducible promoter were only produced when glucose became limited. From the onset of the stationary phase the amount of extracellular TFH and of intracellular β-galactosidase increased similarly, but much slower and to lower final values as during growth in LB medium. β-galactosidase activity reached 780 Miller units. Hence, it seems that transcription from P_{xylA} is repressed during exponential growth of *B. megaterium*.

Most remarkable are the significant discrepancies observed when cultivating *B. megaterium* WH323 (Δ*xylA*) in complex (LB) and defined (A5) medium (Table 7). These were summarized in Table 6 for the pH controlled batch cultivations. Firstly, it was not only the growth behaviour as characterized by lag phase and maximal growth rate which differed but, particularly, the amounts of overflow metabolites generated and reconsumed during the cultivation course. The temporal formation of over 10 fold higher concentrations of metabolites in A5 have to be attributed predominantly to the larger availability of the carbon source (glucose) and the higher growth rate which typically leads to metabolic overflow.

Table 7. Comparison of *B. megaterium* WH323 (Δ*xylA*) batch cultivations (at 37 C, pH 7) with LB and A5 medium

Feature regarded	LB	A5
Lag phase	long (10 h)	short (5 h)
μ_{max}	0.58 h^{-1}	0.72 h^{-1}
Overflow metabolites	low (0.4 g L^{-1})	high (5 g L^{-1})
Expression of heterologous gene via P_{xylA} promoter (checked by β-Gal activity)	exponential growth phase	stationary phase
Promoter strength (derived from β-Gal-activity)	high	low
Main TFH secretion	exponential. growth phase	stationary phase
Cell associated insoluble TFH fraction	low	high
General extracellular protease activity	low	high

Secondly, by determination of the activity of the cytoplasmatic β-galactosidase the expression of heterologous genes under control of the same P_{xylA} promoter was pursued. Though in both cultivations the inducer xylose was present in high concentration from the very beginning the expression patterns differed largely. In LB medium expression started at the exponential growth phase whereas in A5 medium expression was only observed during stationary phase. In both media the β-galactosidase showed initially a rather steep increase, but later it only increased slowly (Figure 16). The expression levels of the heterologous β-galactosidase gene as indicated by the intracellular enzyme activities were about 2.2 fold higher in LB than in A5. Therefore, the strengths of the *xylA* promoter and the effectiveness of its

derepression by the applied inducer are very different in the two media. These findings clearly indicate that gene regulation and expression are significantly affected by medium composition. It is assumed that the complex medium contains constituents like amino acids and smaller peptides which are responsible for the observed higher expression levels.

Thirdly, the secretion of TFH in the used media mainly ran concomitantly with the production of β-galactosidase. This suggests that the location of preTFH to the *trans* side of the cytoplasmic membrane is proper folding and its releasing across the outer cell wall appears to happen quickly after expression. However, the activity of the SEC system for translocation of preTFH can not be judged from the results of this study. In a recent study with *B. subtilis* in complex medium expression of the important *secA* gene (preprotein translocase) was only temporarily observed in the exponential growth phase (Herbort *et al*., 1999). The preprotein translocase for exporting native proteins exhibited a maximal value at the end of the exponential growth phase and strongly declined when approaching the stationary phase. This agrees well with the course of the secreted TFH in LB medium. This concordance and the low fraction of aggregated TFH in the cells allow the conclusion that gene expression and secretion occur in LB medium simultaneously during exponential growth. Contrarily, in the A5 medium gene expression was observed in the stationary phase at a reduced level. Significant amounts of the preprotein remain located in cell-associated form. This indicates that in A5 medium production and secretion (including folding) are not appropriately tuned. Obviously, one or several of the translocation and folding steps limit export into the culture broth.

IV.1.2.3 Secretion of TFH in a *B. megaterium* fed-batch cultivation of high cell densities (HCDC)

Recently, *B. megaterium* was grown to high cell densities of up to 80 g_{CDW} L^{-1} in a glucose limited fed-batch cultivation (Hollmann & Deckwer, 2004; Malten *et al.*, 2005b). Here, a feed and induction protocol was used that was established before to ensure the highest productivity per cell for intracellular produced GFP (Biedendieck *et al.*, 2007). For the secretion of TFH, the high cell density production process was further optimized by controlling the xylose concentration after induction (Figure 17). The initial glucose concentration in the batch phase was set to 30 g L^{-1}. After exhaustion of the glucose (11.7 h), feed solution 1 was fed exponentially into the

growing culture setting the growth rate to 0.14 h^{-1}. Its actual value was measured as 0.136 h^{-1}. About 5 h after starting the fed-batch, *tfh* expression was induced by addition of 5 g L^{-1} xylose. At this time with a biomass of around 15 g_{CDW} L^{-1} feeding was switched to feed solution 2 containing also 5 g L^{-1} xylose. This strategy maintained in the bioreactor a constant level of xylose independent of the exponential feeding profile as demonstrated by HPLC analysis.

Acetate, succinate and pyruvate were the major organic acids produced during HCDC as detected by HPLC analysis. Isobutyrate and propionate amounts were negligible. 3 g L^{-1} pyruvate, 5.8 g L^{-1} acetate, and 5.9 g L^{-1} succinate were produced in the batch and feeding phase by *B. megaterium* as overflow metabolites due to high glucose consumption rates under aerobic conditions. In the fed batch phase the cells consumed successively these alternative carbon sources, when glucose became limiting (Figure 17B). The high concentration of succinate which peaked at the beginning of the induction phase was remarkable. In the batch as well as the feeding phase the pO_2 in the culture medium was always kept above 20 % air saturation. Hence, activity of fermentative pathways such as the succinate-propionate pathway (Gottschalk, 1986) cannot be assumed and the measured by-products are predominantly due to metabolic overflow. Similar extracellular metabolite distributions have been observed in HCDC of *B. megaterium* (Hollmann & Deckwer, 2004) and *E. coli* as well (Dresler *et al.*, 2006; Korz, 1993).

After starting the induction by addition of xylose a steep increase of secreted TFH activity was observed for about 4 h. The secreted TFH activity per cell reached its maximum of 187 U g_{CDW}^{-1} already 3.7 h after induction of *tfh* gene expression, but decreased in the next 5 h to 112 U g_{CDW}^{-1}.

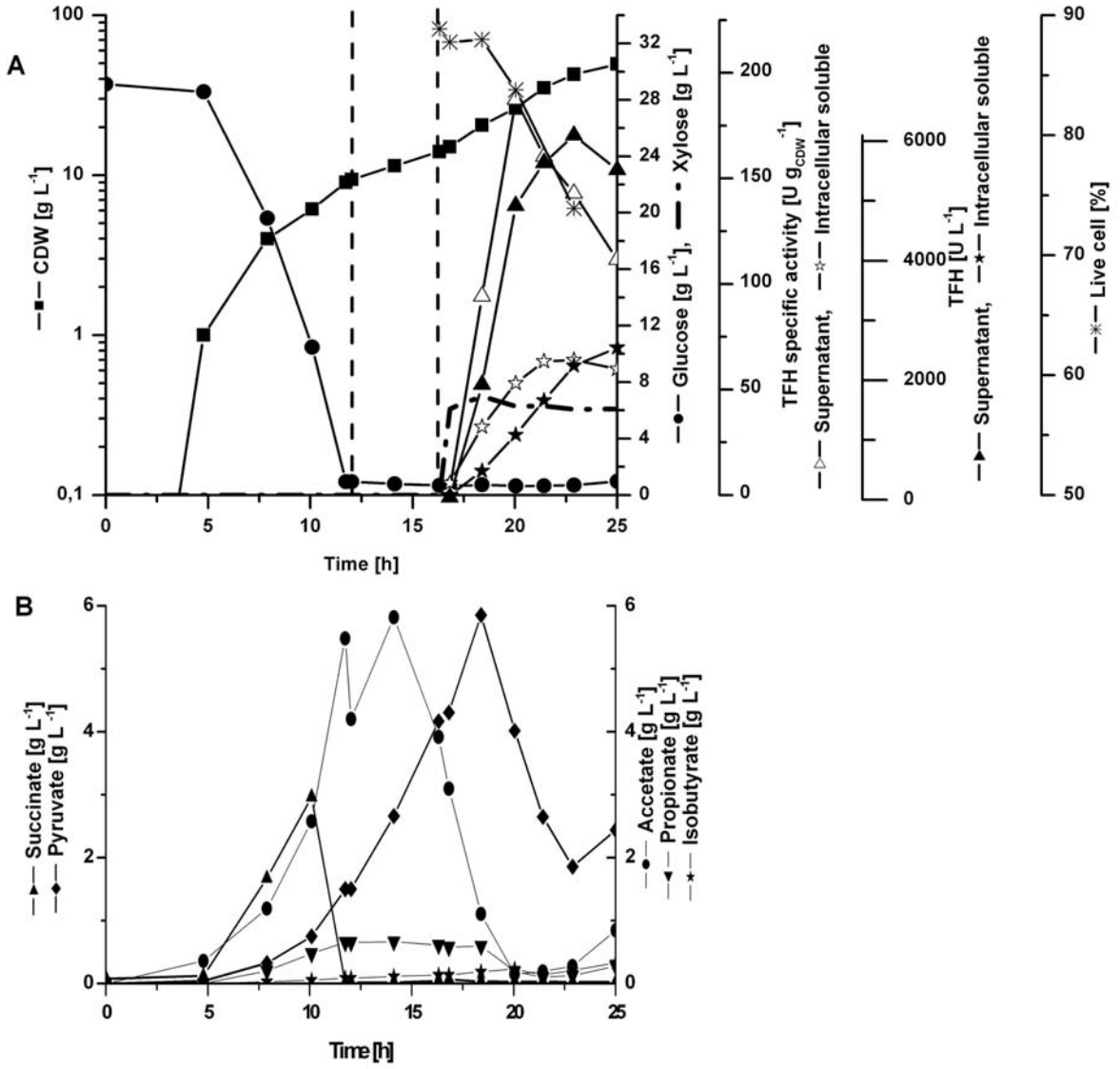

Figure 17. Production of TFH in high cell density cultivation using *B. megaterium* WH323 (Δ*xylA*) carrying pYYBm9. (A) After 30 g L^{-1} glucose was consumed in the batch phase, the exponential feed began at 12 h as indicated by the first dashed line. Expression of *tfh* was induced at 16.8 h as indicated by the second dashed line by addition of 5 g L^{-1} xylose. (B) Metabolites in growth medium as detected by HPLC.

The further increase in cell density, while the cellular TFH productivity decreased at the same time, raised the volumetric TFH activity to its maximum of 6098 U L^{-1} at 6 h after induction. In the next 2 h the volumetric TFH activity decreased to 5520 U L^{-1}. Therefore, the cultivation was stopped. The dry cell weight reached up to 49.5 g_{CDW} L^{-1}. In this process, the export of TFH was also accompanied by an increased transport of the neutral protease (Figure 18). The decline of TFH at later times was due to the action of extracellular proteases and probably the intracellular protease after cell lysis since the number of live cells started to decrease about 2 h after induction. This is in contrast to previous studies on the production of

heterologous dextransucrase (Malten *et al.*, 2005b) and levansucrase (Malten *et al*., 2006) using *B. megaterium* MS941 and WH320. This was the first time that secretion of the heterologous protein was observed at high cell density conditions with a culture growing at low rate. In MS941 not even any production and export of dextransucrase was detected in HCDC, whereas using WH320 protein production was found but the recombinant protein was not exported and accumulated in aggregated form in the cells. The secretion of TFH in WH323 supports the hypothesis that smaller molecular mass proteins can be successfully secreted by *B. megaterium*, probably because they fold easier after translocation. However, in HCDC the secretion was not complete since TFH activity was also found in the intracellular fraction. The intracellular soluble specific TFH activity reached its maximal value of 64 U g_{CDW}^{-1} at 5 h after induction of *tfh* gene expression but decreased in the last 2 h to 59.6 U g_{CDW}^{-1}. In contrast the volumetric activity from intracellular soluble TFH increased fast from 80 U L^{-1} to 2245 U L^{-1} 6 h after induction of gene expression and reached slowly 2546 U L^{-1} in the last 2 h.

IV.1.2.4 Cell viability and protein production during *Bacillus megaterium* high cell density cultivation

The effect of recombinant protein production on the viability of *B. megaterium* cells was analyzed by flow cytometry. For this purpose *B. megaterium* cell populations were stained with propidium iodide (PI), a hydrophobic fluorophore only passing damaged cell membranes. Dead cells incorporated more PI than living cells leading to a stronger red fluorescence signal in the FL3 channel. Furthermore, cellular autofluorescence led to a weak signal distribution in the green fluorescence channel FL1. Hence, *B. megaterium* cells were separated into live and dead subpopulations on a FL1-FL3 dot blot. An analysis of the samples from HCDC before and after induction of gene expression (Figure 17A)

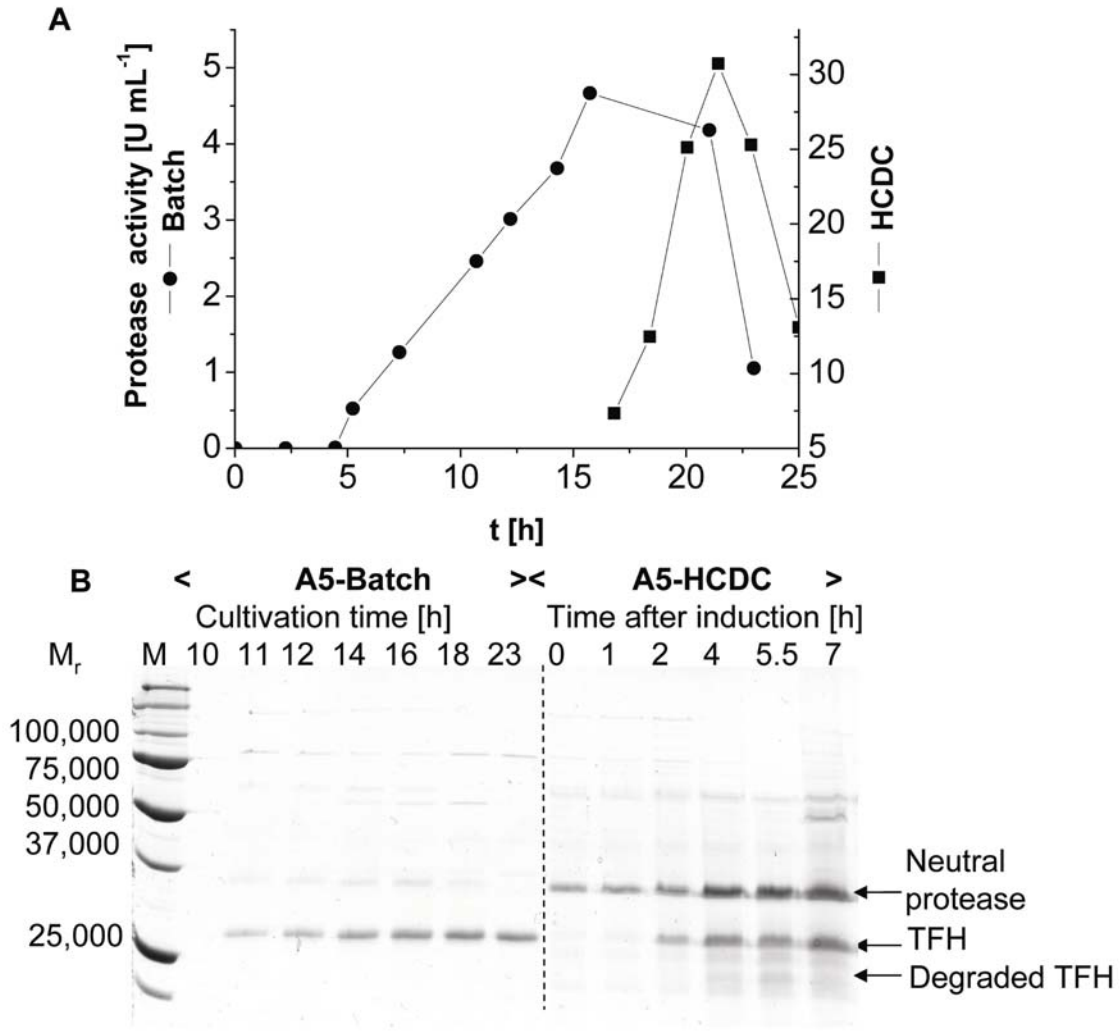

Figure 18. Protease secretion by *B. megaterium* WH323 (*xylA*). (A) Protease produced in batch cultivation with A5 medium (-●-) compared to the production in HCDC after induction at 15.8 h (-■-). (B) Extracellular proteins from 15 µL unconcentrated growth medium were analyzed by SDS-PAGE stained by Coomassie Brilliant Blue G250. Samples were taken at indicated cultivation and induction times, respectively.

indicated that before induction 88.8 % cells were alive, which decreased only slight to 83.7 % 2 h after induction. Hence, induction of foreign protein production had only a minor effect on the viability of the cell population up to 2 hours after induction. However, the amount of the living cells decreased constantly in the next 6 h to 73.8 %. Correspondingly, the specific TFH activity decreased but the volumetric TFH activity still increased in the next 4 h caused by the intracellular TFH liberation during cell lysis. The following decline of volumetric TFH activity was mainly caused by the action of the neutral protease in the HCDC.

For comparison of the secretome from batch and HCDC samples the extracellular proteins from the growth medium were analyzed by SDS-PAGE without prior concentration (Figure 18B). In accordance with activity measurements, TFH concentrations were stronger in samples from the HCDC than from the batch cultivation. However, in HCDC another exoprotein with a relative molecular mass of 35,000 was secreted much stronger than in the batch cultivation. N-terminal amino acid sequencing identified this protein as the neutral protease NprM, which is still present in *B. megaterium* WH323 (Δ*xylA*). Therefore, protease production was also determined for batch and fed-batch cultivations. The results of the activity tests by using an azocasein assay were in a good agreement with the SDS-PAGE analysis (Figure 18A). The maximal protease activity in HCDC culture medium was 30.7 U mL^{-1} and only 4.7 U mL^{-1} in batch medium. Prior induction in HCDC only 4.3 U mL^{-1} protease were observed. Protease production was strongly induced when *tfh* expression was started by xylose addition. In the batch cultivation with A5 medium protease production was firstly observed along with cell growth and continued in the stationary phase. In both cultivation strategies the protease activity exhibited a sharp decline at high cultivation times when growth ceased or was very low. This might be due to decreasing production and insufficient stability caused by autoproteolytic activity.

IV.1.2.5 Secretion of TFH in *B. megaterium* in steady-state and transient continuous cultures

In high cell density cultivation, glucose and subsequently produced metabolites might accumulate leading to a repression of protein production. In a continuous cultivation these accumulation should not occur due to the continuous exchange of the culture medium. Furthermore, this is also an economical strategy and often performed in industry because of the continuous protein production. Recently, the effect of the specific growth rate on protease production during continuous cultivations was investigated for the production of savinase (EC 3.4.21.62), an extracellular alkaline protease from a non-sporulating strain of *B. clausii* (Christiansen & Nielsen, 2002). In this study, a feeding and induction strategy was developed for the TFH production in the continuous cultivation of *B. megaterium*. It was established from the work of Fürch and co workers, 2006a. The secretion of TFH in continuous cultivation was studied at two different dilution rates (0.1 and 0.4 h^{-1}) by adding xylose as inducer for the protein production. When the dilution rate was changed from 0.1 to 0.4 h^{-1}, a

transition phase was introduced with a dilution rate of 0.25 h^{-1} in order to help the cells to adapt to the new settings. When the dilution rate was 0.4 h^{-1}, the glucose concentration in the feed solution was increased from 30 to 50 g L^{-1} in order to increase the amount of cell mass during the cultivation (Figure 19). Such a high glucose concentration was not used at a lower dilution rate because of the overflow metabolism. Steady state was reached after at least four residence times after the end of the batch phase and each shift to a new dilution rate.

First, TFH was produced at a dilution rate of 0.1 h^{-1}. The initial glucose concentration in the batch phase was set to 30 g L^{-1}. After exhaustion of the glucose (9.5 h), the same solution as used in the batch cultivation was fed continuously into the growing culture. The dilution rate was set to 0.1 h^{-1}. Glucose concentration during the cultivation is shown in figure 19. At a growth rate of 0.1 h^{-1} glucose accumulated in the cultivation medium to a maximum of 9.1 g L^{-1}, then was consumed to 7.0 g L^{-1}. Acetate and succinate were the major organic acids produced during continuous cultivation as detected by HPLC analysis.

Pyruvate, Isobutyrate, formiate and propionate formation were negligible under used conditions. 4.32 g L^{-1} acetate and 1.15 g L^{-1} succinate were produced in the batch phase by *B. megaterium* as overflow metabolites due to high glucose consumption rates under aerobic conditions. During the cultivation at D = 0.1 h^{-1} acetate was consumed to 1 g L^{-1} and kept constant. The succinate concentration did not change after the batch cultivation.

About 42.5 h after starting the continuous cultivation at 0.1 h^{-1} *tfh* expression was induced by addition of 5 g L^{-1} xylose into the bioreactor. At the same time the feed solution was changed to a solution also containing 5 g L^{-1} xylose. A steep increase of secreted TFH activity was observed for about 5 h with a maximal increase of 1.1 mg TFH $L^{-1}h^{-1}$. The secreted TFH activity per cell reached its maximum of 421 U g_{CDW}^{-1} 48 h after induction of *tfh* gene expression and at the same time reached its maximum volumetric activity value of 5410 U L^{-1}. The intracellular TFH activity curve showed a similar pattern. A maximum of 445 U L^{-1} intracellular TFH activity was also reached 48 h after induction.

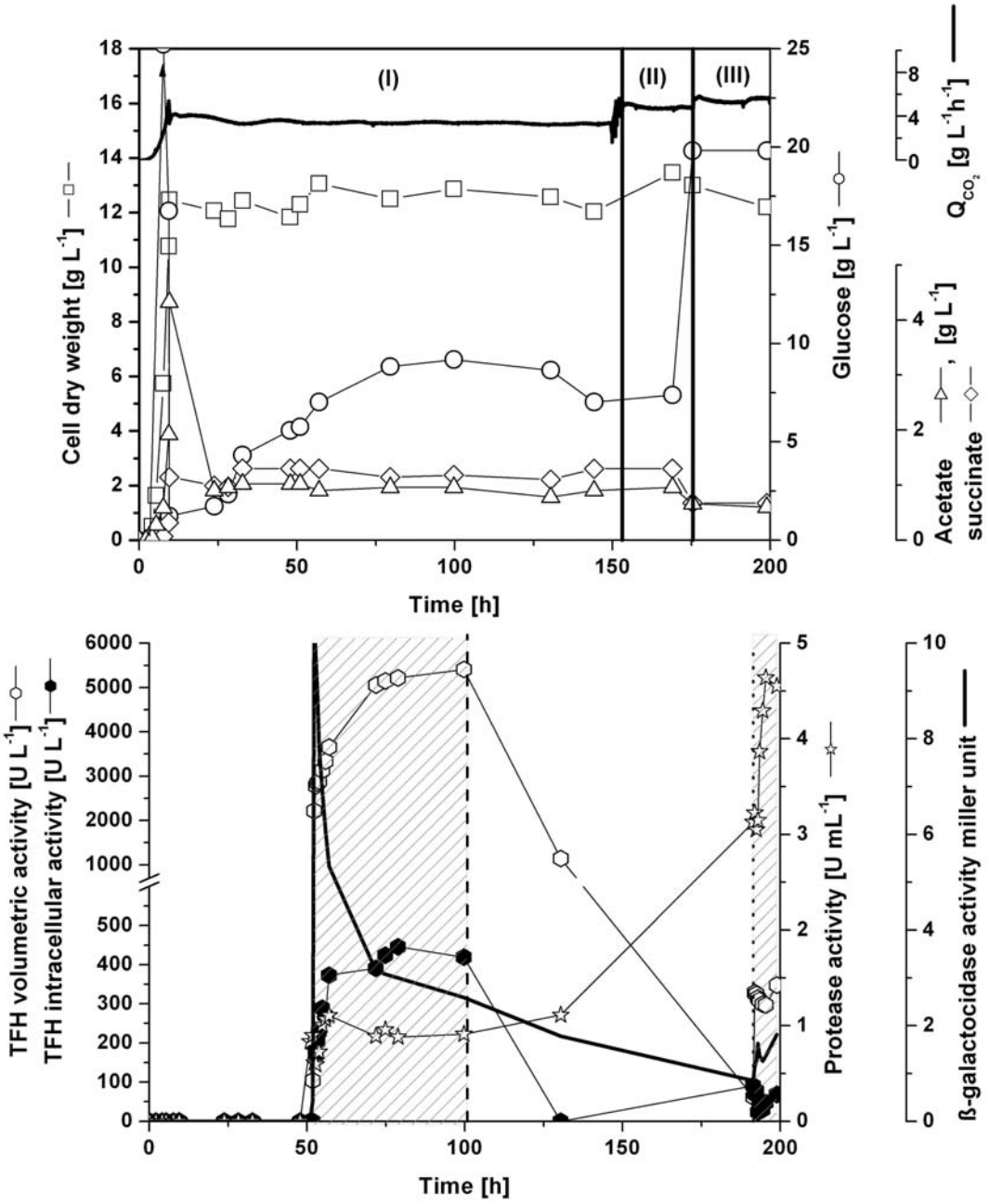

Figure 19. TFH production and export by *B. megaterium* WH323 (Δ*xylA*) using a continuous cultivation. WH323 (Δ*xylA*) containing pYYBm9 was cultivated using A5 medium at three different dilution rates (D): (I) D = 0.1 h^{-1} (II) D = 0.25 h^{-1} (III) D = 0.4 h^{-1} indicated by black lines. Up to 170 h 30 g L^{-1} glucose was present in the feeding solution before the glucose concentration was increased to 50 g L^{-1}. Expression of *tfh* was first induced by addition of 0.5 % (w/v) xylose from 52 h to 101 h at D = 0.1 h^{-1} and from 191 h to 199 h at D = 0.4 h^{-1} indicated by dashed areas.

49 h after induction xylose was washed out by changing back to a feed solution without xylose. A concomitant decrease of secreted TFH activity (20 µg TFH $L^{-1}h^{-1}$) was observed. After 91 h still 62 U L^{-1} TFH were left in the culture medium. The intracellular TFH activity decreased to zero already 30 h after the switch. A complete replacement of the bioreactor volume is already reached after 10 h. Hence, xylose

was absent, the TFH production ceased and the produced TFH in the medium should be washed out. However, after 91 h TFH was still present. The only explanation for the longer retardation of the TFH can be a time consuming protein transport process through the membrane and cell wall.

The glucose accumulation and consumption was dependent on the *tfh* induction by xylose. When xylose was added to induce *tfh*, the glucose concentration increased rapidly to 9 g L^{-1}. This was previously also observed in the high cell density cultivation. When the induction was stopped, the glucose was consumed again.

Second, the transition phase was carried out at a dilution rate of 0.25 h^{-1}. The dilution rate was increased to 0.25 h^{-1} at 153.5 h. This step was set up as an intermediate stage to give the cells time to adapt its physiology to a faster growth condition. Glucose and metabolites concentrations remained constant.

Third, the TFH was produced at a dilution rate of 0.4 h^{-1}. At 175.4 h, the dilution rate was increased to 0.4 h^{-1}. To supply sufficient carbon source the new feed solution contained 50 g L^{-1} glucose instead of 30 g L^{-1} (feed solution 3). This led to a constant cell dry weight of 13 g L^{-1} during the continuous cultivation. When the higher dilution rate was introduced, glucose accumulated rapidly to a maximum of 20 g L^{-1}. This indicated that the maximal glucose uptake rate did not increase with a higher dilution rate. This phenomenon was also observed by Nielsen and co-workers (Christiansen & Nielsen, 2002). Due to the higher dilution rate acetate and succinate decreased to a level of 1 g L^{-1} and 0.6 g L^{-1}, respectively (Figure 19).

The second induction of gene expression by adding 5 g L^{-1} xylose into the bioreactor began at 191.4 h, 16 hours after setting the dilution rate to 0.4 h^{-1}. At the same time the feed solution was changed to the one containing 5 g L^{-1} xylose. However, maximal TFH activity of 329 U L^{-1} was found 0.5 h after the second induction. In the next 4 h it decreased to 297 U L^{-1}. Therefore, the cultivation was stopped. A maximum of 6 U g_{CDW}^{-1} intracellular TFH activity was reached 1 h after induction.

During the cultivation at different dilution rates the expression of a chromosomal *lacZ* gene under the control of the same promoter P_{xylA} in was studied. The β-galactosidase gene was expressed immediately after xylose addition and reached its maximum (11 Miller units) after 0.5 h. In the next 5 h, the amount of β-galactosidase decreased to 5.5 Miller units and further decreased during the washing out of xylose. During the second gene induction by xylose addition, the activity of β-galactosidase

increased from 1.4 to 1.8 Miller units showing a similar production curve as intracellular TFH. The whole β-galactosidase expression suited well to the TFH production which was controlled by the same promoter system.

During the cultivation at different dilution rates, the export of TFH was also accompanied by an increased transport of the neutral protease (Figure 19). At higher dilution rates protease production increased. Four times more protease was produced when the dilution rate increased from 0.1 to 0.4. The decline of TFH at this time was most likely due to the action of extracellular proteases.

Carbon dioxide in the off gas was produced constantly when a certain dilution rate was set. In addition, carbon dioxide increased when the dilution rate was increased. In the batch as well as the feeding phase the pO_2 in the culture medium was always kept at above 20 % air saturation.

Comparing to the high cell density cultivation, less metabolites were produced during the whole cultivation which indicated a more efficient strategy for protein production. By using the continuous cultivation TFH specific activity was improved 6.6-fold from 64 U g_{CDW}^{-1} to 421 U g_{CDW}^{-1}.

IV.1.2.6 Purification of His_6-tagged TFH

IV.1.2.6.1 Purification of secreted TFH from different culture media

As shown above, His_6-tagged TFH was successfully produced and secreted into the growth medium of WH323 (Δ*xylA*) carrying pYYBm9. Next, TFH was successfully purified using Ni-affinity chromatography. The different growth media showed an influence on the purification efficiency. The LB medium from batch cultivation and A5 medium in HCDC were chosen for TFH purification studies. Different pre-treatments of the media were tested prior incubation with the Ni-affinity material. As a control experiment also the media without pre-treatment was used. Because TFH is even stable at elevated temperatures the supernatant was heated to 50 °C for 10 min in order to precipitate less stable exoproteins. Alternatively, in order to lower the salt concentration and adjust the pH for further purification steps the sample was dialyzed against 20 mM sodium phosphate buffer. Due to the observed proteolytic degradation of TFH, 1 mM Pefabloc was added as protease inhibitor. However, SDS-PAGE analysis indicated that some degradation of TFH remained (data not shown).

Table 8. Affinity chromatography purification of His_6-tagged TFH secreted by WH323-pYYBm9 grown in LB batch cultivation and HCDC (A5 medium). Prior affinity chromatography the supernatant was pre-treated: no pre-treatment (1), 50 °C for 10 min (2), 18 h dialysis at 4 °C (3). Data given refer to supernatant (a), recovered purified product by elution from affinity matrix (b), none bound fraction (c).

Cultivation		Total activity [U]	Protein amount [µg]	Specific activity [U $mg_{protein}^{-1}$]	Yield [%]	Purification factor
LB 1	a	37	238	157	100	1.0
	b	20	41	494	54	3.2
	c	2			5	
LB 2	a	35	213	162	100	1.0
	b	17	37	471	50	2.9
	c	1			2	
LB 3	a	23	147	159	100	1.0
	b	13	42	310	55	1.9
	c	1			6	
HCDC 1	a	49	203	240	100	1.0
	b	25	83	307	52	1.3
	c	29			59	
HCDC 2	a	47	221	213	100	1.0
	b	23	63	367	49	1.7
	c	21			46	
HCDC 3	a	29	161	178	100	1.0
	b	10	45	215	34	1.2
	c	9			32	

Results are summarized in Table 8. The error of measurements was less than 10 %. TFH in LB medium from the batch culture bound efficiently to the affinity material. Less TFH binding was observed for the A5 medium of the HCDC. This might be attributed to the presence of additional interfering proteins in the HCDC medium as exhibited by SDS-PAGE. However, using LB medium about half of the TFH protein which was bound to the affinity material did not elute. For both media, pre-treatment by dialysis (LB 3 and HCDC 3) yielded the lowest purification factors. This may be caused by irreversible adsorption of TFH to the dialysis membrane. Comparable results were obtained for the control (no pre-treatment) and the heat treated sample. Hence, applying the supernatant of the LB medium cultivation without any pre-treatment directly to the affinity material is the method of choice.

IV.1.2.6.2 Purification of secreted TFH using different methods

In order to improve the yield and the purification efficiency different purification strategies were tested for purification of the secreted TFH from continuous cultivation.

Table 9. Comparison of three different purification strategies of His_6-tagged TFH secreted by WH323-pYYBm9 grown in continuous cultivation using A5 medium. (1) Sartobind IDA 75 Metal Chelate Membrane Adsorbers (Sartorius AG, Goettingen, Germany), with a prefiltration of the media with a cut off of 0.2 µm. (2) Chelating Sepharose Fast Flow Gel. (3) ProPur Sample IMAC Pack (Nunk, Wiesbaden, Germany). Data given refer to supernatant (a), recovered purified product by elution from affinity matrix (b), none bound fraction (c).

Material Method	Fractions	Total activity [U]	Protein amount [µg]	Specific activity [U $mg_{protein}^{-1}$]	Yield [%]	Purification factor
(1)	a	3167	91000	35	100	1
	0,2 µm	2678	86000	31	85	0.89
	b	1022	3000	340	32	9.7
	c	1359	64000	21	43	
(2)	a	2.8	91	30	100	1
	b	0,86	7	122	31	4
	c	0.96	50	19	34	
(3)	a	2.8	91	30	100	1
	b	0.66	7	101	24	3.3
	c	0.63	38	17	23	

In addition to the previously used chelating Sepharose Fast Flow gel (Amersham Bioscience; Freiburg; Germany) two new commercial systems named ProPur IMAC Pack (Nunk; Wiesbaden; Germany) and Sartobind IDA 75 metal chelate membrane adsorbers (Sartorius AG; Goettingen; Germany) were tested. These systems are usually chosen due to easy and rapid handling at a low cost. A rapid processing avoids the proteolytic degradation of TFH. Furthermore, solving the problem of insufficient elution from the Chelating Sepharose was attempted. Propur and Sartobind belong to a new generation of Immobilized Metal Affinity Chromatography (IMAC) purification devices. The most common matrix for IMAC is Ni-NTA, but in the new system iminodiacetic acid (IDA) is used for metal complexation showing a high

affinity to Ni metal ions. Results are summarized in (Table 9). The purification factor was improved from 4 to 9.7 (2.4 fold) by using Sartobind IDA 75 Metal Chelate Membrane Adsorbers instead of Chelating Sepharose Fast Flow Gel. However, during the pre-filtration with 0.2 µm filter 15 % of enzyme activities are lost. The yield was similar compared to other strategies after the purification. The lowest purification factor and yield was obtained using ProPur IMAC Pack probably due to the short binding time. Reloading of the none bound fraction to the column did not improve the purification.

IV.1.2.6.3 Ultrafiltration, size exclusion chromatography and concentration of eluted TFH

Since imidazole may strip a metal ion cofactor from the target protein, an irreversible precipitation can occur, if the purified proteins are stored at - 20 °C or - 80 °C, caused by the high amount of imidazole in the elution buffer. Hence, imidazole is removed by diafiltration using ultrafiltration concentrators or rapid dialysis against an appropriate buffer. Here, the ultrafiltration step led to an 10-fold concentration of TFH, but only 32 % of the TFH after Ni-affinity chromatography were recovered (Table 10).

Table 10. Purification and recovery of the His_6-tagged TFH secreted by WH323-pYYBm9 grown in A5 continuous cultivation after Ni–affinity chromatography using Sartobind IDA 75 metal chelate membrane adsorbers.

Purification steps	Total units [U]	Protein amount [µg]	Specific activity [U mg $_{protein}^{-1}$]	Yield [%]	Purification factor
Supernatant	3167	91000	35	100	1
Filtration	1022	3000	340	32	9.7
Gel filtration	796	1814	439	25	12.5
Concentration	483	1385	349	15	9.9

Next, the target protein was further purified by size exclusion chromatography. The bed volume of the column was 319 mL. The void volume was 96 mL. According to the calibration equation TFH was eluted at 200 mL (data not shown). In this fraction also active enzyme was found. Imidazole and other small molecules from the Ni-affinity chromatography elution medium led to a large peak at 300 mL. After metal chelate affinity chromatogram using Sartobind IDA 75 metal chelate membrane adsorbers relative high amounts of hydrolyzing activity remained in the none-bound fraction (Table 10). Using size-exclusion chromatography it was further studied if this non-bound fraction contained TFH which did not bind to the Ni-affinity material. A

clearly peak was also appeared at 100 mL with 30 U L^{-1} volumetric activity in the TFH assay (data not shown). This active protein was eluted at around void volume. Hence, it could be aggregated TFH with a larger molecular mass. The aggregation may also explain why this TFH did not bind to the affinity column.

IV.1.3 Discussion

Dresler *et al*. (2006) studied the production of TFH in *E. coli*. The *tfh* gene with DNA encoding a C-terminal His_6-tag and an N-terminal OmpA leader sequence was expressed using a temperature inducible promoter and localized on a free replicating plasmid. The cultivation techniques and methods were similar to that used in this study. However, Dresler *et al*. (2006) also observed considerable release of TFH into the medium. The secreted amounts of TFH of the present work and that using *E. coli* as host (Dresler *et al.*, 2006) were compared in Table 11. For the batch cultivations with LB medium and the HCDC with synthetic medium the results are comparable for the two systems. This is a considerable progress (50 – 100-fold) compared to the production of TFH in the wild type *Thermobifida fusca* strain (Dresler *et al.*, 2006; Gouda *et al.*, 2002).

Table 11. TFH production in *E. coli* and *B. megaterium*

Cultivation	**Medium**	***B. megaterium* WH323**		***E. coli* TG 1**	
		U g_{CDW}^{-1}	**U L^{-1}**	**U g_{CDW}^{-1}**	**U L^{-1}**
Batch	**LB**	**2651**	**7953**	**4000**	**8000**
Batch	**A5**	**116**	**886**	**770**	**7300**
HCDC	**A5**	**187**	**6098**	**76/227***	**5500/12000***
Chemostat					
D = 0.1	**A5**	**421**	**5410**		
D = 0.4	**A5**	**6**	**25**		

* dependent on feeding rate in induction phase (temperature shift)

Using a high cell density cultivation the maximum secreted TFH specific activity reached 187 U g_{CDW}^{-1} and was higher than that obtained in batch cultivation with A5 medium. The volumetric TFH activity in the culture broth passed a maximum about 2 to 3 h later and it was 6098 U L^{-1} (Table 11, Figure 17). In view of the increased experimental efforts to carry out HCDC this result was, however, disappointing as an even higher volumetric secreted TFH activity of about 7953 U L^{-1} was achieved in the batch process with LB medium (Figure 16). A further cultivation optimization process

in a chemostat with A5 medium clearly demonstrated that the protein was produced efficiently at lower growth rates. Similar amount of TFH in the supernatant were produced compared to TFH production using HCDC, but with a 2.4-fold higher specific activity. Hence, production of TFH in pH controlled batch reactors using LB medium or with semi defined A5 medium in a continuous cultivation has to be recommended on the basis of the findings of the present study.

For the production in LB medium also better results were obtained in the purification in comparison to HCDC and batch cultivation. Furthermore, Sartobind IDA 75 metal chletate membrane adsorbers was found out to be more efficient as it has a 2.4-fold and 3-fold higher purification factor than with common used Chelating Sepharose Fast Flow Gel and Propur Sample IMAC Pack, respectively. Further medium optimization as performed for PGA production may still improve TFH production.

IV.1.4 Summary for the recombinant production and secretion of TFH using *B. megaterium*

After codon optimization TFH was successfully produced and secreted by a recombinant *B. megaterium* strain. A strain lacking the xylose utilization system increased the TFH yield and made the system applicable for long-term gene induction in batch and fed-batch cultivations. From the specific activity of purified TFH it can be concluded that 2.9 mg TFH L^{-1} were secreted in shaking flask cultivation with LB medium. This was further increased to 18.1 mg L^{-1} in a pH controlled batch cultivation. With A5 medium applying a high-cell density cultivation compared to a pH controlled batch the secretion was increased 7-fold to 13.9 mg L^{-1}. Finally, using a continuous cultivation 12.3 mg L^{-1} TFH was secreted and the productivity was improved 2.3-fold to 421 U g $_{CDW}^{-1}$ compared to the production in high cell density cultivation.

IV.2 Recombinant Penicillin G amidase (PGA) production and export using *B. megaterium*

In the second part of the thesis, *B. megaterium* was used to produce a homologous penicillin G amidase. This enzyme is not present in the employed production strains, but was cloned from *B. megaterium* ATCC 14945 and placed under control of the xylose inducible promoter P_{xylA} using the expression plasmids pRBBm23 and pRBBm49.

IV.2.1 Rationale of the experimental approach for PGA production in *B. megaterium*

First, in order to stabilize the desired product PGA in the growth medium the influence of calcium ions and the extracellular protease NprM on enzyme stability and activity were investigated. Subsequently, the leader peptide of the extracellular lipase LipA from *B. megaterium* was tested for the improvement of PGA export. Gene induction using the promoter P_{xylA} was analyzed in a *xylA* mutant strain to prevent inducer utilization. Finally, medium optimization and up scaling were approached systematically.

IV.2.1.1 Increased recombinant PGA production and secretion using *B. megaterium* by the addition of calcium ions

Previous investigations of homologous PGA production in *E. coli* identified calcium as an important factor for protein folding and maturation (Ignatova *et al*., 2005; Kasche *et al*., 2005). An amino acid sequence alignment of PGA from *B. megaterium* and *E. coli* showed that all active site amino acids were conserved. However, an overall amino acid sequence identity of only 28.4 % was observed (Table 12). Firstly, both PGAs have the Ser1 residue at the N-terminal of β-chain contributing to the active site. The Ser1 residue functions as both a nucleophile and a catalytic base to enhance nucleophilicity (Lee *et al*., 2000; Oinonen & Rouvinen, 2000). Secondly, both PGAs from *E. coli* and *B. megaterium* carry the identical amino acid residues forming the oxyanion hole. An intermediate oxyanion tetrahedral transition state helps stabilizing the substrate through hydrogen bonding. The reaction intermediate is formed by the nucleophilic attack of the N-terminal hydroxyl group of Ser1: β onto the carbonyl carbon of the substrate peptide bond. Thirdly, the conserved calcium ion coordination sphere suggests that also *B. megaterium* PGA utilizes the calcium ion bound at the lip of the active site to aid in stabilization of the active site and in

connecting the two subunits. Fourthly, the highly conserved critical amino acid residues for autoproteolysis assure the active centre formation of mature PGA after cleavage of the signal peptide and the linker peptide. Hence, although the degree of sequence identity is low, structurally important amino acids and as a consequence enzyme function were found conserved, indicating homology at the structural level.

Table 12. Comparison of *E. coli* and *B. megaterium* PGA based on alignment of their amino acid sequences (McVey *et al.*, 2001)**.**

Organism	Nucleophile	Close to Nucleophile	Close to N_α	Autoproteolysis	Oxyanion hole	Substrate binding	Calcium ion coordination
E. coli	Ser1 β	Gln23 β	Asn241 β Gln23 β	Ser1 β Lys10 β	Ala69 β Asn241 β Gln23 β	Phe24 β Phe57 β Ser67 β	Phe71 β Asp73 β Phe146 α Glu152 α Val75 β Asp76 β
B. megaterium	Ser1 β	Gln23 β	Asn246 β Gln23 β	Ser1 β Lys10 β	Ala69 β Asn246 β Gln23 β	Phe57 β	Asp76 β Phe147 α Glu153 α

Hence, the influence of calcium ions on the activity of *B. megaterium* PGA was tested. The complete *pga* gene was cloned into the *Bsr*GI/*Sac*I site of pMM1522 placing its expression under control of the xylose inducible promoter. The new vector pRBBm23 was transformed into protoplasted *B. megaterium* MS941 cells. This *B. megaterium* strain is deficient in the major extracellular protease NprM due to deletion of the corresponding gene. Significant stabilization of exported proteins by *B. megaterium* MS941 was reported before (Malten *et al.*, 2005a; Wittchen & Meinhardt, 1995). The influence of different calcium ion concentrations on the secretion of recombinant PGA was tested in shaking flask cultivations. Comparing the addition of various calcium ion concentrations to the complex LB growth medium demonstrated that 2.5 mM $CaCl_2$ was optimal for PGA production (Figure 20 + Figure 21). Three hours after induction 189.4, 489.9, and 287.3 U PGA g_{CDW}^{-1} were measured in the growth medium containing none, 2.5, and 5 mM $CaCl_2$, respectively. The addition of 2.5 mM $CaCl_2$ increased the amount of secreted PGA 2.6-fold (Figure 20) and has no influence on the cell growth compared to the culture without $CaCl_2$ addition (Figure 21). Furthermore, addition of 5 or 10 mM $CaCl_2$ resulted in lower amounts of biomass which is probably due to growth inhibition by higher concentration of calcium ions (Figure 21). Therefore, 2.5 mM $CaCl_2$ were added to the growth medium for recombinant PGA production in all following experiments.

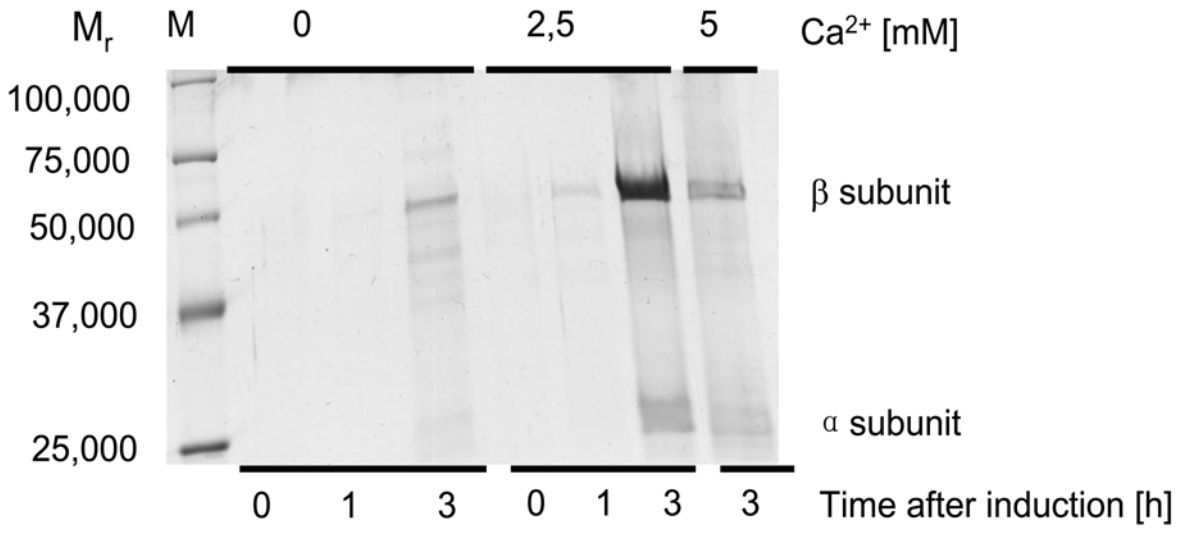

Figure 20. Influence of calcium ions on PGA production and export. *B. megaterium* MS941 carrying pRBBm23 (encoding SP_{pga}-PGA) was cultivated in LB medium with indicated concentrations of $CaCl_2$. Proteins from 1.5 mL cell-free growth medium were precipitated by ammonium sulphate, analyzed by SDS-PAGE and stained with Coomassie Brilliant Blue G250. Lane M shows Precision Plus Protein Standard (Bio-Rad, München, Germany).

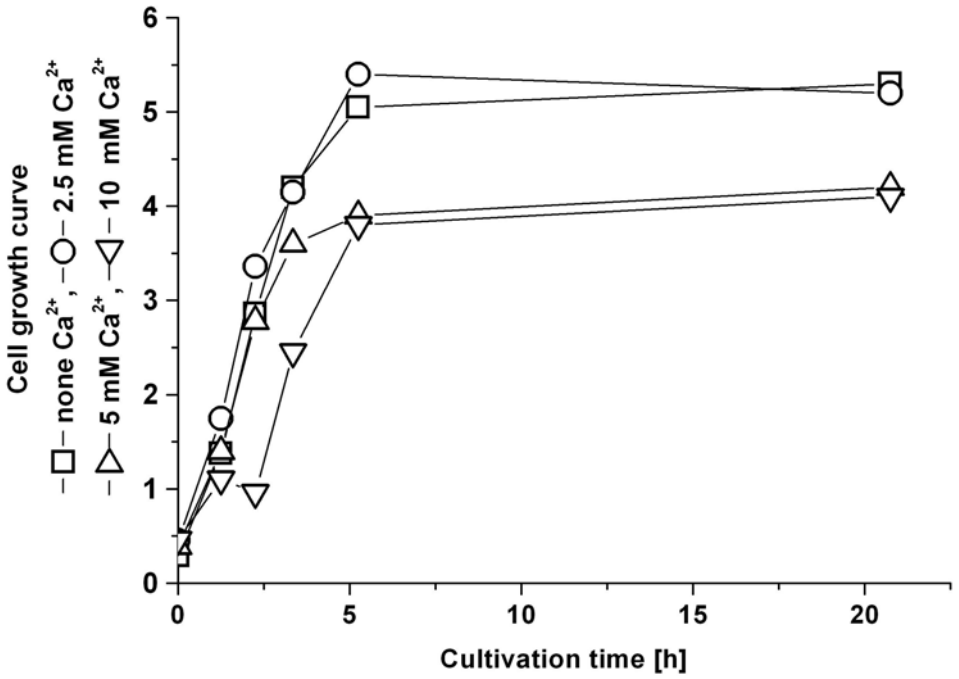

Figure 21. Influence of calcium ions on cell growth. *B. megaterium* MS941 carrying pRBBm23 (encoding SP_{pga}-PGA) was cultivated in LB medium with indicated concentrations of $CaCl_2$.

IV.2.1.2 Characterization of secreted *B. megaterium* PGA

The *pga* gene was initially cloned with the 5' region encoding its mature signal peptide SP_{pga}. SDS-PAGE analysis of the extracellular proteins of recombinant *B. megaterium* carrying pRBBm23 (encoding SP_{pga}-PGA) revealed two subunits of PGA with relative molecular masses (M_r) of 30,000 (α-chain) and 60,000 (β-chain) (Figure 20). The N-terminal amino acid analysis of both recombinant exported proteins indicated that the α-chain started at amino acid residue 25 (GEDKNEGVKVVR) while the N-terminal amino acid sequence of the β-chain SNAAIVGSEKSATGN corresponded to residues 266 to 279. Hence, the α- and β- subunit of PGA range from residue 25 to 265 and from 266 to 802 with calculated molecular masses of 27,753 Da and 61,394 Da, respectively. These calculated masses corresponded well to the experimentally observed masses of the subunits and suited perfectly the report by Panbangred *et al*. (Panbangred *et al*., 2000). The native signal peptide sequence was deduced as MKTKWLISVIILFVFIFPQNLVFA.

IV.2.1.3 The signal peptide of the extracellular lipase LipA increases PGA export in *B. megaterium*

In previous works, the signal peptide of the *B. megaterium* extracellular esterase LipA (SP_{lipA}) was successfully used for the secretion of *Lactobacillus reuteri* levansucrase (Malten *et al*., 2006) and *T. fusca* hydrolase. In order to analyze the efficiency of the LipA signal peptide for the secretion of recombinant *B. megaterium* PGA, protein secretion mediated by SP_{lipA} and by its natural signal peptide (SP_{pga}) were compared. *B. megaterium* strain MS941 carrying the plasmid pRBBm49 encoding a SP_{lipA}-PGA fusion and the plasmid pRBBm23 encoding the native PGA (SP_{pga}-PGA) were cultivated in LB medium, respectively. A maximum of 380.0 and 230.0 U PGA g_{CDW}^{-1} were measured for the exported PGA using the SP_{lipA} and SP_{pga}, respectively. Hence, changing the original signal peptide of PGA to the one of LipA improved the amount of secreted PGA 1.7-fold (Table 13).

Table 13. Stepwise improvement of PGA production and export using *B. megaterium*. *B. megaterium* MS941 carried a *nprM* knock out, whereas YYBm1 combined the *nprM* knock out with a *xylA*$^-$ knock out. The plasmid pRBBm23 (encoding SP_{pga}-PGA) and the plasmid pRBBm49 (encoding SP_{lipA}-PGA). Media were supplemented with 2.5 mM $CaCl_2$, LB1 includes tryptone from Oxoid, LB2 was prepared with tryptone from Bacto, AA: amino acid solution, MM: MOPSO based minimal medium, SF: shaking flask cultivation. Batch: pH controlled fermentation. The purified enzyme has a specific activity of 45 U $mg_{protein}^{-1}$ (Yang *et al*., 2001). Standard deviations performed experiments were below 10 %.

Strain	Plasmid	Medium*	Cultivation	PGA activity [U g_{CDW}^{-1}]	PGA [mg L^{-1}]
MS941	pRBBm23	A5	SF	6.0	0.3
MS941	pRBBm23	A5	Batch	17.0	4.2
MS941	pRBBm23	LB1	SF	230.0	25.0
MS941	pRBBm49	LB1	SF	385.0	36.0
MS941	pRBBm49	LB2	SF	500.0	20.0
YYBm1	pRBBm23	LB1	SF	280.0	33.0
YYBm1	pRBBm49	LB1	SF	390.0	41.0
YYBm1	pRBBm49	LB2	SF	830.0	22.0
YYBm1	pRBBm49	MM	SF	0.0	0.0
YYBm1	pRBBm49	MM + 0.5 x AA	SF	170.0	11.0
YYBm1	pRBBm49	MM + 1 x AA	SF	330.0	35.0
YYBm1	pRBBm49	MM + 2 x AA	SF	200.0	28.0
YYBm1	pRBBm49	LB2	Batch	640.0	25.0
YYBm1	pRBBm49	MM + 1 x AA	Batch	320.0	29.0
MS941	pRBBm23	A5 + Glu feed	HCDC	0.8	0.9
YYBm1	pRBBm23	A5 + Glu feed	HCDC	7.6	5.9
YYBm1	pRBBm23	A5 + Glu feed Early induction	HCDC	0.7	0.7
YYBm1	pRBBm49	LB + Glu feed	HCDC	48	25.0

IV.2.1.4 Construction of a *B. megaterium* strain deficient in xylose utilization and the extracellular protease NprM

HPLC analysis of growth medium of batch cultivations with MS941 carrying pRBBm23 (encoding SP_{pga}-PGA) in A5 medium indicated the utilization of xylose as carbon source after the majority of glucose in the growth medium was consumed. In order to improve target gene induction efficiency, a constant level of the inducer xylose during cultivation had to be guaranteed. This was achieved by constructing a stable strain deficient in xylose utilization (Rygus *et al*., 1991). In agreement with this assumption, the use of the *xylA* knock-out mutant strain *B. megaterium* WH323 (Δ*xylA*) in protein production using the xylose inducible promoter resulted in higher yields of intracellularly produced heterologous protein (Biedendieck *et al.*, 2007). However, a major drawback of WH323 was an increased secretion of the neutral extracellular protease NprM. *B. megaterium* MS941 employed in this study lacks

NprM (Malten *et al*., 2005b; Wittchen & Meinhardt, 1995). Hence, a strain deficient in xylose utilization based on *B. megaterium* MS941 was constructed by interrupting the gene encoding the xylose isomerase *xylA* with the *cat* gene mediating chloramphenicol resistance. The new strain was named YYBm1. The phenotype and genotype of this new strain were analyzed. In order to test the stability of strain YYBm1, the growth characteristic of the first and later generations were compared.

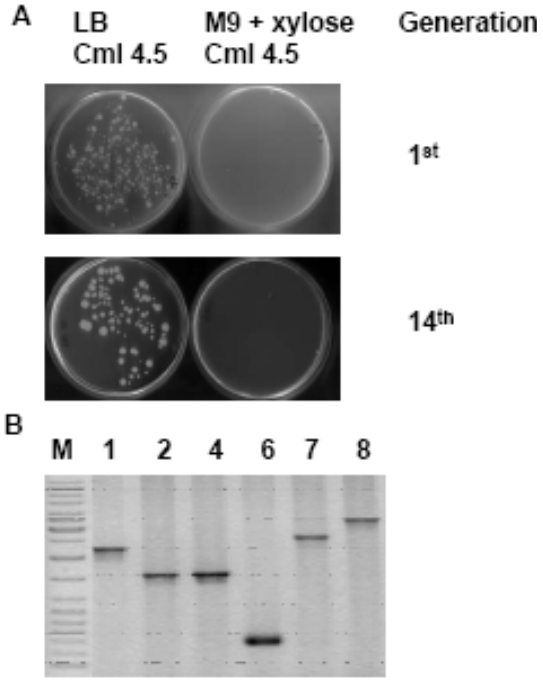

Figure 22. YYBm1 phenotype and genotype test. (A) Different generation of YYBm1 cell inoculated in LB liquid medium at 42 °C for 12 h. Cells were diluted to 100 cells μL^{-1} and incubated on agar plate of complex LB medium and M9 minimal medium with 1 % (w/v) xylose as sole carbon source. 4.5 µg mL^{-1} chloramphenicol (*cml*) were used for antibiotic selection. The single colony was picked up and further inoculated on the two plates. Phenotypes were compared after 1st and 14th generation inoculation. (B) Correct integration of the *cml* cassette into the *xylA* gene was tested by PCR with corresponding pairs of primers.

Gel band Nr.	PCR primer	PCR theoretical size	PCR Experimental size	Predicted fragment
1	xylR_for cmL_rev	2008	+	*xylR-xylA'-cml*
2	cmL_for xylB_rev	1518	+	*cml-'xylA-xylB*
4	putative4_for xylB_rev	1432	+	*xylA'-'xylA-xylB*
6	pcr_ery_s pcr_ery_antis	561	+	*ery*
7	xylR_for' xylB_rev'	2330	+	*xylR-xylA-xylB*
8	pcr_ery_s xylB_rev'	3037	+	*ery-xylA-xylB*

One generation was defined as a 12 h cultivation of the strain in LB liquid medium without chloramphenicol antibiotic at 42 °C. Thereafter, one percent medium with cells was inoculated with new LB medium for the next generation. The cells of the first and later generations were diluted to 100 cell μL^{-1} and further plated and

cultivated on agar plates with LB medium and minimal medium with xylose as sole carbon source. *B. megaterium* YYBm1 of the first and the 14th generation grew on the LB agar plate with chloramphenicol and did not grow on minimal medium with xylose as sole carbon source (Figure 22A). Hence, *B. megaterium* YYBm1 was deficient in xylose utilization and showed a stable phenotype over multiple generations. The corresponding genotype of YYBm1 was analyzed by PCR. The amplified fragments suggest the presence of the *cml* and *ery* antibiotic resistance gene. Usually, the obtained phenotype is only present after a second crossover, which also eliminates the erythromycin resistance. However, observed results suggest that the inactivation of the *xylA* occurred already after the first crossover. Due to the shown stability of this *xylA*$^-$ phenotype this strain was further used (Figure 22B).

Next, the xylose metabolization of *B. megaterium* strains MS941(Δ*nprM*), WH320, YYBm1 (Δ*nprM*, *xylA*$^-$) and WH323 (Δ*xylA*) was compared. These strains were cultivated in minimal medium with glucose as sole carbon source.

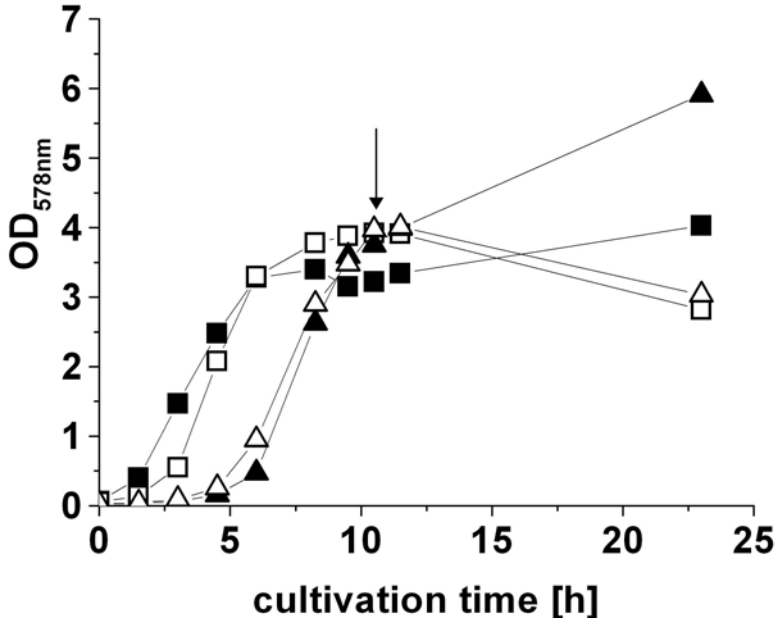

Figure 23. *B. megaterium* YYBm1 is deficient in xylose utilization. Shaking flask cultivation of *B. megaterium* strain MS941 (Δ*nprM*) (■), YYBm1 (Δ*nprM*, *xylA*$^-$) (□), WH320 (▲), and WH323 (Δ*xylA*) (Δ) in minimal medium with glucose as initial carbon source. At the beginning of the stationary phase, 5 g L^{-1} xylose was added as second carbon source into the growth medium (indicated by arrow).

When glucose in the growth medium was consumed, all *B. megaterium* strains stopped growing and entered the stationary phase (Figure 23). After addition of xylose as second carbon source, the strains MS941 and WH320 entered into a

second exponential phase of growth, whereas cells of the strains YYBm1 and WH323 died. Hence, YYBm1 and WH323 were unable to utilize xylose as carbon source (Figure 23). Consequently, the *xylA nprM* double mutant YYBm1 revealed the expected phenotype. When tested in protein production experiments, YYBm1 secreted 390.0 U PGA per gram CDW compared to 380.0 U PGA per gram CDW by MS941 (Table 13). Comparing the two strains for the export of PGA carrying its natural leader peptide an increase of 1.2-fold (230 vs. 280 U g_{CDW}^{-1}) in the specific activity was observed (Table 13).

IV.2.1.5 Optimization of the gene induction strategy

Next, early and late induction of gene expression by the addition of xylose were compared. When the inducer xylose was added right at the beginning of the cultivation, the maximal specific activity was reached 7.5 h after the start of cultivation.

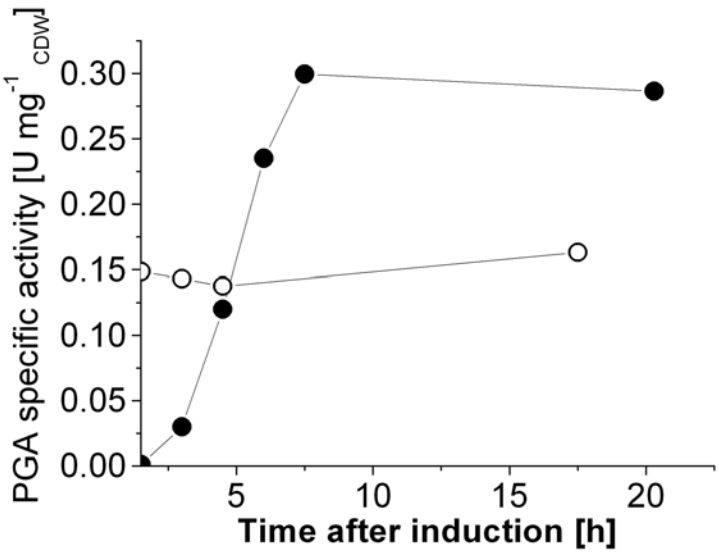

Figure 24. Early and late induction of PGA production by xylose addition to the growth medium. *B. megaterium* YYBm1 (Δ*nprM*, *xylA*⁻) containing pRBBm23 was grown in LB medium. Induction of gene expression took place at the beginning of cultivation (●) and at OD 4 (○) by adding 0.5 % (v/w) xylose into the growth medium.

Similar final activities were reached when xylose was added at an OD_{578nm} of 0.4. An induction of gene expression at higher optical density, *e.g.* at OD_{578nm} 4, led to a faster appearance of PGA activity after induction, however, just half the amount of PGA was obtained compared to the early induction (Figure 24). Hence, 5 g L^{-1} xylose was added right at the beginning of the cultivation for recombinant PGA production in the following experiments.

IV.2.1.6 Optimization of the complex growth medium

Next, the effects of the addition of tryptones from two different companies to the complex growth medium were investigated. PGA secretion by MS941 carrying pRBBm49 (encoding SP_{lipA}-PGA) in LB medium was improved 1.8-fold to 36.0 mg L^{-1} by utilizing tryptone from Oxoid (Wesel, Germany) instead of that from Bacto (Heidelberg, Germany) (Table 13). These two tryptones varied in the concentrations of contained amino acids, especially in the amount of arginine, aspartic acid, and tyrosine. Used Oxoid versus Bacto tryptone contain 5.53 % to 3.03 % arginine, 7.31 % to 6.11 % aspartic acid, and 3.1 % to 1.42 % tyrosine, respectively. 1.8 times more PGA (41 mg L^{-1}) was secreted by YYBm1 (Δ*nprM*, *xylA*$^-$) carrying pRBBm49 (encoding SP_{lipA}-PGA) in LB medium utilizing Oxoid tryptone compared to Bacto tryptone (Table 13). For MS941 (Δ*nprM*) and YYBm1 a maximal OD_{578nm} of 14 were reached during cultivation with Oxoid tryptone. Only OD_{578nm} of 4 and 6 were reached by MS941 and YYBm1, respectively, when grown in LB containing Bacto tryptone. Interestingly, in contrast to the volumetric activity the specific activity is 1.4- and 2-fold higher for PGA obtained from cultivations of *B. megaterium* MS941 and YYBm1 using tryptone from Bacto instead of Oxoid, respectively (Table 13). Another difference in cultivation with these two media was the production of an extracellular immune inhibitor A metalloprotease like protein Q73BM2 (M_r = 84,400) in the presence of tryptone from Oxoid (Figure 25). The production of this protein was observed before for *B. megaterium* by Wang and co workers (Wang *et al*., 2006). The protein was identified using the MASCOT program with MALDI-TOF/MS data and the strain-specific protein database “bmgMECI”.

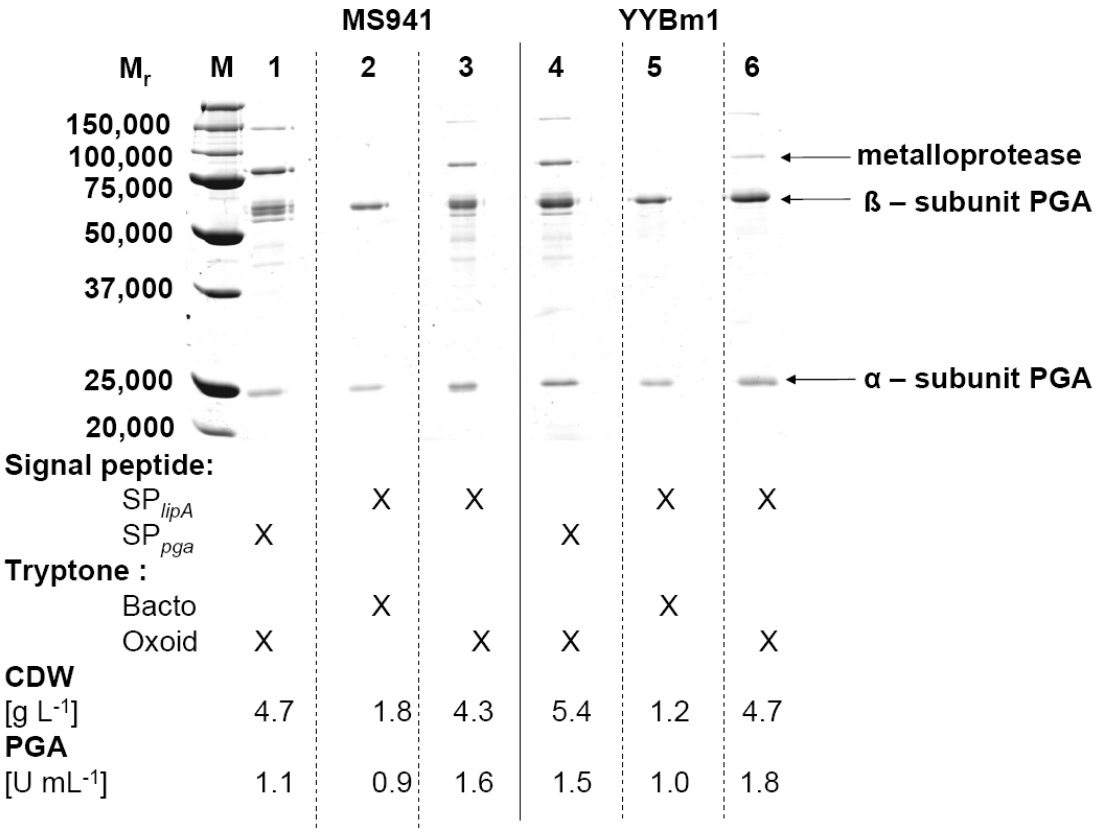

Figure 25. Comparison of different leader peptides for the production and export of *B. megaterium* PGA. PGA was produced in shaking flask cultivation of *B. megaterium* MS941 (Δ*nprM*) and YYBm1 (Δ*nprM*, *xylA*$^-$) carrying either pRBBm23 (encoding SP$_{pga}$-PGA) or pRBBm49 (encoding SP$_{lipA}$-PGA) in LB medium containing tryptone from different companies. At an OD_{578nm} of 0.4, *pga* expression was induced by the addition of 5 g L^{-1} xylose to the growth medium. Samples were taken at various time points after induction. Proteins from 10 µL unconcentrated growth medium were separated by SDS-PAGE and stained with Coomassie Brilliant Blue G250. Biomass concentration and PGA volumetric activity 24 h after induction of recombinant gene expression are shown.

IV.2.1.7 From complex to mineral medium

For the control and subsequent directed optimization of the fermentation process defined mineral media are desired. Moreover, these mineral media usually are less cost intensive compared to complex media. Therefore, we systematically developed a mineral medium for PGA production and export in *B. megaterium*. First, the previously developed semi-defined A5 medium (Malten *et al.*, 2005b) containing 0.5 g L^{-1} yeast extract and a newly developed mineral medium based on MOPSO buffer were tested in comparison to complex medium.

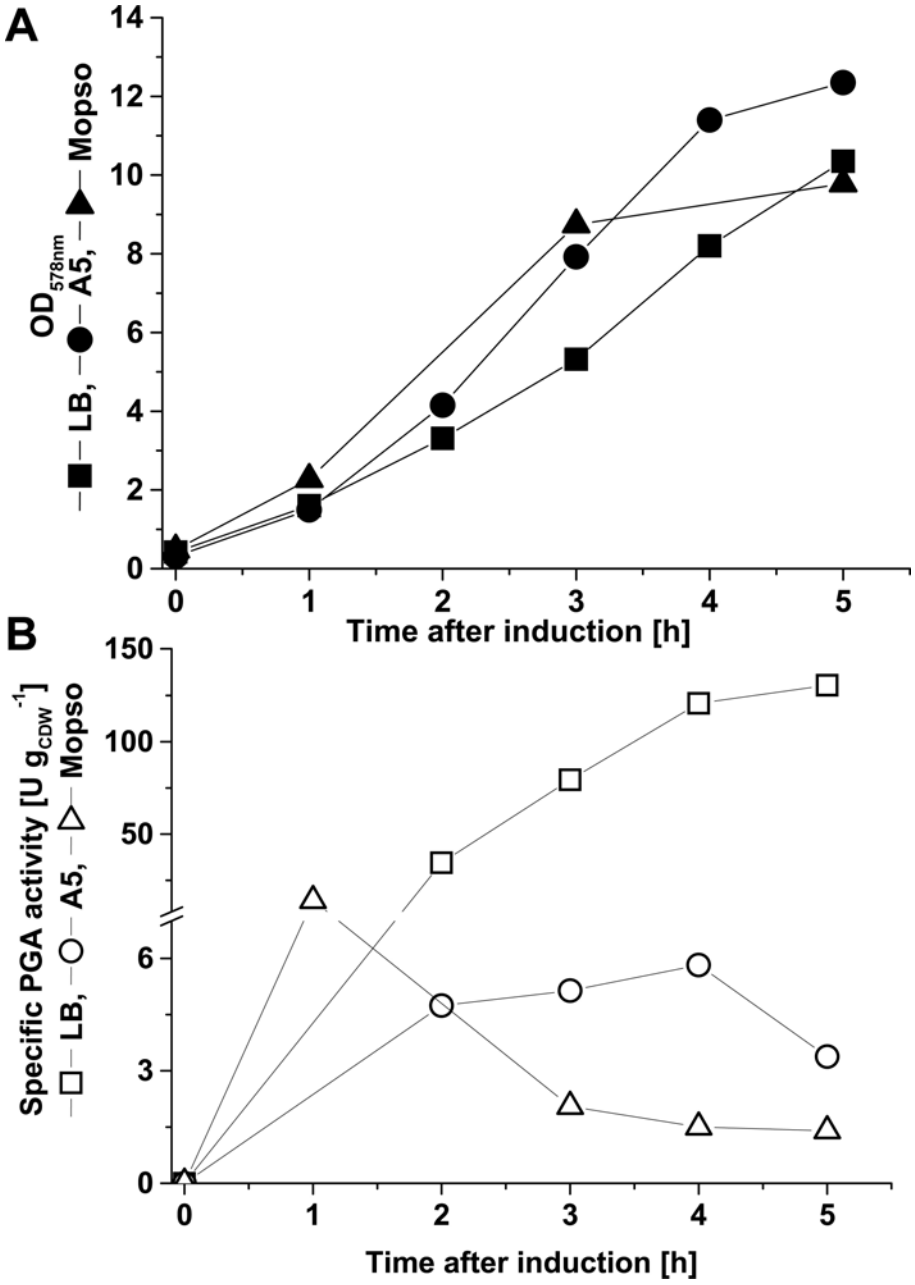

Figure 26. Comparison of growth media for PGA production and export using *B. megaterium* in shaking flask cultivation. MS941 (Δ*nprM*) carrying pRBBm23 (encoding SP_{pga}-PGA) grew in LB (square), A5 (circle), and MOPSO (triangle) medium. The *pga* expression was induced at OD_{578nm} of 0.4 by adding 5 g L^{-1} xylose. (A) Solid symbols represent the measured growth curve. (B) Open symbols represent specific PGA activity.

Growth and secretion of PGA were initially compared for the different media in shaking flask cultivations of *B. megaterium* MS941 carrying pRBBm23 (encoding SP_{pga}-PGA) (Figure 26). Using complex medium, maximal specific PGA activity of 131 U g_{CDW}^{-1} was reached 5 h after induction of *pga* expression. Cultivation in semi-defined A5 medium led to a drastic 22-fold reduction (maximum of 6.0 U g_{CDW}^{-1}) while in MOPSO derived medium specific PGA activity was reduced 9.4-fold (maximum of

14 U g_{CDW}^{-1}) (Figure 26). Although the MOPSO derived mineral medium was a protein and amino acid free medium, similar cell densities were reached compared to complex medium. In addition, higher specific PGA activities compared to the semi-defined A5 medium were achieved. Hence, we started to optimize the MOPSO-based medium by systematic supplementation of nutrients to increase PGA production and export.

Acevedo *et al*. (1973) and Pinotti *et al*. (2000) showed the requirement of certain amino acids for a high production of PGA in *B. megaterium* ATCC14945 (Acevedo & Cooney, 1973; Pinotti *et al.*, 2000). Hence, for improving the productivity in minimal medium, the influence of the amino acid addition on PGA secretion was investigated. Free amino acids as arginine, proline, histidine, and asparagines were selectively added to the medium including glucose as carbon source and casein as nitrogen source (Pinotti *et al*., 2000). Here, growth and PGA production of *B. megaterium* YYBm1 (Δ*nprM*, *xylA*$^-$) carrying pRBBm49 (encoding SP_{lipA}-PGA) was systematically investigated in 96-well microtiter plates.

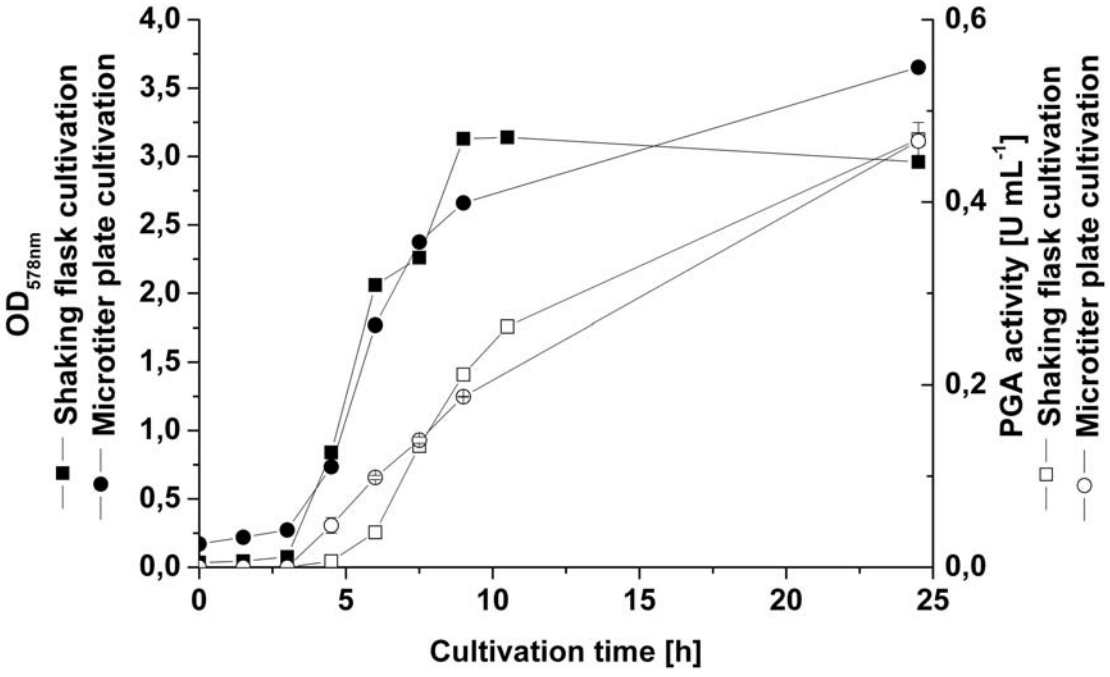

Figure 27. Cultivation and PGA production in microtiter plates. *B. megaterium* YYBm1 (Δ*nprM*, *xylA*$^-$) carrying pRBBm49 (encoding SP_{lipA}-PGA) was cultivated in LB medium using microtiter plates and shaking flasks. Cell growth from microtiter plate cultivation was measured with a spectrophotometer at OD_{578nm} and Multiskan Ascent photometer at OD_{580nm}. PGA activity measurements were performed as described in material and methods.

The expression of *pga* was induced at the beginning of cultivation. First, the cell growth and protein production characteristics were compared to shaking flasks cultivations using LB medium. Similar cell growth curves and comparable amounts of enzyme were achieved at the end of cultivations (Figure 27). Hence, the microtiter plates allow cultivation comparable to shaking flasks with the advantage of high through-put. Next, according to their corresponding metabolic pathways (Michal, 1999), the 20 amino acids were grouped into 7 families: I. glycine and serine; II. valine, leucine and isoleucine; III. alanine; IV. glutamine, glutamic acid, proline, and arginine; V. histidine; VI. lysine, threonine, methionine, aspartic acid, cysteine, and asparagine; VII. phenylalanine, tyrosine, and tryptophan. Seven different combinations of amino acid solutions were prepared each time excluding one group. Cell growth and PGA production were investigated using *B. megaterium* strain YYBm1 carrying the plasmid pRBBm49 (encoding SP_{lipA}-PGA) (Figure 28). If group II, IV or VII were excluded, specific activity of PGA increased up to 1.9-, 1.8- and 2.5-fold, respectively. Without group V (histidine), specific activity of PGA was not increased significantly comparing to the combination when group II, IV or VII were excluded (Figure 28). This indicated that histidine should be added into the medium as a supplement in order to improve the PGA productivity. The highest increase in PGA production was observed when amino acids from group VII were excluded. Group VII contains the aromatic amino acids (F, Y, W) which are usually produced from the pentose phosphate pathway. The minimal medium supplemented with all amino acids excluding group VII was chosen for the described scale-up experiments from microtiter plate over shaking flasks to the bioreactor. However, an even higher amount of PGA was found in the supernatant when group II, IV, and VII were excluded together from the medium when testing all the combinations among these three groups in a combinatorial test (Figure 29). These were arranged as following: addition of 20 amino acids excluding (1) group II, (2) group IV, (3) group VII, (4) group II and group IV, (5) group II and group VII, (6) group IV and group VII and (7) all three groups group II, IV and VII. The highly reproducible result convinced us that the microtiter plate cultivation technique was an easy, economical and reliable method for medium optimization.

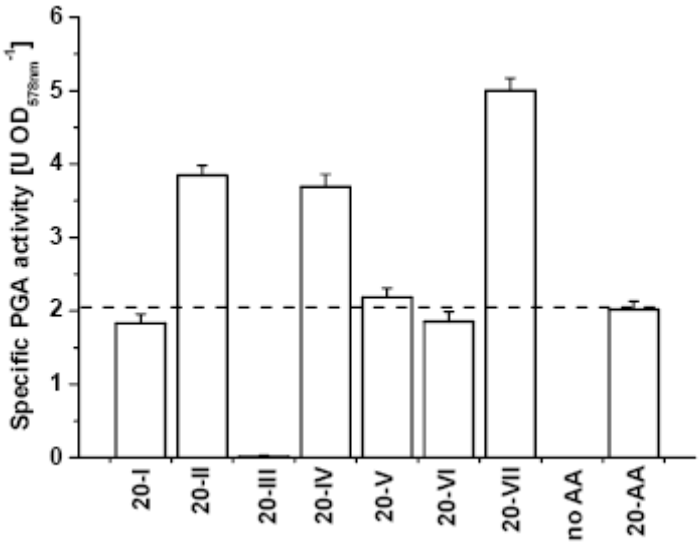

Figure 28. Minimal medium optimization with supplements of different combination of amino acids solutions in the microtiter plate. Strain YYBm1 (Δ*nprM*, *xylA*⁻) carrying plasmid pRBBm49 (encoding SP_{lipA}-PGA) was cultivated. Supplements of 20 amino acids excluding each time one group of the amino acids were added to the minimal medium, which were shown as 20 – group number of amino acid. Minimal medium without any supplements of amino acids and with 20 amino acids were tested as negative and positive control.

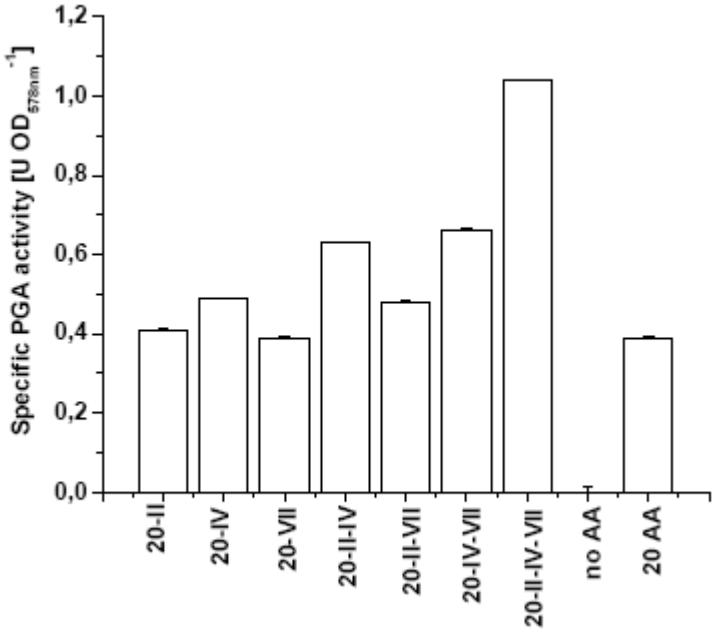

Figure 29. Minimal medium in microtiter plate optimization using combinatorial arrangement with *B. megaterium* strain YYBm1 carrying pRBBm49 (encoding SP_{lipA}-PGA). From the supplementation of 20 amino acids each time different amino acids combinations were excluded (shown as 20 – group number of amino acid). Minimal medium without any supplements of amino acids and with 20 amino acids were tested as negative and positive control.

Next, the amount of added amino acids solution was optimized in shaking flask cultivations (Figure 30). *B. megaterium* strain YYBm1 carrying plasmid pRBBm49 (encoding SP_{lipA}-PGA) was cultivated in 100 mL minimal medium with a final concentration of none, 0.5 x, 1 x, and 2 x of the amino acids solution excluding the group VII amino acids. The 2 x addition of the amino acids solution led to increased final cell density at the end of the cultivation. However, optimal PGA production was obtained in minimal medium with 1 x addition of the amino acid solution, which was also verified by SDS-PAGE analysis of extracellular proteins (data not shown). These results indicated that amino acids were essential for PGA production, but the higher concentration of amino acid, here the double amount, limited PGA production.

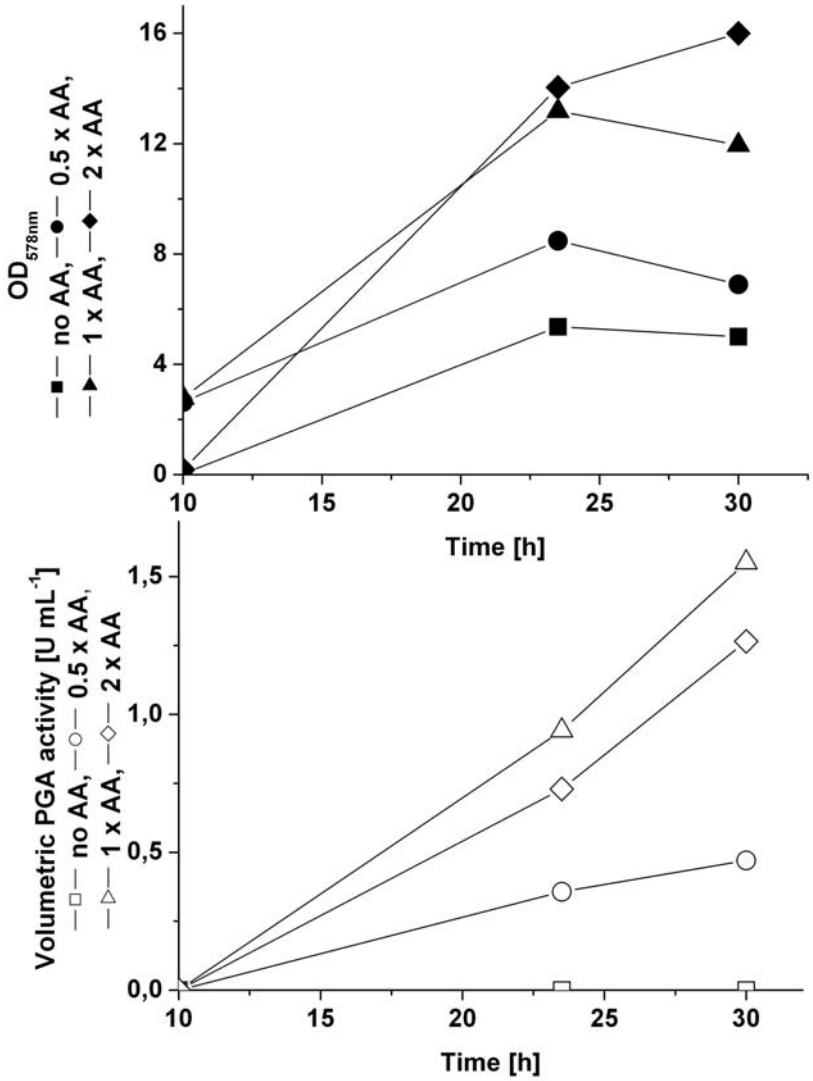

Figure 30. The influence of the amino acids concentration on cell dry weight and PGA activity. Shaking flask cultivations of YYBm1 carrying pRBBm49 (encoding SP_{lipA}-PGA) were performed. No amino acids in the medium was shown as square (■,□), concentration of 0.5 x amino acids solution was shown as circle (●,○), concentration of 1 x amino acids solution was shown as up triangle (▲,Δ), concentration of 2 x amino acids solution was shown as rhombus (◆,◇)

IV.2.1.8 Upscale of PGA production using *B. megaterium* to a 2 liter bioreactor

Finally, this optimized minimal medium containing 1x amino acids solution excluding group VII amino acids was used for an upscale in a pH controlled 2 L bioreactor (Figure 31). As control, LB complex medium with tryptone from Bacto was tested. 29.0 mg L^{-1} PGA were produced by YYBm1 carrying pRBBm49 (encoding SP_{lipA}-PGA) using the optimized minimal medium. This was a slight 1.1-fold increase compared to PGA production in the complex medium. For the first time, a higher volumetric productivity was reached in a batch cultivation using a defined minimal medium compared to an undefined complex medium. However, after cultivation in LB medium, the specific PGA activity was still 2 times higher than after cultivation in minimal medium due to the 2 times higher biomass production in minimal medium.

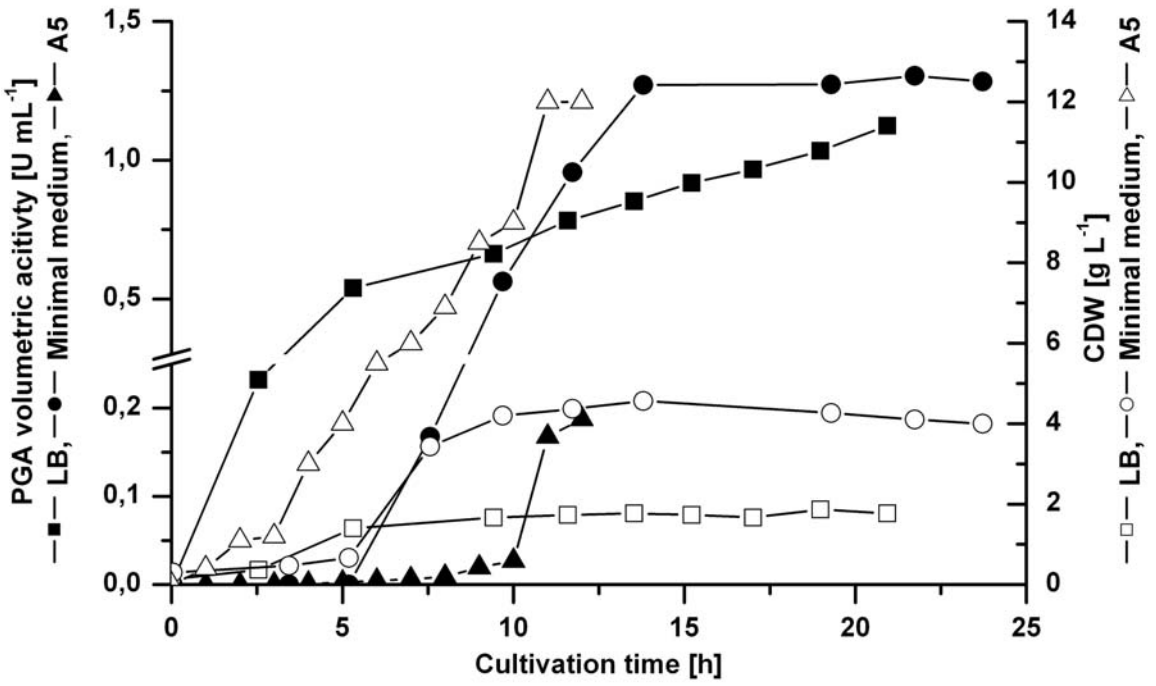

Figure 31. Up scaling of PGA production and export using *B. megaterium* in a 2 L bioreactor. The pH controlled batch cultivation of *B. megaterium* YYBm1 carrying pRBBm49 (encoding SP_{lipA}-PGA) was performed in complex medium (square) and optimized minimal medium (circle). *B. megaterium* MS941 carrying pRBBm23 (encoding SP_{pga}-PGA) was grown in semi-defined A5 medium (triangle). For induction of recombinant gene expression, 5 g L^{-1} xylose were added at the beginning of the cultivation. Samples were taken at indicated time points to determine cell dry weight (open) and PGA volumetric activity (solid).

Next, the obtained improvements in the bioreactor were compared to a bioreactor cultivation performed at the beginning of the study. This comparison of the described complex and minimal medium with a pH-controlled batch cultivation of *B. megaterium* strain MS941 carrying pRBBm23 (encoding SP_{pga}-PGA) using A5 semi-defined

medium excluding calcium ions (Figure 31) provided insights into the improvement process via the different described steps. In cultivations using either LB or minimal medium, PGA secretion started in the exponential phase, whereas in a cultivation using semi-defined A5 medium it started in the stationary phase. Finally, only 4.2 mg PGA per liter growth medium were obtained using strain MS941 carrying pRBBm23 (encoding SP_{pga}-PGA) in A5 medium. Hence, using the newly constructed strain YYBm1 deficient in xylose utilization, the signal peptide of LipA, an optimized minimal medium supplemented with calcium ions and a defined mix of amino acids the volumetric PGA productivity was improved 7-fold resulting in 29.0 mg PGA per liter growth medium.

IV.2.1.9 Secretion of PGA in a *B. megaterium* fed-batch cultivation of high cell densities

IV.2.1.9.1 Experimental approach for high cell density cultivations

First, in order to study the improvement of PGA production after strain optimization fed-batch cultivation with *B. megaterium* MS941 and the optimized YYBm1 in A5 semi-defined medium was investigated. Subsequently, an early induction strategy was applied to the high cell density cultivation using strain YYBm1 cultivated in A5 semi-defined medium. Finally, considering the stress conditions under the high cell density cultivation with A5 semi-defined medium, strain YYBm1 was cultivated in LB medium while feeding a high concentrated glucose solution and early induction of PGA production. Due to the high cost of amino acids, optimized minimal medium was not applied in these fed-batch cultivations.

IV.2.1.9.2 Comparison of B. megaterium strain MS941 and YYBm1 carrying pRBBm23 (SP_{pga}-PGA) in high cell density cultivation

First of all, PGA production was compared between strain MS941 and YYBm1 carrying pRBBm23 (SP_{pga}-PGA) in high cell density cultivation (Figure 32 + Figure 33). First, a HCDC (No.1) was carried out using MS941 (Δ*nprM*) carrying pRBBm23 (encoding SP_{pga}-PGA). An initial glucose concentration of 3 g L^{-1} was used in the batch phase (Figure 32A). After exhaustion of the glucose (7.8 h), feed solution was fed exponentially into the growing culture setting the growth rate to 0.14 h^{-1}. Its actual value was measured as 0.13 h^{-1}. About 24.4 h after starting the fed-batch *pga* expression was induced by addition of 5 g L^{-1} xylose at a biomass of around 52 g_{CDW} L^{-1}.

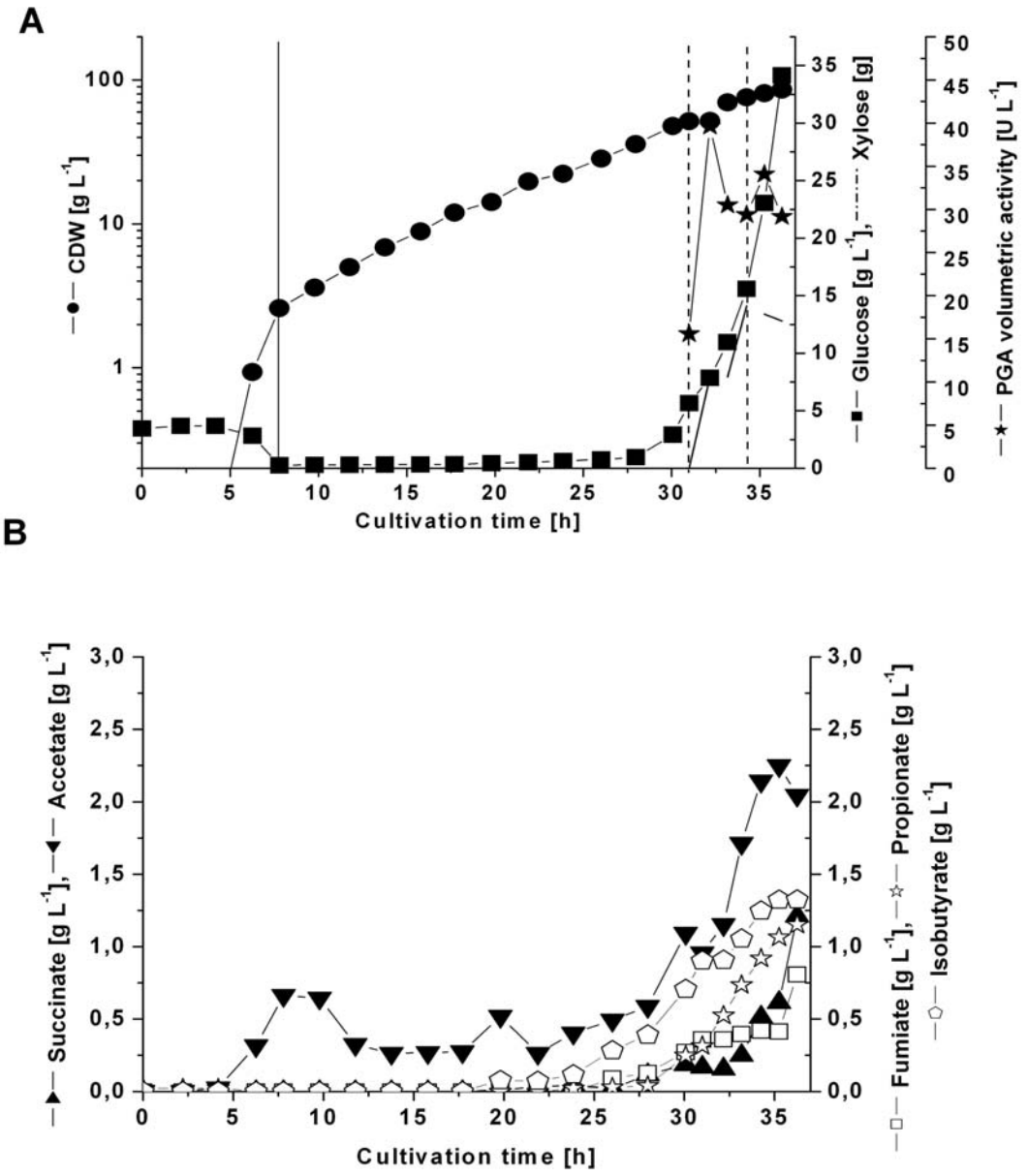

Figure 32. Production of PGA in high cell density cultivation using *B. megaterium* MS941 carrying pRBBm23 (encoding SP_{pga}-PGA) in A5 medium. (A) After the initial 3 g L^{-1} glucose were consumed in the batch phase exponential feed began at 7.8 h as indicated by the first solid line. Expression of *pga* was induced at 32.2 h as indicated by the first dashed line by addition of 5 g L^{-1} xylose. At 34.2 h second induction as indicated by the second dashed line was done by addition of another 5 g L^{-1} xylose. (B) Metabolites in growth medium were identified and quantified using HPLC.

After induction, glucose accumulated quickly in the medium caused by a decrease in growth rate to 0.12 h^{-1}. At the same time a steep increase of PGA secretion was observed for about 1 h reaching a maximum of 40 U L^{-1}. Thereafter, it decreased in the next 1 h to 30 U L^{-1} accompanied by a decreasing amount of xylose in the medium and an increase in cell mass. Therefore, a second induction was started by adding 5 g L^{-1} xylose into the culture medium in order to keep the induction efficiency.

Again PGA activity increased slightly up to 35 U L^{-1} in the next hour. Then it decreased again. However, the cellular PGA productivity decreased during the whole induction time demonstrating that probably not enough xylose was present for an efficient induction. Therefore, the cultivation was stopped. The cell dry weight reached up to 86 g_{CDW} L^{-1}. 2.3 g L^{-1} acetate was the major organic acid produced during HCDC (No.1) as detected by HPLC analysis. Succinate, fumiate, pyruvate, isobutyrate, and propionate amounts were less than 1.5 g L^{-1}. 0.7 g L^{-1} acetate was produced in the batch phase by *B. megaterium* as overflow metabolite due to high glucose consumption rates under strictly aerobic conditions. In the fed batch phase the cells consumed successively this alternative carbon source, when glucose became limiting (Figure 32). The enhanced amount of all metabolites during the induction was due to the accumulation of glucose which reached up to 34 g L^{-1} in the culture medium.

The second HCDC (No.2) was carried out using the same medium as in the first HCDC (No.1) using YYBm1 (Δ*nprM*, *xylA*$^-$) carrying PRBBm23 (encoding SP_{pga}-PGA) (Figure 33). After exhaustion of the initial 4.5 g L^{-1} glucose after 6.1 h in the batch phase, feed solution was added exponentially into the growing culture setting the growth rate to 0.12 h^{-1}. Its actual value was measured as 0.10 h^{-1}. About 30 h after starting the fed-batch *pga* expression was induced by addition of 5 g L^{-1} xylose at a biomass concentration of around 34.8 g_{CDW} L^{-1}. After induction, 3.2 g L^{-1} glucose was accumulated in 30 min from 4.4 to 7.6 g L^{-1}. Again the accumulation was caused by the decrease in growth rate. However, the glucose was consumed again in the next 2 h to around 3 g L^{-1} in the medium. After induction, a steep increase of secreted PGA activity was observed with a constant production rate of up to 265 U L^{-1}. This was almost a 7-fold improvement compared to the PGA production (40 U L^{-1}) using *B. megaterium* stain MS941 with the same plasmid and under the same cultivation conditions. However, cells grew very slowly during the induction. An increase of cell dry mass from 34.8 to 37.1 g L^{-1} was achieved within the next 8 h. Therefore, the cultivation was stopped.

Acetate, succinate, and pyruvate were the major organic acids produced during HCDC (No.2) as detected by HPLC analysis. Isobutyrate and propionate amounts were around 1 g L^{-1} during the cultivation. 0.8 g L^{-1} acetate were produced in the batch phase by *B. megaterium* as overflow metabolite similar to strain MS941. In the fed batch phase the cells consumed successively this alternative carbon source,

when glucose became limiting (Figure 33B). 1.9 g L^{-1} pyruvate, 2.4 g L^{-1} acetate, and 2.6 g L^{-1} succinate were produced at the beginning of induction due to the accumulation of glucose. However, they were consumed again during the further cultivation reaching levels of 0.4, 0.5, 0.6 g L^{-1}, respectively.

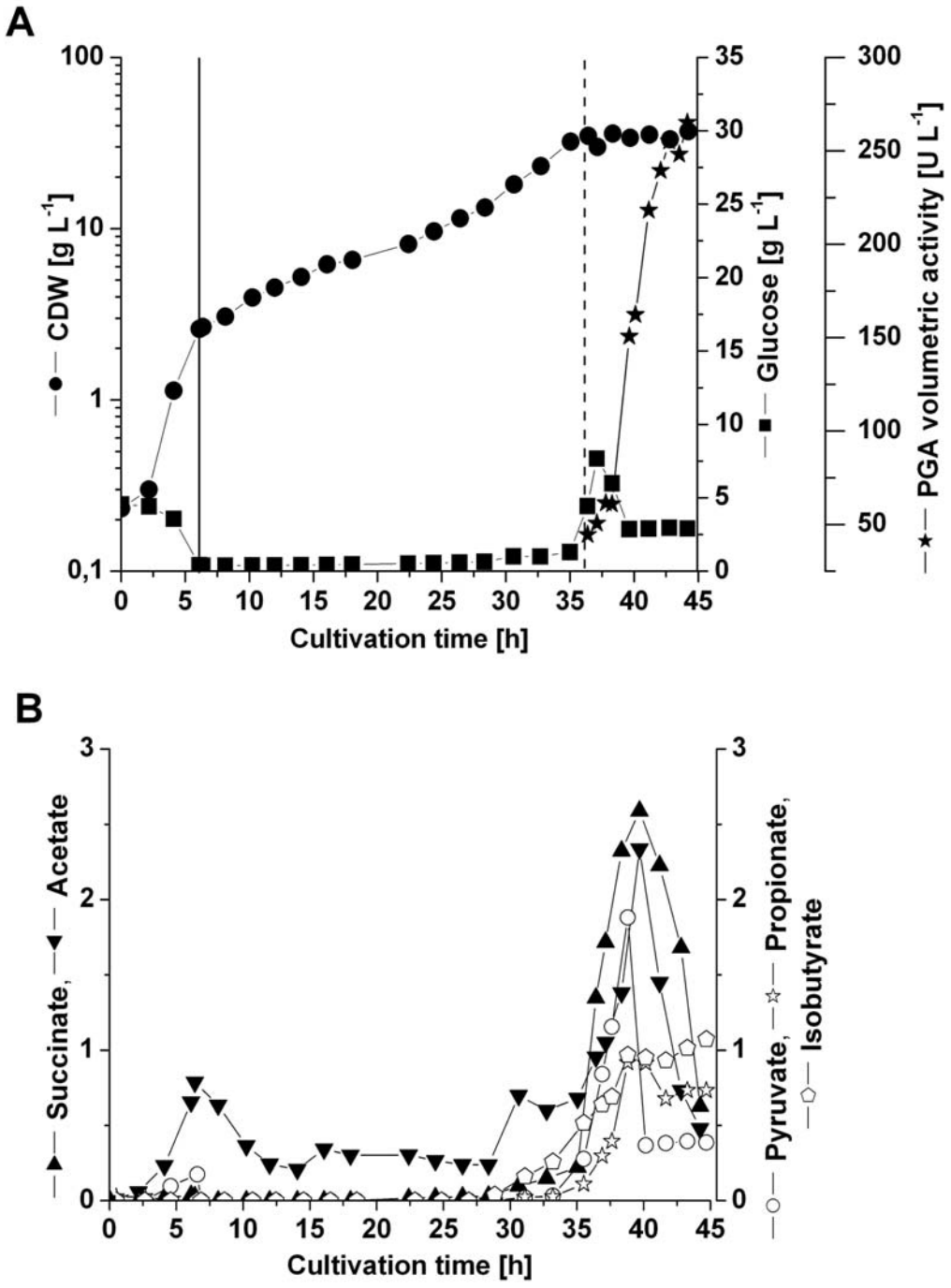

Figure 33. Production of PGA in high cell density cultivation using *B. megaterium* YYBm1 carrying pRBBm23 (encoding SP_{pga}-PGA) in A5 medium. (A) After 4.5 g L^{-1} glucose was consumed in the batch phase exponential feeding began at 6.1 h as indicated by the first solid line. Expression of *pga* was induced at 36.4 h as indicated by the first dashed line by addition of 5 g L^{-1} xylose. (B) Metabolites in growth medium were identified and quantified using HPLC.

By using strain YYBm1 (Δ*nprM*, *xylA*$^-$), PGA volumetric activity was increased almost 7-fold. However, only half of the cell density was reached comparing to MS941 after fed-batch cultivation.

IV.2.1.9.3 Early induction of pga gene expression in a high cell density cultivation with B. megaterium strain YYBm1 carrying pRBBm23 (encoding SP_{pga}-PGA)

Next, the secretion of PGA in fed-batch cultivation was further optimized in two different strategies using strain YYBm1 (Δ*nprM*, *xylA*$^-$). Either by a cultivation in A5 defined medium or LB complex medium. First, in order to see the improvement of protein production the new developed strain YYBm1 was cultivated in fed-batch of high cell densities using the semi-defined A5 medium with an induction of *pga* expression at the beginning of the cultivation (Figure 34). This was done, because the cells stopped to grow after induction in previous HCDC (No.2) using YYBm1 and only 37.1 g cell dry weight per liter were finally produced. The xylose utilization deficiency of strain YYBm1 enabled to use an induction by adding of the inducer xylose at the beginning of the cultivation. This may release the physiological stress occurring suddenly after induction at high cell densities. In this HCDC (No.3), strain YYBm1 carrying pRBBm23 (encoding SP_{pga}-PGA) was cultivated in the same semi-defined A5 medium, but with xylose addition at the beginning. After exhaustion of the glucose after 7.4 h in the batch phase, the feed solution was added exponentially to the growing culture setting the growth rate to 0.1 h^{-1}. Its actual value was measured as 0.09 h^{-1}. After 30 h of feeding, the volumetric PGA activity reached its maximal value of 31 U L^{-1}. Subsequently, it began to decrease and could not be increased by a second induction made at 43 h. The xylose concentration was not constant during the cultivation especially when cell mass increased. Xylose as inducer could be transported into the cells by the xylose transporter XylT in order to begin the induction. Hence, at a higher cell mass more xylose might be present inside the cells reducing the extracellular concentration. Remarkably, in only 3 h biomass was increased from 44 to 71 g L^{-1} and 30 g L^{-1} glucose accumulated before the beginning of the second induction.

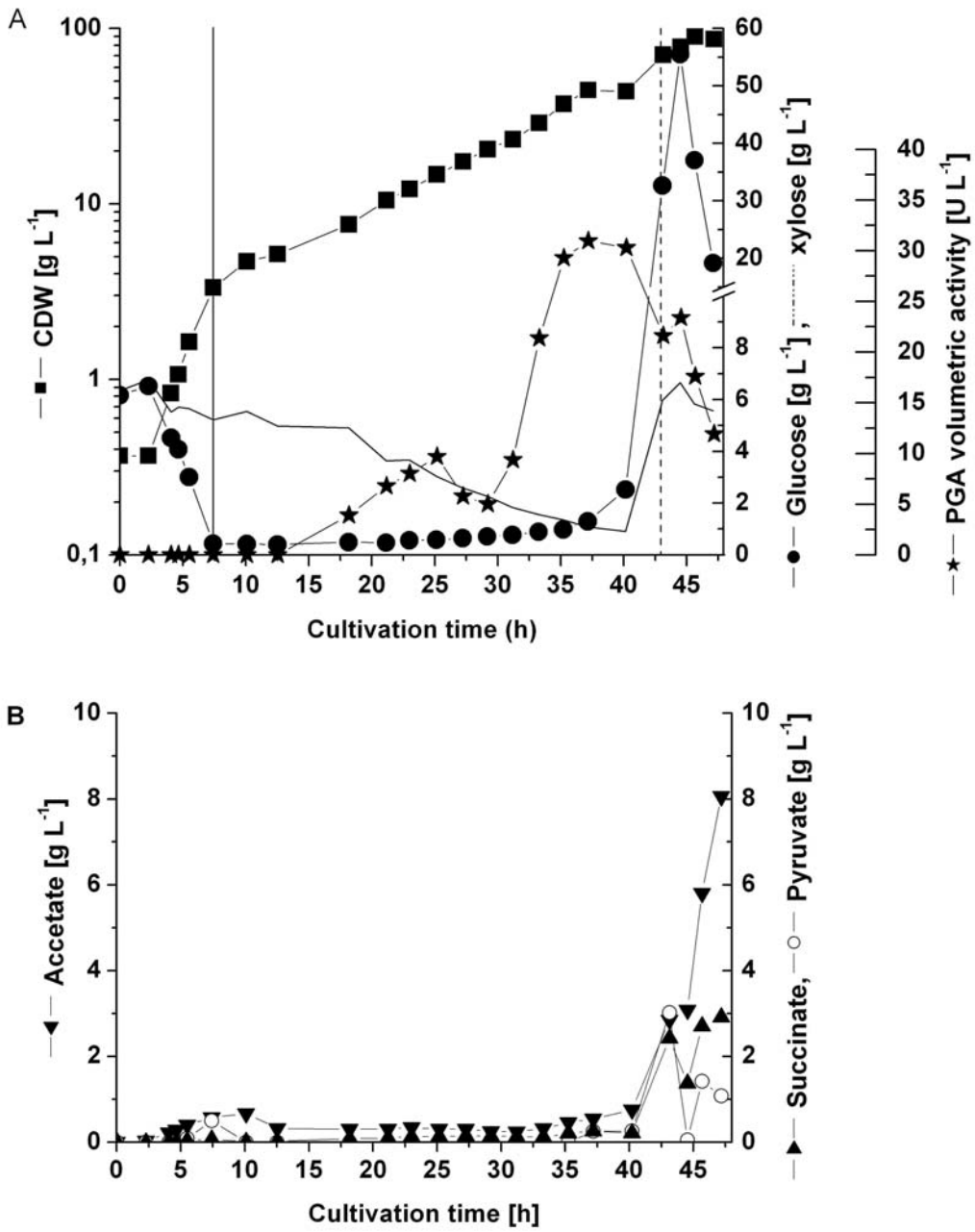

Figure 34. Production of PGA in high cell density cultivation using *B. megaterium* YYBm1 carrying pRBBm23 (encoding SP_{pga}-PGA). (A) After 4.5 g L^{-1} glucose was consumed in the batch phase exponential feed began at 7.4 h as indicated by the first solid line. Expression of *pga* was induced at the beginning of cultivation by addition of 5 g L^{-1} xylose. At 44 h a second time of 5 g L^{-1} xylose was added as indicated by the dashed line. (B) Metabolites in growth medium were identified and quantified using HPLC.

After the second induction, glucose first reached a level of 56 g L^{-1} and was then consumed again to 20 g L^{-1}. However, a slight increase of secreted PGA from 21 to 23 U L^{-1} was found in the medium 30 min after second induction. Unfortunately, the PGA activity began to decrease afterwards. Therefore, the cultivation was stopped with a 90 g L^{-1} cell dry weight at the end of the cultivation.

Acetate, succinate, and pyruvate were the major organic acids produced during HCDC as detected by HPLC analysis. Isobutyrate and propionate amounts were negligible. Eight g L^{-1} acetate, 3 g L^{-1} succinate, and 1 g L^{-1} pyruvate were produced at the end of the cultivation due to the accumulation of glucose in the medium.

IV.2.1.9.4 Fed-batch cultivation with LB medium in a batch phase using strain YYBm1 carrying pRBBm49 (encoding SP_{lipA}-PGA)

In the first part of this thesis it was shown that TFH was more intensively produced in complex medium compared to semi-defined medium. Further, considering the stress conditions in high cell density cultivation, a new strategy was investigated to produce PGA in a fed batch cultivation in LB medium. LB medium can supply small peptides which are important for high level heterologous protein production. A glucose solution was exponentially fed into the bioreactor in order to provide a carbon source for further cell growth (Figure 35).

This HCDC strategy No.4. was carried out with strain YYBm1 carrying pRBBm49 (encoding SP_{lipA}-PGA). Based on the xylose utilization deficiency of strain YYBm1, again an induction at the beginning of the cultivation was applied. After 12.4 h, the batch phase was finished reaching a low cell mass of 3 g_{CDW} L^{-1}. The maximal cell growth rate was 0.4 h^{-1}. PGA volumetric activity increased constantly to 857 U L^{-1} before the glucose feeding was started. Feed solution was added exponentially to the growing culture setting the growth rate to 0.14 h^{-1}. However, its actual value was measured as 0.08 h^{-1}. After 3 h of feeding, the PGA volumetric activity reached its maximal value of 1129 U L^{-1}. Subsequently, volumetric activity began to decrease although the xylose concentration was kept constant during the cultivation. However, a slight increase of secreted PGA in the medium was found after 6 h from 462 to 482 U L^{-1} after a second addition of 5 g L^{-1} xylose to increase the concentration of inducer in the culture medium. Unfortunately, this increase lasted only for 2 h with a maximum of 513 U L^{-1}. Remarkably, 94 g L^{-1} glucose accumulated from beginning of the cultivation until the second induction, but were consumed to 62 g L^{-1} at the end of the cultivation. Correspondingly, a larger cell growth rate was also found shortly after the second induction with a μ of 0.1 h^{-1}. Overall, 23.5 g cell dry weight L^{-1} were produced after this fed batch cultivation. This low final cell density may be caused by using LB medium in the batch phase because using LB medium usually less biomass is produced comparing to A5 medium. However, an almost 30-fold improvement of the volumetric PGA activity was reached by using this new strategy compared to the

high cell density cultivation using strain MS941 carrying pRBBm23 (SP_{pga}-PGA) (1129 U L^{-1} vs. 40 U L^{-1}).

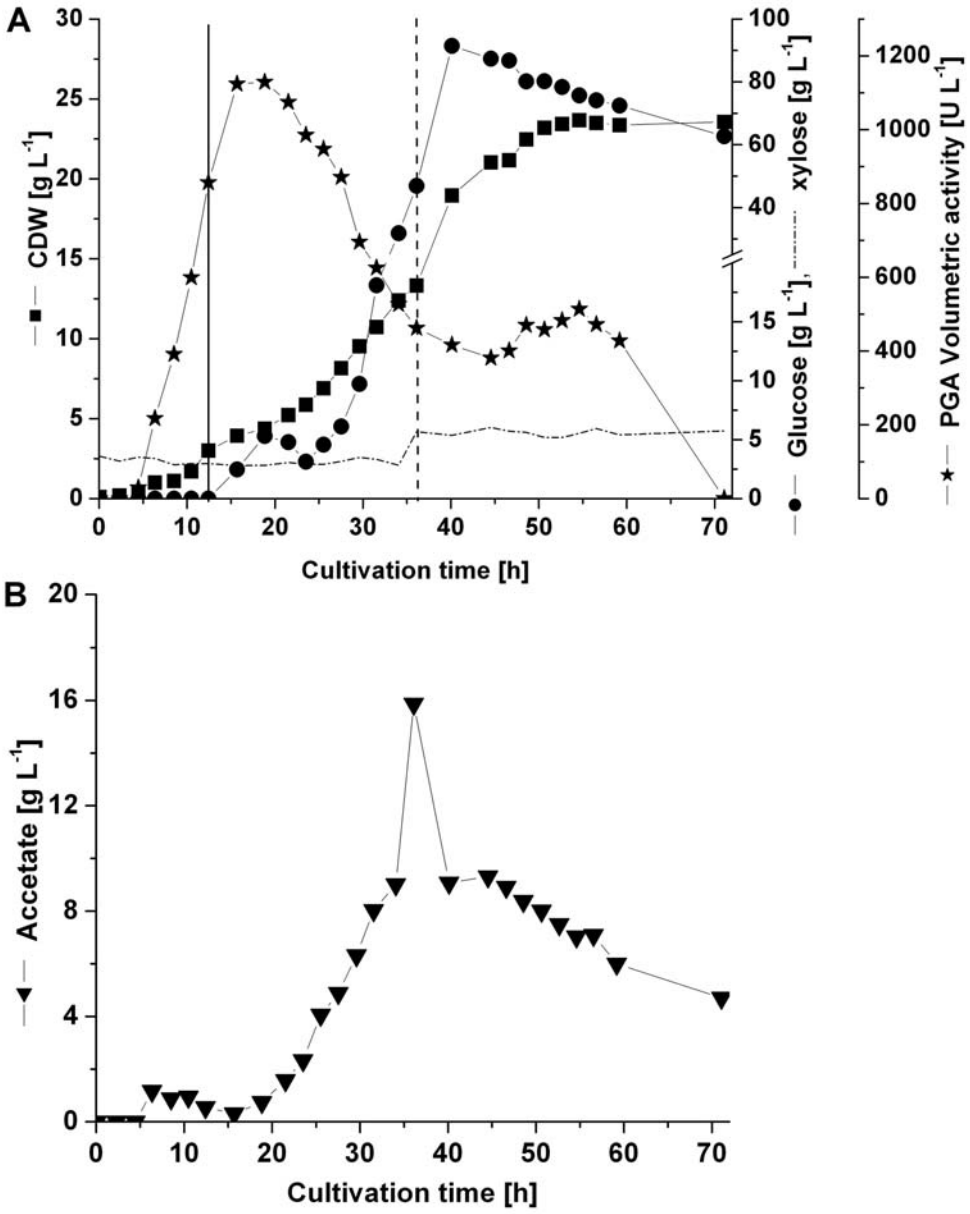

Figure 35. Production of PGA in high cell density cultivation using *B. megaterium* YYBm1 carrying pRBBm49 (encoding SP_{lipA}-PGA). (A) After the batch phase exponential feeding began at 12.4 h with 100 g L^{-1} glucose as indicated by the first solid line. Expression of *pga* was induced at the beginning of the cultivation by addition of 5 g L^{-1} xylose. At 36.1 h a second addition of 5 g L^{-1} xylose was done indicated by the dashed line. (B) Metabolites in the growth medium were identified via HPLC.

Acetate was the only major organic acid produced during HCDC as detected by HPLC analysis. A maximal of 16 g L^{-1} acetate were produced before the second

induction. Then it was consumed to 4.7 g L^{-1} until the end of cultivation. This showed a similar phenomenon as glucose as carbon source.

IV.2.2 Discussion

This study demonstrated the importance of the right composition of the growth medium. Amino acids were found to have a major influence on the recombinant PGA production. Difference in the amino acid composition of Oxoid and Bacto tryptone led not only to a 1.8-fold higher PGA production, but also influenced the secretome. Only in growth medium containing Oxoid tryptone a metalloprotease was produced. This also indicates limitation in the amino acid metabolism, which the organism tries to overcome by utilization the extracellular protein sources. The influence of supplying the right amino acid set was demonstrated by reaching higher volumetric PGA concentration in a batch cultivation compared to the complex medium. In this study 1305 U L^{-1} PGA volumetric activity was obtained comparing to the wild type strain *B. megaterium* ATCC14945 with a maximum of 131 U L^{-1} in a batch cultivation. Also in a recombinant production in *B. subtilis* only 613 U L^{-1} were reached (Table 14). Outlined enzyme activity results were compared after the original enzyme activity from literature was converted to the relative value according to the NIPAB assay at 37 °C since absolute protein amounts are not given by the mentioned PGA productions. Therefore, observed differences between the various *B. megaterium* production strains might be due to differences in the employed enzymatic test systems. However, a *B. megaterium* ATCC 14945 mutant was established reaching very high PGA production of 9060 U L^{-1}. This might due to the exponential growth-related promoter that has extended function in LB, an enriched medium where *Bacillus* cells form spores poorly.

High cell density cultivation are desirable for high time-volume yields, but were not successful in this study when a semi-defined medium (A5) was used. However, a similar volumetric PGA concentration was obtained compared to the ones produced in batch cultivations when complex medium with a glucose feeding were used. Unfortunately, the obtained low specific PGA activity demonstrated that at least 10-fold improvement should be theoretically reachable by supplying the correct mix of amino acids. A further study could be done by optimizing the developed defined minimal medium with a supplementation of amino acids for high cell density cultivation. A systems biotechnology approach with the systematic high throughput

determination of transcriptome, cytoplasmic proteome, secretome, and especially the metabolome for the various growth and protein production conditions will finally help us to determine the important cellular parameters involved in the observed protein production behaviour. This information might provide a solid base for the directed further metabolomic engineering of *B. megaterium* for optimal protein production and export. It will help us to identify existing bottlenecks and allow for systematic bioengineering solutions.

Table 14. Comparison of PGA production in this study to literature data.

Strain	**Enzyme activity* (equivalent to NIPAB assay at 37 °C)**		**Enzyme production**			**Reference**
	[U L^{-1}]	[U mg_{CDW}^{-1}]	Growth Medium	Cultivation	T (°C)	
B. megaterium YYBm1	1823	385	LB1	SF	37	This study
B. megaterium YYBm1	1553	329	MM	SF	37	This study
B. megaterium YYBm1	1305	320	MM+ 1 x AA	Batch	37	This study
B. megaterium ATCC14945	61.3		complex medium	SF	37	Pinotti *et al*., 2000
B. megaterium ATCC14945	131 114	41 85	complex medium Defined medium	Batch Batch	30 30	Illanes *et al*., 1994
B. megaterium ATCC14945	3241		Defined medium with 19 mg L^{-1} Na_2SO_4	chemostat D = 0.06 h^{-1}	30	Acevedo & Cooney, 1973
B. megaterium UN-cat	9060		LB	SF	30	Panbangred *et al*., 2000
B. subtilis	613		LB	SF	37	Kang *et al*., 1991

*The calculation was carried out according to the formula which was developed by Dr. Anton. Roß in HZI:

PGA activity using NIPAB assay at 37 °C = 0.3 x 1.48 x activity measured by PenG assay at 37 °C

PGA activity using PenG assay at 30 °C = 0.67 x PGA activity using PenG assay at 37 °C

IV.2.3 Summary

A systematic improvement of the recombinant production and export of *B. megaterium* ATCC14945 penicillin G amidase using *B. megaterium* was performed. The addition of 2.5 mM calcium ions increased the specific activity by 2.6-fold.

Exchange of its natural signal peptide by the one of the *B. megaterium* extracellular lipase LipA increased secretion by 1.7-fold. A *B. megaterium* strain deficient in the extracellular protease NprM and in xylose utilization (Δ*xylA*) was developed allowing for stable extracellular proteins and long time induction of gene expression by xylose. Next, a defined minimal medium with defined amino acid additions for high yield PGA production was developed. PGA production was successfully scaled up to 2 L controlled batch fermentations. Finally, PGA production in high cell density cultivations was 30-fold improved by the combined optimization of the signal peptide, the strain and the cultivation strategy optimization.

V Literature

Acevedo, F. & Cooney, C. L. (1973). Pencillin amidase production by *Bacillus megaterium*. *Biotechnol Bioeng* **15**, 493-503.

Aunstrup, K. (1979). Production, isolation, and economics of extracellular enzymes. In *Applied Biochemistry and Bioengineering*, pp. 27-69. New York.

Barg, H. (2003). Gezielte gentechnische Optimierung von *Bacillus megaterium* für die Vitamin B_{12} Produktion. Braunschweig: Technische University Braunschweig.

Barg, H., Malten, M., Jahn, M. & Jahn, D. (2005). Protein and vitamin production in *Bacillus megaterium*. In *Microbial Processes and Products*, pp. 165-184. Edited by J. L. Barredo. Totowa: Humana Press Inc.

Bergquist, P. L., Love, D. R., Croft, J. E., Streiff, M. B., Daniel, R. M. & Morgan, W. H. (1987). Genetics and potential biotechnological applications of thermophilic and extremely thermophilic micro-organisms. *Biotechnol Genet Eng Rev* **5**, 199-244.

Biedendieck, R., Yang, Y., Deckwer, W. D., Malten, M. & Jahn, D. (2007). Plasmid system for the intracellular production and purification of affinity-tagged proteins in *Bacillus megaterium*. *Biotechnol Bioeng* **96**, 525-537.

Bolhuis, A., Venema, G., Quax, W. J., Bron, S. & van Dijl, J. M. (1999). Functional analysis of paralogous thiol-disulfide oxidoreductases in *Bacillus subtilis*. *J Biol Chem* **274**, 24531-24538.

Burger, S., Tatge, H., Hofmann, F., Genth, H., Just, I. & Gerhard, R. (2003). Expression of recombinant *Clostridium difficile* toxin A using the *Bacillus megaterium* system. *Biochem Biophys Res Commun* **307**, 584-588.

Carbone, A., Zinovyev, A. & Kepes, F. (2003). Codon adaptation index as a measure of dominating codon bias. *Bioinformatics* **19**, 2005-2015.

Carlsson, L., Pahlson, C., Bergquist, M., Ronquist, G. & Stridsberg, M. (2000). Antibacterial activity of human prostasomes. *Prostate* **44**, 279-286.

Christiansen, T. & Nielsen, J. (2002). Production of extracellular protease and glucose uptake in *Bacillus clausii* in steady-state and transient continuous cultures. *J Biotechnol* **97**, 265-273.

Dahl, M. K., Degenkolb, J. & Hillen, W. (1994). Transcription of the xyl operon is controlled in *Bacillus subtilis* by tandem overlapping operators spaced by four base-pairs. *J Mol Biol* **243**, 413-424.

Dahl, M. K., Schmiedel, D. & Hillen, W. (1995). Glucose and glucose-6-phosphate interaction with Xyl repressor proteins from *Bacillus* spp. may contribute to regulation of xylose utilization. *J Bacteriol* **177**, 5467-5472.

Dawes, E. A. & Ribbons, D. W. (1964). Some aspects of the endogenous metabolism of bacteria. *Bacteriol Rev* **28**, 126-149.

Debabov, V. (1982). The industrial use of *Bacillis*. In *The Molecular Biology of the Bacillis*, pp. 331-370. New York.

Deckwer, W.-D., Müller, R. J., Van den Heuvel, J. & Kleeberg, I. (2001). Enzyme which cleaves ester groups and which is derived from *Thermomonospora fusca*. Germany.

Deutscher, J., Kuster, E., Bergstedt, U., Charrier, V. & Hillen, W. (1995). Protein kinase-dependent HPr/CcpA interaction links glycolytic activity to carbon catabolite repression in gram-positive bacteria. *Mol Microbiol* **15**, 1049-1053.

Diesterhaft, M. D. & Freese, E. (1973). Role of pyruvate carboxylase, phosphoenolpyruvate carboxykinase, and malic enzyme during growth and sporulation of *Bacillus subtilis*. *J Biol Chem* **248**, 6062-6070.

Dresler, K., van den Heuvel, J., Muller, R. J. & Deckwer, W.-D. (2006). Production of a recombinant polyester-cleaving hydrolase from *Thermobifida fusca* in *Escherichia coli*. *Bioprocess Biosyst Eng* **29**, 169-183.

Forney, L. J. & Wong, D. C. (1989). Alteration of the catalytic efficiency of penicillin amidase from *Escherichia coli*. *Appl Environ Microbiol.* **55**, 2556-2560.

Foster, S. J. & Popham, D. L. (2001). Structure and synthesis of cell wall, spore cortex, teichoic acids, S-layer, and capsules. In *In Bacillus subtilis and its Closest Relatives: from Genes to Cells*, pp. 21-41. Washington, DC: American Society for Microbiology.

Frehel, C. & Ryter, A. (1979). Peptidoglycan turnover during growth of a *Bacillus megaterium* Dap- Lys- mutant. *J Bacteriol* **137**, 947-955.

Frehel, C. & Ryter, A. (1982). Electron microscopic cytochemical study of cell-wall polysaccharides in *Bacillus subtilis* and two strains of *Bacillus megaterium*. *J Ultrastruct Res* **81**, 66-77.

Fürch, T., Hollmann, R., Wittmann, C., Wang, W. & Deckwer, W.-D. (2006). Comparative study on central metabolic fluxes of *Bacillus megaterium* strains in continuous culture using (13)C labelled substrates. *Bioprocess Biosyst Eng*.

Gartner, D., Geissendorfer, M. & Hillen, W. (1988). Expression of the *Bacillus subtilis xyl* operon is repressed at the level of transcription and is induced by xylose. *J Bacteriol* **170**, 3102-3109.

Gellissen, G. (2002). *Production of Recombinant Proteins*: WILEY-VCH Verlag GmbH & Co. KGaA, Weinheim.

Gottschalk, G. (1986). *Bacterial metabolism*, 2nd edn. New York: Springer Verlag.

Gouda, M. K., Kleeberg, I., van den Heuvel, J., Muller, R. J. & Deckwer, W.-D. (2002). Production of a polyester degrading extracellular hydrolase from *Thermomonospora fusca*. *Biotechnol Prog* **18**, 927-934.

Grote, A., Hiller, K., Scheer, M., Munch, R., Nörtemann, B., Hempel, D. C. & Jahn, D. (2005). JCat: a novel tool to adapt codon usage of a target gene to its potential expression host. *Nucleic Acids Res* **33**, 526-531.

Gumpert, J. & Hoischen, C. (1998). Use of cell wall-less bacteria (L-forms) for efficient expression and secretion of heterologous gene products. *Curr Opin Biotechnol* **9**, 506-509.

Haddaoui, E. A., Leloup, L., Petit-Glatron, M. F. & Chambert, R. (1997). Characterization of a stable intermediate trapped during reversible refolding of *Bacillus subtilis* alpha-amylase. *Eur J Biochem* **249**, 505-509.

Harwood, C. R. (1992). *Bacillus subtilis* and its relatives: molecular biological and industrial workhorses. *Trends Biotechnol* **10**, 247-256.

Hefti, M. H., Van Vugt-Van der Toorn, C. J., Dixon, R. & Vervoort, J. (2001). A novel purification method for histidine-tagged proteins containing a thrombin cleavage site. *Anal Biochem* **295**, 180-185.

Henkin, T. M., Grundy, F. J., Nicholson, W. L. & Chambliss, G. H. (1991). Catabolite repression of alpha-amylase gene expression in *Bacillus subtilis* involves a *trans*-acting gene product homologous to the *Escherichia coli lacI* and *galR* repressors. *Mol Microbiol* **5**, 575-584.

Herbort, M., Klein, M., Manting, E. H., Driessen, A. J. & Freudl, R. (1999). Temporal expression of the *Bacillus subtilis secA* gene, encoding a central component of the preprotein translocase. *J Bacteriol* **181**, 493-500.

Hollmann, R. & Deckwer, W.-D. (2004). Pyruvate formation and suppression in recombinant *Bacillus megaterium* cultivation. *J Biotechnol* **111**, 89-96.

Hori, K., Kaneko, M., Tanji, Y., Xing, X. H. & Unno, H. (2002). Construction of self-disruptive *Bacillus megaterium* in response to substrate exhaustion for polyhydroxybutyrate production. *Appl Microbiol Biotechnol* **59**, 211-216.

Hueck, C., Kraus, A. & Hillen, W. (1994). Sequences of *ccpA* and two downstream *Bacillus megaterium* genes with homology to the *motAB* operon from *Bacillus subtilis*. *Gene* **143**, 147-148.

Ignatova, Z., Wischnewski, F., Notbohm, H. & Kasche, V. (2005). Pro-sequence and Ca^{2+}-binding: implications for folding and maturation of Ntn-hydrolase penicillin amidase from *E. coli*. *J Mol Biol* **348**, 999-1014.

Illanes, A., Acevedo, F., Gentina, J. C., Reyes, I., Torres, R., Cartagena, O., Ruiz, A. & Vasquez, M. (1994). Production of penicillin acylase from *Bacillus megaterium* in complex and defined media. *Process Biochemistry* **29**, 263-270.

Jacob, S., Allmansberger, R., Gartner, D. & Hillen, W. (1991). Catabolite repression of the operon for xylose utilization from *Bacillus subtilis* W23 is mediated

at the level of transcription and depends on a *cis* site in the *xylA* reading frame. *Mol Gen Genet* **229**, 189-196.

Jacobs, M., Andersen, J. B., Kontinen, V. & Sarvas, M. (1993). *Bacillus subtilis* PrsA is required in vivo as an extracytoplasmic chaperone for secretion of active enzymes synthesized either with or without pro-sequences. *Mol Microbiol* **8**, 957-966.

John, G. T., Klimant, I., Wittmann, C. & Heinzle, E. (2003). Integrated optical sensing of dissolved oxygen in microtiter plates: a novel tool for microbial cultivation. *Biotechnol Bioeng* **81**, 829-836.

Kang, J. H., Hwang, Y. & Yoo, O. J. (1991). Expression of penicillin G acylase gene from *Bacillus megaterium* ATCC 14945 in *Escherichia coli* and *Bacillus subtilis*. *J Biotechnol* **17**, 99-108.

Kasche, V., Ignatova, Z., Markl, H., Plate, W., Punckt, N., Schmidt, D., Wiegandt, K. & Ernst, B. (2005). Ca^{2+} is a cofactor required for membrane transport and maturation and is a yield-determining factor in high cell density penicillin amidase production. *Biotechnol Prog* **21**, 432-438.

Kleeberg, I., Welzel, K., Vandenheuvel, J., Müller, R. J. & Deckwer, W.-D. (2005). Characterization of a new extracellular hydrolase from *Thermobifida fusca* degrading aliphatic-aromatic copolyesters. *Biomacromolecules* **6**, 262-270.

Korz, D. J. (1993). Entwicklung von Prozeßstrategien zur Kultivierung von *Escherichia coli* zu hohen Zelldichten. Munich: Technical University of Munich.

Kraus, A., Hueck, C., Gartner, D. & Hillen, W. (1994). Catabolite repression of the *Bacillus subtilis xyl* operon involves a *cis* element functional in the context of an unrelated sequence, and glucose exerts additional *xylR*-dependent repression. *J Bacteriol* **176**, 1738-1745.

Kutzbach, C. & Rauenbusch, E. (1974). Preparation and general properties of crystalline penicillin acylase from *Escherichia coli* ATCC 11105. *Hoppe Seylers Z Physiol Chem* **355**, 45-53.

Lao, G. & Wilson, D. B. (1996). Cloning, sequencing, and expression of a *Thermomonospora fusca* protease gene in *Streptomyces lividans*. *Appl Environ Microbiol* **62**, 4256-4259.

Lee, H., Park, O. K. & Kang, H. S. (2000). Identification of a new active site for autocatalytic processing of penicillin acylase precursor in *Escherichia coli* ATCC11105. *Biochem Biophys Res Commun* **272**, 199-204.

Leloup, L., Haddaoui el, A., Chambert, R. & Petit-Glatron, M. F. (1997). Characterization of the rate-limiting step of the secretion of *Bacillus subtilis* alpha-amylase overproduced during the exponential phase of growth. *Microbiology* **143**, 3295-3303.

Malten, M. (2005). Protein production and secretion in *B. megaterium*. Braunschweig: Technische Universität Braunschweig.

Malten, M., Nahrstedt, H., Meinhardt, F. & Jahn, D. (2005a). Coexpression of the type I signal peptidase gene *sipM* increases recombinant protein production and export in *Bacillus megaterium* MS941. *Biotechnol Bioeng* **91**, 616-621.

Malten, M., Hollmann, R., Deckwer, W.-D. & Jahn, D. (2005b). Production and secretion of recombinant *Leuconostoc mesenteroides* dextransucrase DsrS in *Bacillus megaterium*. *Biotechnol Bioeng* **89**, 206-218.

Malten, M., Biedendieck, R., Gamer, M., Drews, A. C., Stammen, S., Buchholz, K., Dijkhuizen, L. & Jahn, D. (2006). A *Bacillus megaterium* plasmid system for the production, export, and one-step purification of affinity-tagged heterologous levansucrase from growth medium. *Appl Environ Microbiol* **72**, 1677-1679.

Marsic, N., Roje, S., Stojiljkovic, I., Salaj-Smic, E. & Trgovcevic, Z. (1993). In vivo studies on the interaction of RecBCD enzyme and lambda Gam protein. *J Bacteriol* **175**, 4738-4743.

Mason, J. M., Fajardo-Cavazos, P. & Setlow, P. (1988). Levels of mRNAs which code for small, acid-soluble spore proteins and their LacZ gene fusions in sporulating cells of *Bacillus subtilis*. *Nucleic Acids Res* **16**, 6567-6583.

McVey, C. E., Walsh, M. A., Dodson, G. G., Wilson, K. S. & Brannigan, J. A. (2001). Crystal structures of penicillin acylase enzyme-substrate complexes: structural insights into the catalytic mechanism. *J Mol Biol* **313**, 139-150.

Meens, J., Frings, E., Klose, M. & Freudl, R. (1993). An outer membrane protein (OmpA) of *Escherichia coli* can be translocated across the cytoplasmic membrane of *Bacillus subtilis*. *Mol Microbiol* **9**, 847-855.

Meens, J., Herbort, M., Klein, M. & Freudl, R. (1997). Use of the pre-pro part of *Staphylococcus hyicus* lipase as a carrier for secretion of *Escherichia coli* outer membrane protein A (*OmpA*) prevents proteolytic degradation of OmpA by cell-associated protease(s) in two different gram-positive bacteria. *Appl Environ Microbiol* **63**, 2814-2820.

Michal, G. (1999). *Biochemical pathways*. Heidelberg . Berlin: Spektrum Akademischer Verlag GmbH.

Miller, J. R., Kovacevic, S. & Veal, L. E. (1987). Secretion and processing of staphylococcal nuclease by *Bacillus subtilis*. *J Bacteriol* **169**, 3508-3514.

Millet, J., Acher, R. & Aubert, J. P. (1969). Biochemical and physiological properties of an extracellular protease produced by *Bacillus megaterium*. *Biotechnol Bioeng* **11**, 1233-1246.

Müller, R. J., Schrader, H., Profe, J., Dresler, K. & Deckwer, W.-D. (2005). Enzymatic degradation of poly(ethylene terephthalate): rapid hydrolyse using a hydrolase from *T. fusca*. *Macromolecular Rapid Communications* **26**, 1400-1405.

Nekolny, D. & Chaloupka, J. (2000). Protein catabolism in growing *Bacillus megaterium* during adaptation to salt stress. *FEMS Microbiol Lett* **184**, 173-177.

Noiva, R. (1994). Enzymatic catalysis of disulfide formation. *Protein Expr Purif* **5**, 1-13.

Oinonen, C. & Rouvinen, J. (2000). Structural comparison of Ntn-hydrolases. *Protein Sci* **9**, 2329-2337.

Panbangred, W., Weeradechapon, K., Udomvaraphant, S., Fujiyama, K. & Meevootisom, V. (2000). High expression of the penicillin G acylase gene (*pac*) from *Bacillus megaterium* UN1 in its own *pac* minus mutant. *J Appl Microbiol* **89**, 152-157.

Petit-Glatron, M. F., Grajcar, L., Munz, A. & Chambert, R. (1993). The contribution of the cell wall to a transmembrane calcium gradient could play a key role in *Bacillus subtilis* protein secretion. *Mol Microbiol* **9**, 1097-1106.

Pinotti, L. M., Silva, A. F., Silva, R. G. & Giordano, R. L. (2000). Study of different media for production of penicillin G acylase from *Bacillus megaterium* ATCC 14945. *Appl Biochem Biotechnol* **84-86**, 655-663.

Popham, D. L. (2002). Specialized peptidoglycan of the bacterial endospore: the inner wall of the lockbox. *Cell Mol Life Sci* **59**, 426-433.

Pragai, Z., Tjalsma, H., Bolhuis, A., van Dijl, J. M., Venema, G. & Bron, S. (1997). The signal peptidase II (*lsp*) gene of *Bacillus subtilis*. *Microbiology* **143 (Pt 4)**, 1327-1333.

Priest, F. G. (1977). Extracellular enzyme synthesis in the genus *Bacillus*. *Bacteriol Rev* **41**, 711-753.

Primrose, S. B. & Ehrlich, S. D. (1981). Isolation of plasmid deletion mutants and study of their instability. *Plasmid* **6**, 193-201.

Rygus, T. & Hillen, W. (1991). Inducible high-level expression of heterologous genes in *Bacillus megaterium* using the regulatory elements of the xylose-utilization operon. *Appl Microbiol Biotechnol* **35**, 594-599.

Rygus, T. & Hillen, W. (1992). Catabolite repression of the *xyl* operon in *Bacillus megaterium*. *J Bacteriol* **174**, 3049-3055.

Rygus, T., Scheler, A., Allmansberger, R. & Hillen, W. (1991). Molecular cloning, structure, promoters and regulatory elements for transcription of the *Bacillus megaterium* encoded regulon for xylose utilization. *Arch Microbiol* **155**, 535-542.

Sarath, G., De la Motte, R. S. & Wagner, F. W. (1989). Protease assay methods. In *Proteolytic enzymes*, pp. 25-55. Edited by R. J. Beynon & J. S. Bond. New York: IRL Press.

Saunders, C. W., Schmidt, B. J., Mallonee, R. L. & Guyer, M. S. (1987). Secretion of human serum albumin from *Bacillus subtilis*. *J Bacteriol* **169**, 2917-2925.

Schmidt-Dannert, C., Sztajer, H., Stocklein, W., Menge, U. & Schmid, R. D. (1994). Screening, purification and properties of a thermophilic lipase from *Bacillus thermocatenulatus*. *Biochim Biophys Acta* **1214**, 43-53.

Sharp, P. M. & Li, W. H. (1987). The codon adaptation index-a measure of directional synonymous codon usage bias, and its potential applications. *Nucleic Acids Res* **15**, 1281-1295.

Simonen, M. & Palva, I. (1993). Protein secretion in *Bacillus* species. *Microbiol Rev* **57**, 109-137.

Stahl, S. (1989). A new bacteriocinogenic activity: megacin BII encoded by plasmid pSE 203 in strains of *Bacillus megaterium*. *Arch Microbiol* **151**, 159-165.

Stahl, S. & Olsson, O. (1977). Temperature range variants of *Bacillus megaterium*. *Arch Microbiol* **113**, 221-229.

Stephenson, K. & Harwood, C. R. (1998). Influence of a cell-wall-associated protease on production of alpha-amylase by *Bacillus subtilis*. *Appl Environ Microbiol* **64**, 2875-2881.

Talarico, L. A., Gil, M. A., Yomano, L. P., Ingram, L. O. & Maupin-Furlow, J. A. (2005). Construction and expression of an ethanol production operon in Gram-positive bacteria. *Microbiology* **151**, 4023-4031.

Thwaite, J. E., Baillie, L. W. J., Carter, N. M., Stephenson, K., Rees, M., Harwood, C. R. & Emmerson, P. T. (2002). Optimization of the cell wall microenvironment allows increased production of recombinant *Bacillus anthracis* protective antigen from *B. subtilis*. *Appl. Environ. Microbiol.* **68**, 227-234.

Tjalsma, H., Noback, M. A., Bron, S., Venema, G., Yamane, K. & van Dijl, J. M. (1997). *Bacillus subtilis* contains four closely related type I signal peptidases with overlapping substrate specificities. Constitutive and temporally controlled expression of different *sip* genes. *J Biol Chem* **272**, 25983-25992.

Tjalsma, H., Kontinen, V. P., Pragai, Z., Wu, H., Meima, R., Venema, G., Bron, S., Sarvas, M. & van Dijl, J. M. (1999). The role of lipoprotein processing by signal peptidase II in the Gram-positive eubacterium *Bacillus subtilis*. Signal peptidase II is required for the efficient secretion of alpha-amylase, a non-lipoprotein. *J Biol Chem* **274**, 1698-1707.

Tokunaga, M., Loranger, J. M., Wolfe, P. B. & Wu, H. C. (1982). Prolipoprotein signal peptidase in *Escherichia coli* is distinct from the M13 procoat protein signal peptidase. *J Biol Chem* **257**, 9922-9925.

Valle, F., Balbas, P., Merino, E. & Bolivar, F. (1991). The role of penicillin amidases in nature and in industry. *Trends Biochem Sci* **16**, 36-40.

van Wely, K. H., Swaving, J., Freudl, R. & Driessen, A. J. (2001). Translocation of proteins across the cell envelope of Gram-positive bacteria. *FEMS Microbiol Rev* **25**, 437-454.

Vitikainen, M., Pummi, T., Airaksinen, U., Wahlstrom, E., Wu, H., Sarvas, M. & Kontinen, V. P. (2001). Quantitation of the capacity of the secretion apparatus and requirement for PrsA in growth and secretion of alpha-amylase in *Bacillus subtilis*. *J Bacteriol* **183**, 1881-1890.

Wang, W., Sun, J., Hollmann, R., Zeng, A. P. & Deckwer, W.-D. (2006). Proteomic characterization of transient expression and secretion of a stress-related metalloprotease in high cell density culture of *Bacillus megaterium*. *J Biotechnol* **126**, 313-324.

Wittchen, K. D. & Meinhardt, F. (1995). Inactivation of the major extracellular protease from *Bacillus megaterium* DSM319 by gene replacement. *Appl Microbiol Biotechnol* **42**, 871-877.

Wu, S. C., Yeung, J. C., Duan, Y., Ye, R., Szarka, S. J., Habibi, H. R. & Wong, S. L. (2002). Functional production and characterization of a fibrin-specific single-chain antibody fragment from *Bacillus subtilis*: effects of molecular chaperones and a wall-bound protease on antibody fragment production. *Appl Environ Microbiol* **68**, 3261-3269.

Xia, J. (2005). Charakterisierung des Lyophilisates des Kulturüberstandes einer *Thermobifida fusca* Kultivierung unter Berücksichtigung von Dimerisierung der *Thermobifida fusca* Hydrolase. Braunschweig: TU-Braunschweig.

Yamane, T. & Shimizu, S. (1984). Fed-batch techniques in microbial process. In *Advances in Biochemical Engineering and Biotechnology*, pp. 145-194. Berlin: Springer Verlag.

Yang, S., Huang, H., Zhang, R., Huang, X., Li, S. & Yuan, Z. (2001). Expression and purification of extracellular penicillin G acylase in *Bacillus subtilis*. *Protein Expr Purif* **21**, 60-64.

Yuan, G. & Wong, S. L. (1995). Isolation and characterization of *Bacillus subtilis groE* regulatory mutants: evidence for *orf39* in the *dnaK* operon as a repressor gene in regulating the expression of both *groE* and *dnaK*. *J Bacteriol* **177**, 6462-6468.

VI Danksagung

Mein Mentor, Herr Prof. Dr. Wolf-Dieter Deckwer, gab mir nicht nur die Möglichkeit an einem interessanten, anwendungsbezogenen Thema zu forschen, sondern auch ein lockeres Arbeitklima mit viel Freiheit, unter dem Motto „Sie wollen doch in 10 Jahren promovieren. Ich habe schon promoviert“. Er hat mich an die Anleitung und Planung meiner Doktorarbeit herangeführt. Besonders bei der Diskussion der Ergebnisse war mir sein Rat eine große Hilfe. Nach diesen 3 Jahren Promotion, habe ich beim ihm nicht nur das Forschen, sondern auch den Ernst der Arbeit und den Humor des Lebens kennengelernt habe. Deshalb gilt ihm ein ganz spezieller Dank. Sein Tod im Oktober traf mich unerwartet nicht nur und sondern auch schmerzlich.

Mein ganz besonderer Großer Dank gilt Prof. Dr. Dieter Jahn, der es mir ermöglicht hat, in seiner Arbeitsgruppe molekularbiologische Arbeiten durchzuführen. Besonders dankbar bin ich für die Übernahme der Betreuung meiner Doktorarbeit seit Oktober. In Gesprächen und Diskussionen hat er mich motiviert und unterstützt. Immer wieder und hat er mir weitergeholfen, wenn ich Hilfe brauchte. Mit seinem Vertrauen hat er mich jederzeit bestärkt.

Als nächstes möchte ich mich bei Prof. Dr. Siegmund Lang für die freundliche Übernahme des Korreferates und Prof. Dr. Stefan Dübel für die Leitung der Prüfungskommission bedanken.

Auch ohne meine tollen Mitarbeiter der „M*egaterium*“ und „TU-BCE“ Gruppen wäre diese Arbeit nie zustande gekommen. Für die schöne Zeit und Zusammenarbeit geht an alle ein ganz besonderer Dank. Dabei sei vor allem Dr. Marco Malten zu erwähnen, nicht weil er nun mein Ehrmann ist, sonder dafür daß er mich geduldig in die molekularen Laborarbeiten eingeführt hat und jederzeit als Erster meine Arbeit liest und korrigiert. Darüber hinaus sei besonders Dr. Rebekka Biedendieck für die nette Zusammenarbeit und ihre Genauigkeit gedankt.

Meiner Kollegin Karolin Dresler danke ich für ihre Unterstützung, zahlreiche Tipps und Diskussionen und besonders die lustige Zeit im „TU-BCE“ Labor. Ganz besonderer Dank geht an Dr. Rajan Hollmann, dafür daß er am Anfang meiner Promotionszeit auch um Mitternacht am Bioreaktor einen klaren Kopf behielt, wenn ich ihn aus dem Bett klingelte. Martin Gamer, Tobias Fürch und Dominik Sieblitz und auch meinen Hiwis Isam Haddad und Sopna Josef sei für die Hilfe und die gute Atmosphäre gedankt.

Rat durfte ich mir auch immer wieder bei den „PostDocs“des Arbeitskreises holen, sowie bei den SFB-Kollegen. Hier sei ganz besonders Frau Dr. Wei Wang und Dr. Jochen Mueller für die Unterstützung und Diskussion gedankt. Frau Rita Getzlaff (HZI) und Dr. Anton Ross (HZI) halfen mir bei der N-terminalen Sequenzierungen bzw. dem PGA Aktivitätstest gerne weiter.

Abschließend möchte ich meinen Eltern, besonders meiner großartigen Mutter danken, daß sie mir überhaupt die Chance gegeben hat, diese Doktorarbeit in Deutschland zu machen und immer an mich geglaubt hat.